

DESIGN AND IMPLEMENTATION OF REFLECTIONLESS FILTERS

A THESIS SUBMITTED TO  
THE GRADUATE SCHOOL OF NATURAL AND APPLIED SCIENCES  
OF  
MIDDLE EAST TECHNICAL UNIVERSITY

BY

ALİ İHSAN ÇUBUKÇU

IN PARTIAL FULFILLMENT OF THE REQUIREMENTS  
FOR  
THE DEGREE OF MASTER OF SCIENCE  
IN  
ELECTRICAL AND ELECTRONICS ENGINEERING

MAY 2016



Approval of the thesis:

**DESIGN AND IMPLEMENTATION OF REFLECTIONLESS FILTERS**

submitted by **ALİ İHSAN ÇUBUKÇU** in partial fulfillment of the requirements  
for the degree of **Master of Science in Electrical and Electronics Engineering**  
**Department, Middle East Technical University** by,

Prof. Dr. M. Gülbin Dural Ünver  
Dean, Graduate School of **Natural and Applied Sciences** \_\_\_\_\_

Prof. Dr. Gönül Turhan Sayan  
Head of Department, **Electrical and Electronics Engineering** \_\_\_\_\_

Prof. Dr. Nigün Günalp  
Supervisor, **Electrical and Electronics Engineering Dept., METU** \_\_\_\_\_

Prof. Dr. Nevzat Yıldırım  
Co-Supervisor, **Electrical and Electronics Engineering Dept., METU** \_\_\_\_\_

**Examining Committee Members:**

Prof. Dr. S. Sencer Koç  
Electrical and Electronics Engineering Dept., METU \_\_\_\_\_

Prof. Dr. Nilgün Günalp  
Electrical and Electronics Engineering Dept., METU \_\_\_\_\_

Prof. Dr. Nevzat Yıldırım  
Electrical and Electronics Engineering Dept., METU \_\_\_\_\_

Prof. Dr. Şimşek Demir  
Electrical and Electronics Engineering Dept., METU \_\_\_\_\_

Prof. Dr. Adnan Köksal  
Electrical and Electronics Engineering Dept., Hacettepe University \_\_\_\_\_

**Date:** 12.05.2016 .

**I hereby declare that all information in this document has been obtained and presented in accordance with academic rules and ethical conduct. I also declare that, as required by these rules and conduct, I have fully cited and referenced all material and results that are not original to this work.**

Name, Last name: Ali İhsan Çubukçu

Signature:

## **ABSTRACT**

### **DESIGN AND IMPLEMENTATION OF REFLECTIONLESS FILTERS**

**ÇUBUKÇU, Ali İhsan**

**M.S., Department of Electrical and Electronics Engineering**

**Supervisor: Prof. Dr. Nilgün GÜNALP**

**Co-Supervisor: Prof. Dr. Nevzat YILDIRIM**

**May 2016, 86 pages**

In this thesis, typical applications of absorptive filters are examined. To better understand the effect of out of band matching of RF and microwave filters on overall system, some experiment setups are constructed and simulations are performed. In addition to this, three types of conventional absorptive filter topologies are analyzed and the realizability of each type is shown by explanation, simulation or measurement. Finally, a recently found method, reflectionless filter structures by Matthew Morgan, is analyzed and various types of reflectionless filters are designed and implemented. Furthermore, some approaches are stated to obtain better filter characteristics with the same topology.

**Keywords :** Absorptive filter, reflectionless filter, out of band matching.

## **ÖZ**

### **YANSIMASIZ SÜZGEÇ TASARIMLARI VE UYGULAMALARI**

**ÇUBUKÇU, Ali İhsan**

**Yüksek Lisans, Elektrik ve Elektronik Mühendisliği Bölümü**

**Tez Yöneticisi: Prof. Dr. Nilgün GÜNALP**

**Ortak Tez Yöneticisi: Prof. Dr. Nevzat YILDIRIM**

**Mayıs 2016, 86 sayfa**

Bu tez çalışmasında, soğurucu süzgeçlerin tipik uygulamaları incelendi. RF ve mikrodalga süzgeçlerin bant dışı uyumluluğunun tüm sisteme olan etkisini daha iyi anlamak adına, bazı deney düzenekleri kuruldu ve benzetim çalışmaları yapıldı. Buna ek olarak, üç çeşit klasik soğurucu süzgeç topolojileri incelendi ve her tipin gerçekleştirilebilirliği; açıklamalar, benzetimler veya ölçümler kullanılarak gösterildi. Son olarak, son zamanlarda Matthew Morgan tarafından bulunan yansımaz süzgeç yapıları analiz edildi ve çeşitli yansımaz süzgeç tipleri tasarlandı ve uygulandı. Ayrıca daha iyi süzgeç karakteristiği elde etmek için aynı topolojide farklı yaklaşımlar üzerinde duruldu.

Anahtar Kelimeler : Soğurucu süzgeç, yansımaz süzgeç, bant dışı uyumluluğu.

**To my beloved mother**

## ACKNOWLEDGMENTS

I wish to express my sincere gratitude to Prof. Dr. Nevzat Yıldırım and Prof. Dr. Nilgün Günalp for their supervision, valuable guidance and helpful suggestions.

I would like to express my appreciation to İrfan Yıldız, Ahmet Özdemir, Salih Can Aksoy, Sinan Kurudere, Akın Özkan, T. Oğuz Topbaş, Taha Akyol and M. Eren Ergüden for their valuable suggestions and advices. I also would like to thank to Meteksan Savunma Sanayii A.Ş. that provides me facilities and materials to finalize the fabrication and measurement processes.

I sincerely thank to my mother Nurgül and my brother Mustafa for being by my side without any condition and exception. This work would never be possible without their support.

I would also like to thank my niece Zeynep Ada and my nephews Yavuz Selim and Metehan for being a part of our family and making our lives pleasant.



## TABLE OF CONTENTS

ABSTRACT .....	v
ÖZ .....	vi
ACKNOWLEDGMENTS .....	viii
TABLE OF CONTENTS.....	ix
LIST OF TABLES .....	xi
LIST OF FIGURES .....	xii

### CHAPTERS

1. INTRODUCTION.....	1
1.1 Introduction .....	1
1.2 Scope of the Thesis and Design Tools.....	2
1.2.1 Organization of the Thesis .....	3
1.2.2 CAD Tools.....	4
2. APPLICATIONS OF ABSORPTIVE FILTERS .....	7
2.1 Introduction .....	7
2.2 Cascaded Microwave Filters .....	7
2.3 Out of Band Effect in Frequency Conversion Applications.....	11
3. METHODS TO REALIZE ABSORPTIVE FILTERS .....	15
3.1 Introduction .....	15

3.2 Absorptiveness by Using Isolator .....	15
3.3 Absorptiveness by Using Multiplexer .....	15
3.4 Absorptiveness by Using 3 dB 90° Coupler .....	19
<b>4. REFLECTIONLESS FILTERS.....</b>	<b>23</b>
4.1 Introduction .....	23
4.2 Theory.....	23
4.3 Design.....	38
4.3.1 Reflectionless Low-Pass Filter Design .....	38
4.3.2 Reflectionless High-Pass Filter Design .....	40
4.3.3 Reflectionless Bandpass Filter Design .....	43
4.3.4 Reflectionless Bandstop Filter Design .....	45
4.4 Realization and Measurement.....	47
4.4.1 Implemented Reflectionless Low-Pass Filters.....	48
4.4.2 Implemented Reflectionless High-Pass Filters.....	50
4.4.3 Implemented Reflectionless Bandpass Filters.....	53
4.4.4 Implemented Reflectionless Bandstop Filters.....	56
<b>5.IMPROVED REFLECTIONLESS FILTERS.....</b>	<b>61</b>
5.1 Introduction .....	61
5.2 Termination Resistor Approach.....	61
5.3 Reflectionless Filter as a Diplexer Approach .....	63
<b>6. CONCLUSION AND FUTURE WORK SUGGESTIONS .....</b>	<b>73</b>
<b>REFERENCES .....</b>	<b>75</b>
<b>APPENDICES.....</b>	<b>77</b>

## LIST OF TABLES

### TABLES

Table 4.1 Relation Between $f_c$ and $f_{tz}$ .....	30
Table 4.2 Summary of Basic Reflectionless Filter Structures .....	37
Table 4.3 Reflectionless Low-Pass Filter Specifications .....	38
Table 4.4 Reflectionless High-Pass Filter Specifications .....	40
Table 4.5 Reflectionless Bandpass Filter Specifications .....	43
Table 4.6 Reflectionless Bandstop Filter Specifications.....	45

## LIST OF FIGURES

### FIGURES

Figure 2.1 Return Loss Comparison for Reflective Bandpass Filters .....	8
Figure 2.2 Insertion Loss Comparison for Reflective Bandpass Filters.....	8
Figure 2.3 Return Loss Comparison for Absorptive Bandpass Filters.....	9
Figure 2.4 Insertion Loss Comparison for Absorptive Bandpass Filters .....	9
Figure 2.5 Characteristics of Cascaded Reflected Low-Pass and High-Pass Filters .....	10
Figure 2.6 Characteristics of Cascaded Absorptive Low-Pass and High-Pass Filters .....	10
Figure 2.7 Return Loss Comparison of Mixer with Reflective and Absorptive Filters .....	12
Figure 2.8 Conversion Loss of Mixer.....	13
Figure 2.9 Conversion Loss of Mixer with Reflective Filter .....	13
Figure 2.10 Conversion Loss of Mixer with Absorptive Filter .....	14
Figure 3.1 a) Low-pass-high-pass diplexer. b) Bandpass-bandstop diplexer. c) Low-pass-bandpass diplexer. d) Bandpass-bandpass diplexer.....	16
Figure 3.2 Synthesized Low-pass – High-pass Diplexer.....	17
Figure 3.3 Simulation Results for Low-pass and High-pass Absorptive Filters ...	17
Figure 3.4 Synthesized Bandpass – Bandstop Diplexer .....	18
Figure 3.5 Simulation Results for Bandpass and Bandstop Absorptive Filters.....	18
Figure 3.6 Explanation of Structure – 1 .....	19
Figure 3.7 Explanation of Structure – 2 .....	20
Figure 3.8 Implemented Absorptive Filter .....	21
Figure 3.9 Measurement Result of Implemented Filter.....	21
Figure 4.1 Symmetric Two Port Network .....	24
Figure 4.2 Even Mode Case for Symmetric Two Port Network .....	24

Figure 4.3 Odd Mode Case for Symmetric Two Port Network .....	24
Figure 4.4 High-Pass Filter Type-1 .....	26
Figure 4.5 High-Pass Filter Type-2 .....	26
Figure 4.6 Derivation of Reflectionless Filter from Dual High-Pass Filters .....	27
Figure 4.7 Reflectionless Low-Pass Filters .....	28
Figure 4.8 Reflectionless High-Pass Filters .....	31
Figure 4.9 Reflectionless Bandpass Filters .....	31
Figure 4.10 Reflectionless Bandstop Filters .....	32
Figure 4.11 Simulation Results for Reflectionless Low-Pass Filter-1 .....	39
Figure 4.12 Simulation Results for Reflectionless Low-Pass Filter-2 .....	39
Figure 4.13 Simulation Results for Reflectionless Low-Pass Filter-3 .....	40
Figure 4.14 Simulation Results for Reflectionless High-Pass Filter-1 .....	41
Figure 4.15 Simulation Results for Reflectionless High-Pass Filter-2 .....	41
Figure 4.16 Simulation Results for Reflectionless High-Pass Filter-3 .....	42
Figure 4.17 Simulation Results for Reflectionless High-Pass Filter-4 .....	42
Figure 4.18 Simulation Results for Reflectionless Bandpass Filter-1 .....	43
Figure 4.19 Simulation Results for Reflectionless Bandpass Filter-2 .....	44
Figure 4.20 Simulation Results for Reflectionless Bandpass Filter-3 .....	44
Figure 4.21 Simulation Results for Reflectionless Bandpass Filter-4 .....	45
Figure 4.22 Simulation Results for Reflectionless Bandstop Filter-1 .....	46
Figure 4.23 Simulation Results for Reflectionless Bandstop Filter-2 .....	46
Figure 4.24 Simulation Results for Reflectionless Bandstop Filter-3 .....	47
Figure 4.25 Lay-out of Reflectionless Low-Pass Filter .....	48
Figure 4.26 Fabricated Reflectionless Low-Pass Filters .....	48
Figure 4.27 Measurement Result of Reflectionless LPF-1 .....	49
Figure 4.28 Measurement Result of Reflectionless LPF-2 .....	49
Figure 4.29 Measurement Result of Reflectionless LPF-3 .....	50
Figure 4.30 Lay-out of Reflectionless High-Pass Filter .....	50
Figure 4.31 Fabricated Reflectionless High-Pass Filters .....	51
Figure 4.32 Measurement Result of Reflectionless HPF-1 .....	51
Figure 4.33 Measurement Result of Reflectionless HPF-2 .....	52

Figure 4.34 Measurement Result of Reflectionless HPF-3 .....	52
Figure 4.35 Measurement Result of Reflectionless HPF-4 .....	53
Figure 4.36 Lay-out of Reflectionless Bandpass Filter .....	53
Figure 4.37 Fabricated Reflectionless Bandpass Filters.....	54
Figure 4.38 Measurement Result of Reflectionless BPF-1 .....	54
Figure 4.39 Measurement Result of Reflectionless BPF-2 .....	55
Figure 4.40 Measurement Result of Reflectionless BPF-3 .....	55
Figure 4.41 Measurement Result of Reflectionless BPF-4 .....	56
Figure 4.42 Lay-out of Reflectionless Bandstop Filter .....	56
Figure 4.43 Fabricated Reflectionless Bandstop Filters.....	57
Figure 4.44 Measurement Result of Reflectionless BSF-1 .....	57
Figure 4.45 Measurement Result of Reflectionless BSF-2 .....	58
Figure 4.46 Measurement Result of Reflectionless BSF-3 .....	58
Figure5.1 Reflectionless Low Pass Filters Constructed by First Approach .....	62
Figure5.2 Simulation Result for First Approach .....	63
Figure5.3 (a) Even Mode Case (b) Even Mode Equivalent for Left Side Circuitry (c) Even Mode Equivalent for Right Side Circuitry .....	64
Figure5.4 (a) Odd Mode Case (b) Odd Mode Equivalent for Left Side Circuitry (c) Odd Mode Equivalent for Right Side Circuitry .....	64
Figure5.5 Dual-Directional Diplexer.....	66
Figure5.6 Reflectionless Filter with Attenuator Sub-network .....	67
Figure5.7 Simulation Result for Reflectionless Filter with Attenuator Sub-network .....	67
Figure5.8 Second Order Reflectionless Filter .....	68
Figure5.9 Third Order Reflectionless Filter .....	69
Figure5.10 Comparison of First, Second and Third Order Reflectionless Filters. ....	69
Figure5.11 Reflectionless Low-Pass Filter with High-Pass Sub-network .....	70
Figure5.12 Comparison of Regular Reflectionless Low-Pass Filter and Reflectionless Filter in Figure 5.9 .....	71

# **CHAPTER 1**

## **INTRODUCTION**

### **1.1 Introduction**

Radio Frequency (RF) - Microwave filters are one of the most important fundamental blocks of microwave radar, communication, or measurement and test systems. The main object of filters in RF – microwave systems is rejecting unwanted signals and transmitting wanted signals with less attenuation and distortion. According to its transmission-rejection characteristics, there are 4 main types of RF – microwave filters which are low-pass, bandpass, high-pass, and band-reject characteristics [1].

Very first theoretical studies and applications are started in the years preceding World War II. Very first significant paper about microwave filtering was published by W. P. Mason and R. A. Sykes in 1937 and there have been a lot of studies about filter topologies, filter synthesis approaches, filter realization techniques and so on [2]. When these studies are examined, it is seen that all of them have reflective stop band until 2004. After 2004, some studies about filters having matched stop band characteristics can be found in literature.

Each microwave component in microwave systems is designed for matched source and matched load. However, this is not valid for real world applications. Especially, if this microwave component is cascaded with a filter, out of band characteristics of filter can affect its performance and it can cause many vital problems in microwave systems. For example, if this microwave component is a high gain amplifier, instability problems can occur even though amplifier is unconditionally stable when it is tested alone [3]. Moreover, out of band performance is also very critical for nonlinear microwave devices such as mixers

and frequency doublers. Filters are widely used after these nonlinear devices to prevent spurious signals caused by themselves. If these filters are reflective in stop band, stop band characteristics of filters affect directly input return loss of nonlinear devices and conversion losses can be problematic because of this.

Because of such problems, nearly ten year old topic, absorptive filters, becomes important. As it can be understood from its name, absorptive filter is nothing but a filter which has low return loss in stop band as well as pass band. In literature, this type of filters can also be described in different names such as “reflectionless filters” and “invulnerable filters”.

The main target of this thesis is to classify different types of absorptive filters and explain the basic theory behind them. These theoretical concepts are verified by using simulations and implementations. For implementation steps of this thesis, some absorptive filters in different frequency ranges, structures and topologies are designed and manufactured.

## **1.2 Scope of the Thesis and Design Tools**

The aim of this thesis is the search for the required cases, design and implementation of different types of absorptive filters operating in different frequency ranges with different structures. Four different design approaches of absorptive filters is mentioned namely absorptiveness by using isolators, absorptive filter formation from multiplexers, absorptiveness in filtering by using 3 dB 90° couplers, and Matthew Morgan’s reflectionless filter topology.

Different tools are used in design and simulation steps. The filter design software FILPRO™ is used to synthesize diplexers. GENESYS™ is also used in synthesis and analysis of some filters.



### 1.2.1 Organization of the Thesis

In Chapter 2, the reason why absorptive filters are needed is analyzed. Some problematic cases that are caused by conventional reflective filters are given by using simulation tools and these cases are realized. The reason behind these problematic cases is explained and performance of absorptive filters is compared with conventional filter performance.

Chapter 3 is devoted for three methods to implement absorptive filters which are absorptiveness by using isolators, absorptive filter formation from multiplexers, and absorptiveness in filtering by using 3 dB 90° couplers. Firstly, some explanations about isolators are given and some features of absorptive filters constructed with isolators are examined. Secondly, another method, implementation of absorptive filters by using multiplexers is handled. For the completeness of this section, what multiplexer is and what are the specialized forms of multiplexers are explained. After these explanations, how a multiplexer can be used as absorptive filters is mentioned and two diplexers are designed by using FILPRO™. Designed diplexers' simulation results are shared and their absorptive filter performances are examined. Finally, last method for Chapter 3 to realize an absorptive filter by using 3 dB 90° coupler is explained. For this purpose, how this type of absorptive filters operates is explained and measurement result of an absorptive filter which is constructed by using this method is presented.

In Chapter 4, Reflectionless Filter, one of the newest topology of absorptive filters found and patented by a Scottish scientist Matthew Morgan, is analyzed and implemented. Firstly, theory behind the reflectionless filters is studied and design method is explained. Secondly; low-pass, high-pass, bandpass and bandstop reflectionless filters are designed and simulated by using GENESYS™. Finally, these filters are implemented and test results are presented in this chapter.

In order to improve suppression or have different filtering characteristics of reflectionless filters, two different approaches are mentioned in Chapter 5. First

of them is constructed by using different termination resistors from characteristic impedance  $Z_0$ . In second approach, reflectionless filter is thought as dual-directional diplexer and some matched networks such as resistive attenuators or other reflectionless filters are connected to internal ports and it is seen that reflectionless property is conserved for matched sub-networks. Simulation results are presented for each examples of belonging approach in this chapter.

### **1.2.2 CAD Tools**

Following CAD tools are used in the design of filters:

The component of the diplexers was synthesized using FILPRO™. FILPRO™ is filter synthesis, transformation and analysis software. This synthesis tool can be used in passive, lumped and distributed topologies in cascade topologies and cross-coupled filters of diverse topologies. Multiplexer configurations, directional couplers and impedance matching circuits can also be designed and analyzed in FILPRO™. This software is developed in Electrical Engineering Department of METU [4].

GENESYS™ is a linear design tool of EAGLEWARE Company. Analysis and tuning of most of the absorptive filters are carried out using linear toolbox of GENESYS™ software. Interdigital filters used in 3 dB 90° coupler method are also synthesized in this tool. In order to see more realistic results of each design, S-parameters of components are imported to GENESYS™ and results are observed [5].

Sonnet®Suites™ is electromagnetic analysis software, which uses method of moments (MoM) to solve the current distribution on the metallization of the analyzed circuit. Final optimization of interdigital filters used to realize the third method of absorptive filter construction given in Chapter 3 is made by using this tool [6].

Layouts of proposed filters are created by using PADS<sup>®</sup> Layout by Mentor Graphics.



## **CHAPTER 2**

### **APPLICATIONS OF ABSORPTIVE FILTERS**

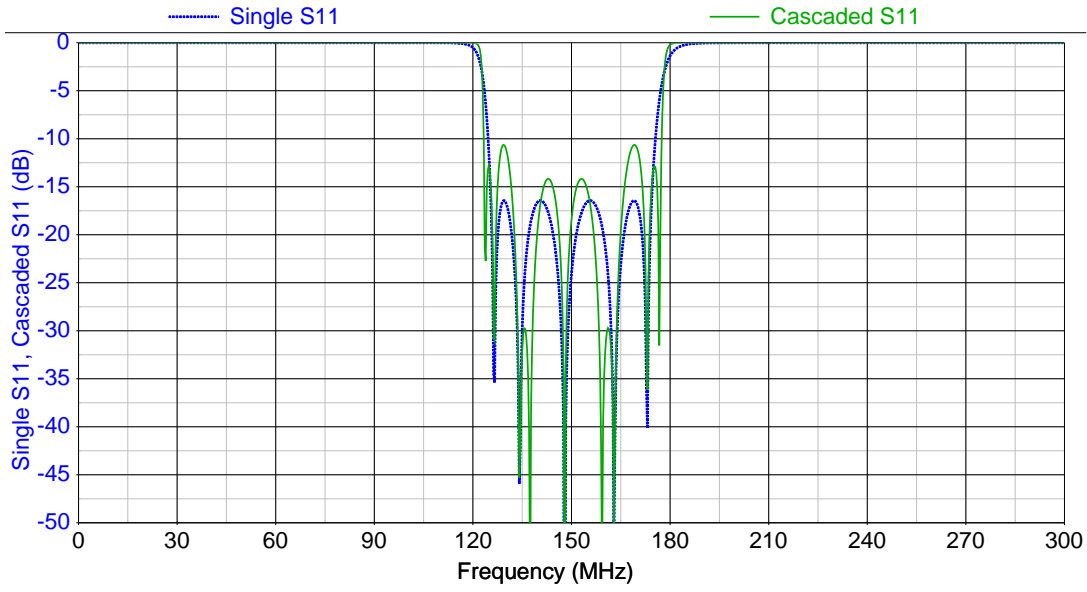
#### **2.1 Introduction**

Each microwave components such as filters, frequency doublers, mixers, amplifiers and so on are designed for matched source and matched load as mentioned in Chapter 1. However, this is not valid for cascaded microwave systems. Therefore, degradations can be observed in system performance of some microwave components especially when they are cascaded with reflective filters. In other words, reflective filters' almost full reflective out of band characteristics can affect performance of other components. In this chapter, some application cases with reflective and absorptive filters are examined and compared.

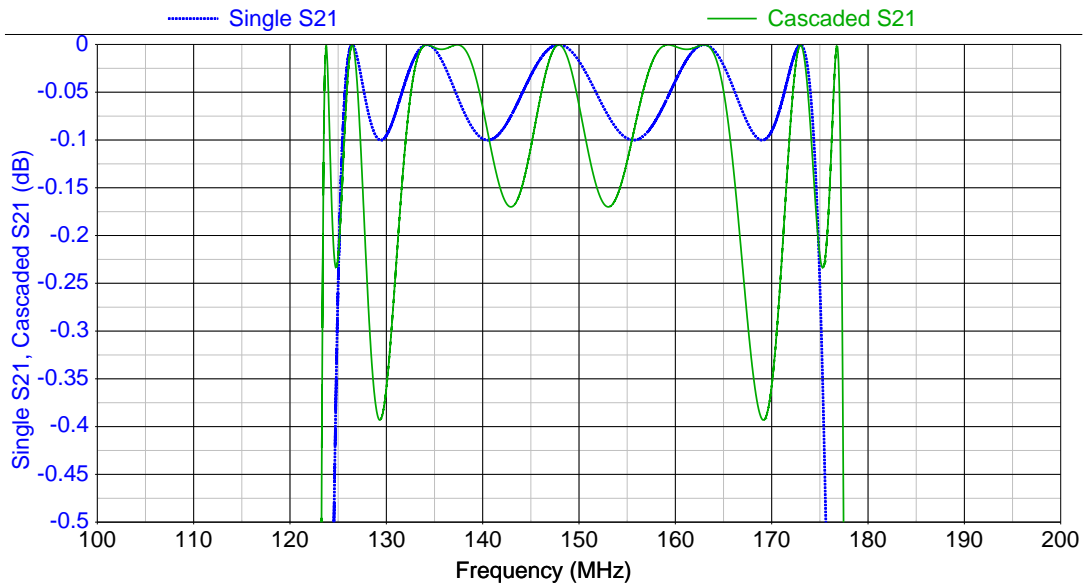
#### **2.2 Cascaded Microwave Filters**

Designers can cascade filters for different purposes such as to have better suppression in stop band and to characterize an overall filter characteristics by combining different filters. However, pass band characteristics of cascaded reflective filters can be distorted because of the standing waves between their reflective stop bands. Therefore, cascading reflective filters can result in unexpected results. On the other hand, absorptive filters can be cascaded as long as filtering demand is satisfied.

Cascaded reflective filter characteristics evaluated by using GENESYS™ linear simulation tool. Firstly, a reflective Chebyshev band pass filter with 0.1 dB ripple between 125-175 MHz pass band is synthesized by using GENESYS™. The comparison of single filter and cascaded filter characteristics are given in Figure 2.1 and Figure 2.2.



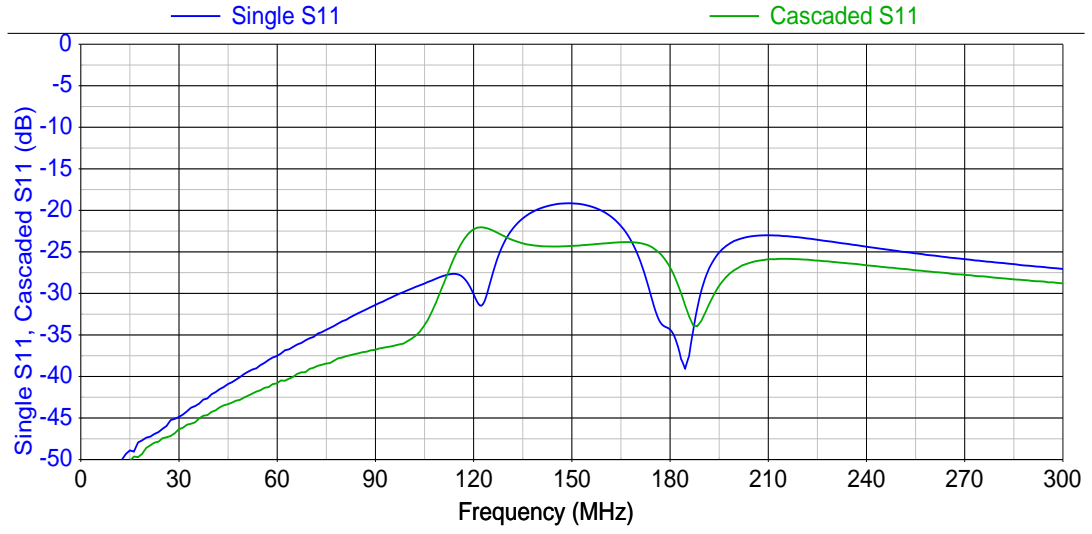
**Figure 2.1:** Return Loss Comparison for Reflective Bandpass Filters



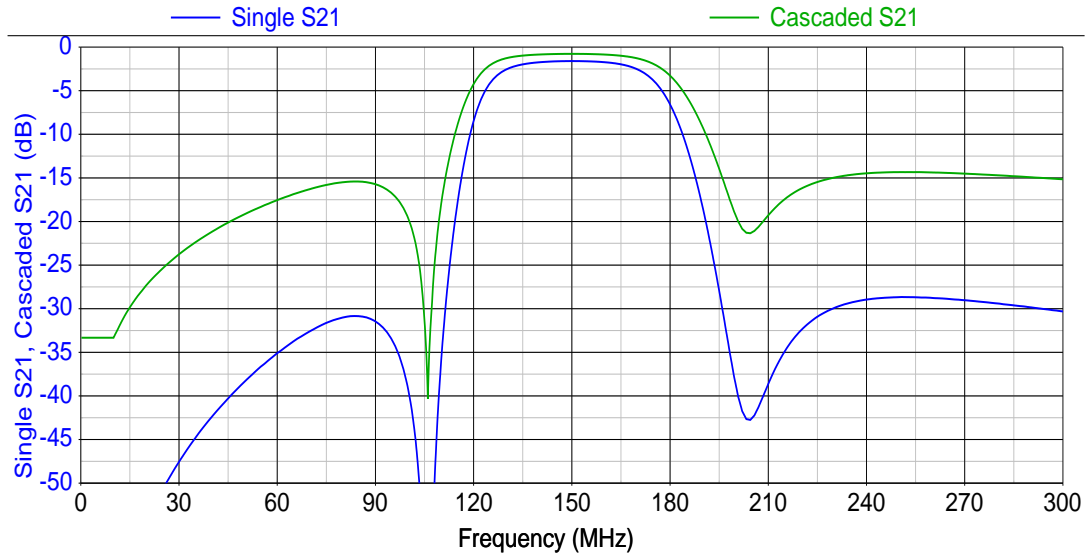
**Figure 2.2:** Insertion Loss Comparison for Reflective Bandpass Filters

As it is seen from Figure 2.1 and Figure 2.2 cascaded performance of reflective filters degrades. Worse return loss and higher ripple in pass band is observed.

By using similar approach, cascaded absorptive filter characteristics is examined by using network analyzer. Results of comparison are given in Figure 2.3 and Figure 2.4. Design procedure of absorptive filters used in this test is given in Chapter 4.

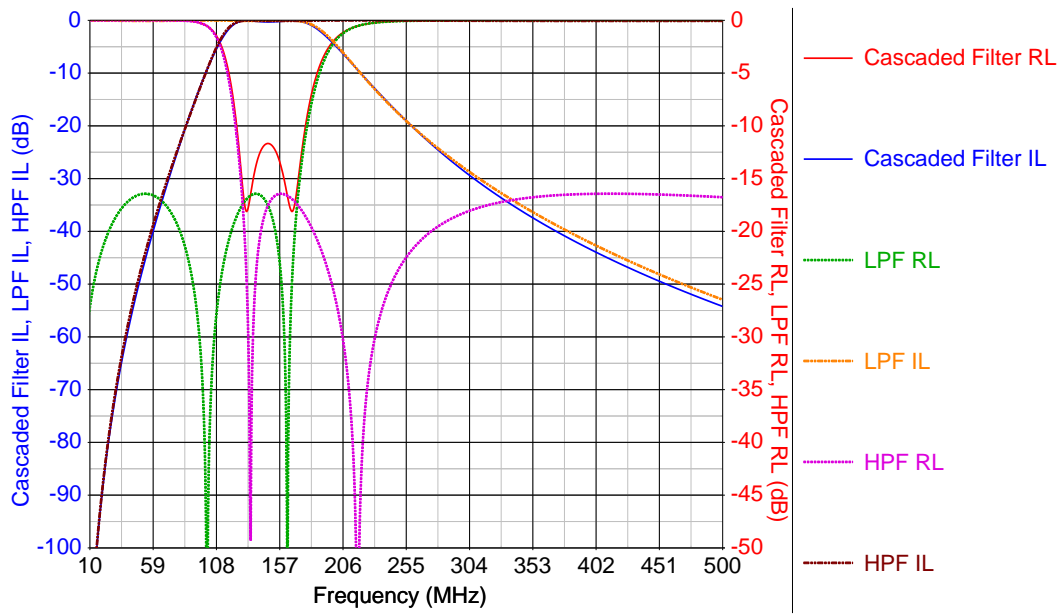


**Figure 2.3:** Return Loss Comparison for Absorptive Bandpass Filters

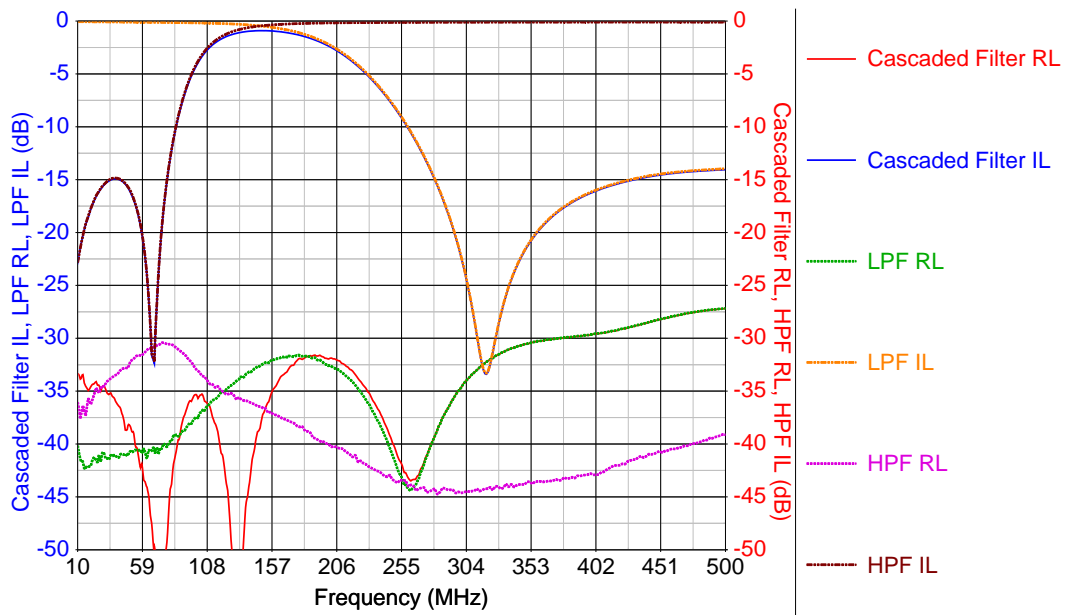


**Figure 2.4:** Insertion Loss Comparison for Absorptive Bandpass Filters

As it is mentioned before, filters are cascaded to obtain not only better suppression but also overall filter characteristics by combining different filters. In order to compare this application with reflective and absorptive filters, a low-pass and a high-pass filter are cascaded and a bandpass filter characteristic is obtained. Results are given in Figure 2.5 and Figure 2.6.



**Figure 2.5:** Characteristics of Cascaded Reflected Low-Pass and High-Pass Filters



**Figure 2.6:** Characteristics of Cascaded Absorptive Low-Pass and High-Pass Filters



According to results given in Figure 2.5, return loss performance of cascaded filter is worse than single filter performances. On the other hand, cascaded absorptive filters return loss characteristics have similar trend to single performance.

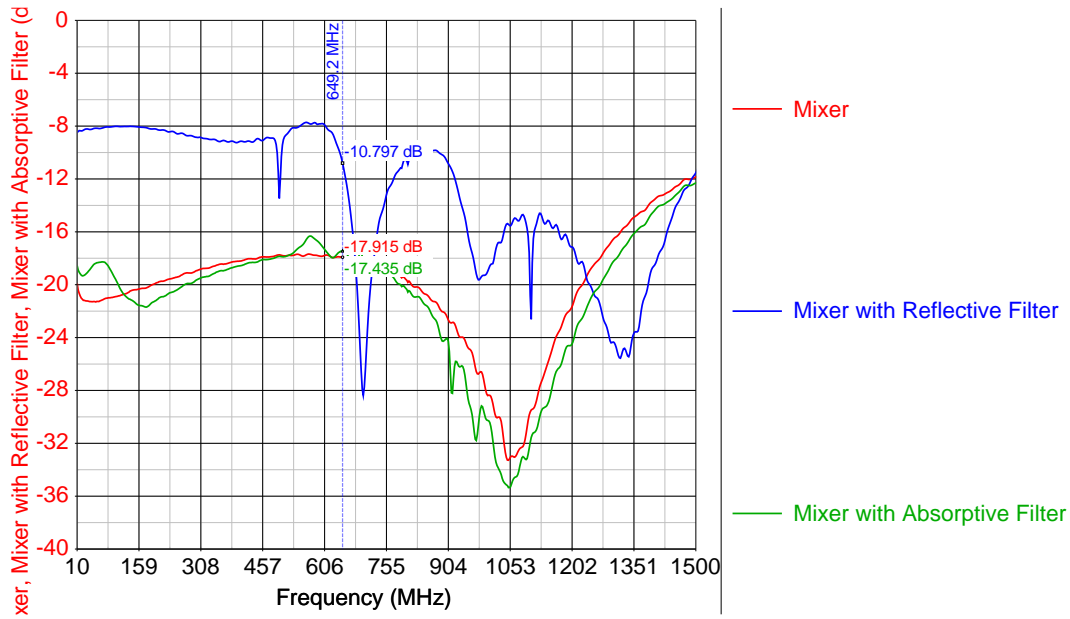
### **2.3 Out of Band Effect in Frequency Conversion Applications**

Mixers are widely used in frequency conversion applications. A mixer is a three-port device which produces sum and difference frequencies of two input signal. Because of nonlinear characteristics of mixer, it can generate wide variety of conversion products [1]. Therefore, filtering is inevitable for systems with mixers.

As it is mentioned, out of band signals are reflected back from filters. This fact can be problematic for filtering applications of mixer products since reflected signals get back to the mixer and they lead more spurious products.

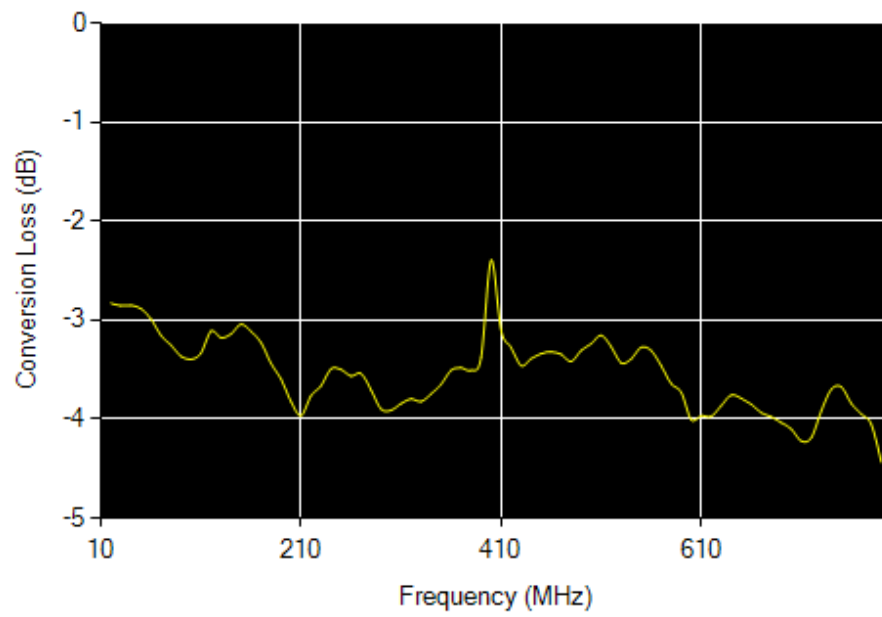
On the other hand, cascaded mixer return loss not only depends on the in band return loss performance of the components used after mixers but also out of band return loss performance because after mixer, out of band can be turned into in band after reversion and this affects overall system return loss negatively. Therefore, using reflective filters with mixers can cause some problems.

In order to explain this kind of problems, a down conversion case is examined. ZX05-5+ mixer of Mini-Circuits<sup>®</sup> Company is used for this test (Appendix A). A fixed LO signal at 800 MHz is applied and return loss of single mixer, mixer with reflective filter centered at 150 MHz and mixer with absorptive filter centered at 150 MHz is measured and following result is obtained.

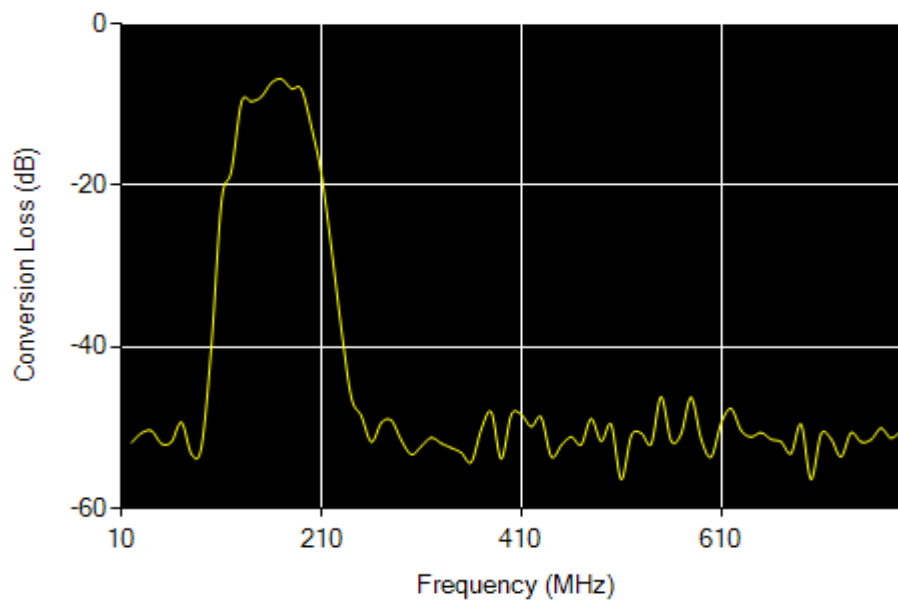


**Figure 2.7:** Return Loss Comparison of Mixer with Reflective and Absorptive Filters

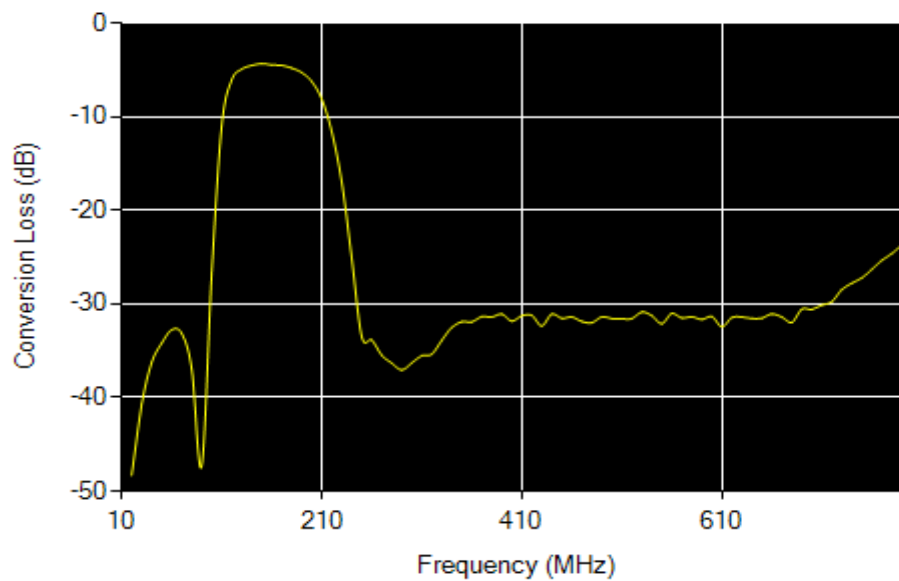
As it is seen from Figure 2.7, return loss of mixer is almost same with mixer with absorptive filter case. However, reflective filter case has worse return loss performance. Return loss also affects conversion loss of the mixer. Therefore, ripples are observed in reflective filter case. The results are shared in Figure 2.8, Figure 2.9 and Figure 2.10.



**Figure 2.8:** Conversion Loss of Mixer



**Figure 2.9:** Conversion Loss of Mixer with Reflective Filter



**Figure 2.10:** Conversion Loss of Mixer with Absorptive Filter

Designers use attenuators to overcome these problems; however, this increases conversion loss. Therefore, using absorptive filters after mixers is a better solution for this kind of problems.

In conclusion, reflective filter characteristics can cause some problems when it is evaluated in system aspect. Burning unwanted signals on terminated loads is preferred rather than reflecting them back by nature. In addition to this, it is seen that out of band performance affects in band performance for some components. Therefore, out of band return loss must be considered as well as in band return loss.

## **CHAPTER 3**

### **METHODS TO REALIZE ABSORPTIVE FILTERS**

#### **3.1 Introduction**

Three methods for realization of absorptive filters are proposed in Chapter 3. First of them is obtained by using isolators. Second type is realized from multiplexers. Last one is constructed from 3 dB 90° couplers.

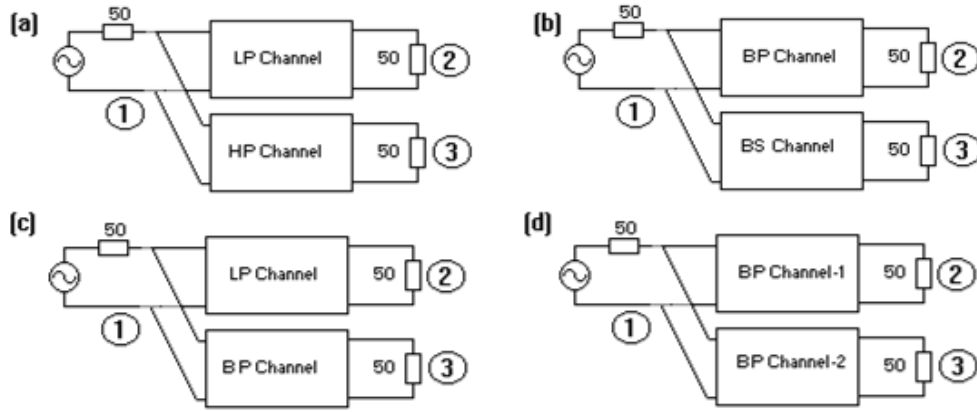
#### **3.2 Absorptiveness by Using Isolator**

Isolator is one of the most commonly used microwave ferrite components. It is a two port device and it has a unidirectional transmission characteristics. Since the reflected power from the load of the isolators are absorbed by isolator instead of reflecting back, they can be used as matching purposes[1].

When an isolator is cascaded with a conventional reflective filter, overall network has absorptive characteristics since the reflected out of band signals are absorbed by isolator. Although this method seems the simplest way to obtain absorptive filters, finding wide band, easy to integrate isolators can be problematic. Therefore, this method is not commonly used in applications.

#### **3.3 Absorptiveness by Using Multiplexer**

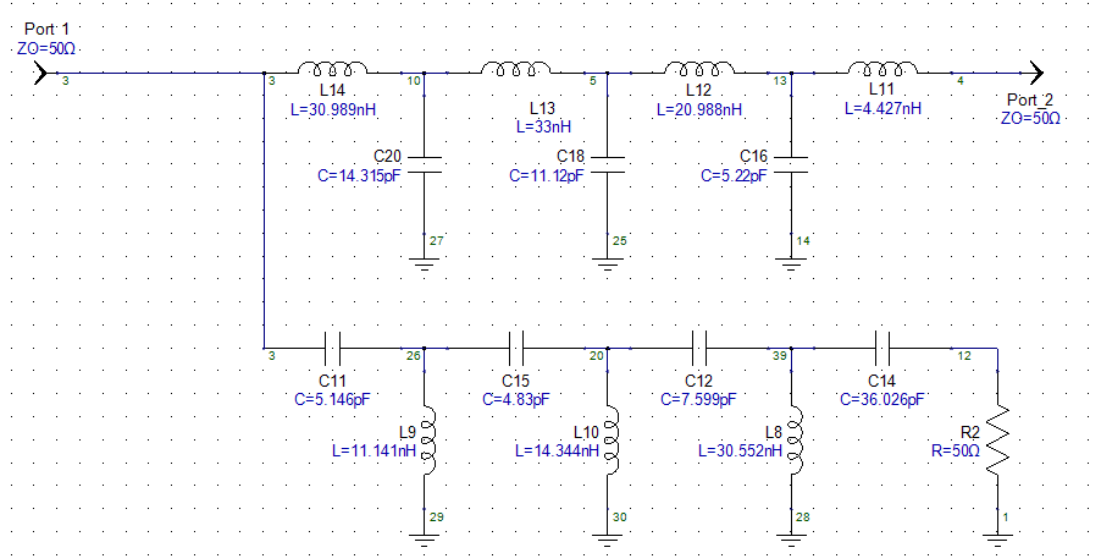
Multiplexers are microwave components that divide bands into channels by using special channel filters. Diplexer is a specialized name for two channeled multiplexer. Similarly, triplexer is for three channeled multiplexer. Typical parallel connected diplexers are given in Figure 3.1[4].



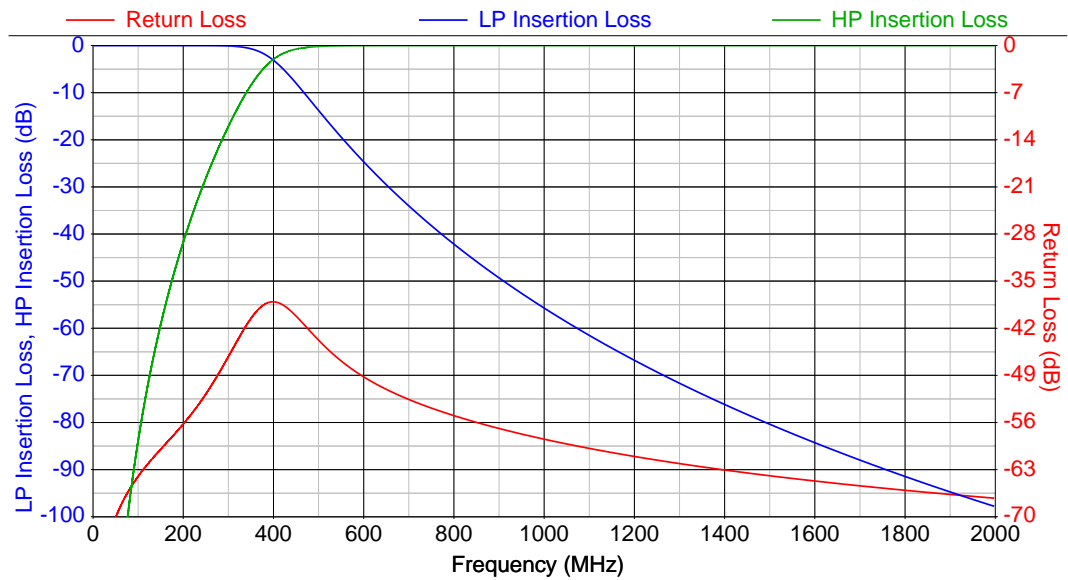
**Figure 3.1:** a) Low-pass-high-pass diplexer. b) Bandpass-bandstop diplexer. c) Low-pass-bandpass diplexer. d) Bandpass-bandpass diplexer[4]

When a channel's output of a multiplexer is terminated, absorptive characteristics occurs in this channel's band at the input of the multiplexer. By using this nature of multiplexers, absorptive filters can be constructed. For example, if the diplexer structure given in Figure 3.1-a is used and high-pass channel is terminated, an absorptive low-pass filter is obtained and vice versa. Similarly, absorptive bandpass and bandstop filters can be created by using the structure given in Figure 3.1-b.

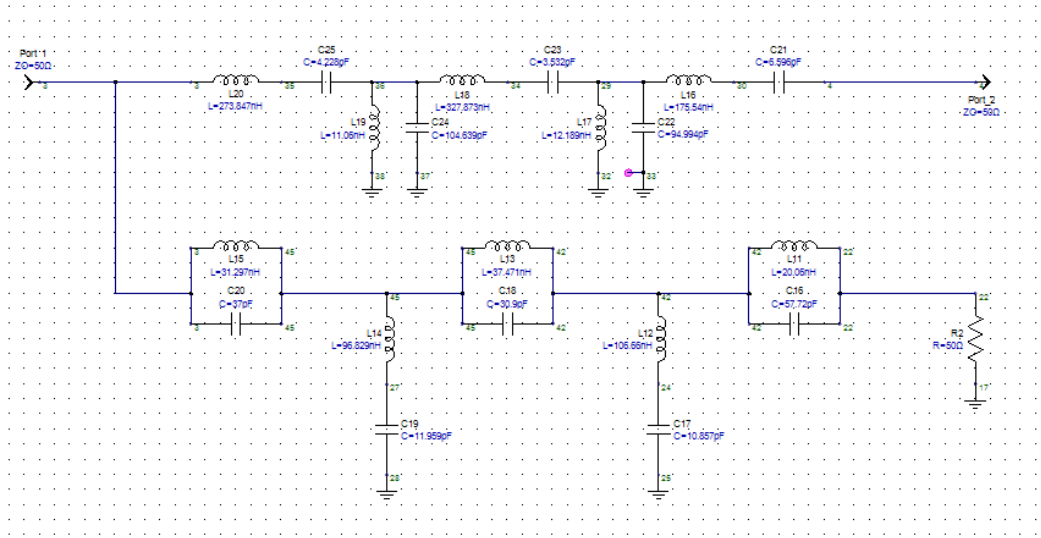
To give examples for this type of absorptive filters, two diplexers are created by using FILPRO™. One of them is low-pass – high-pass diplexer and the other one is bandpass – bandstop diplexer. Synthesized diplexers and their simulation results are given in Figure 3.2, Figure 3.3, Figure 3.4 and Figure 3.5.



**Figure 3.2:** Synthesized Low-pass – High-pass Diplexer



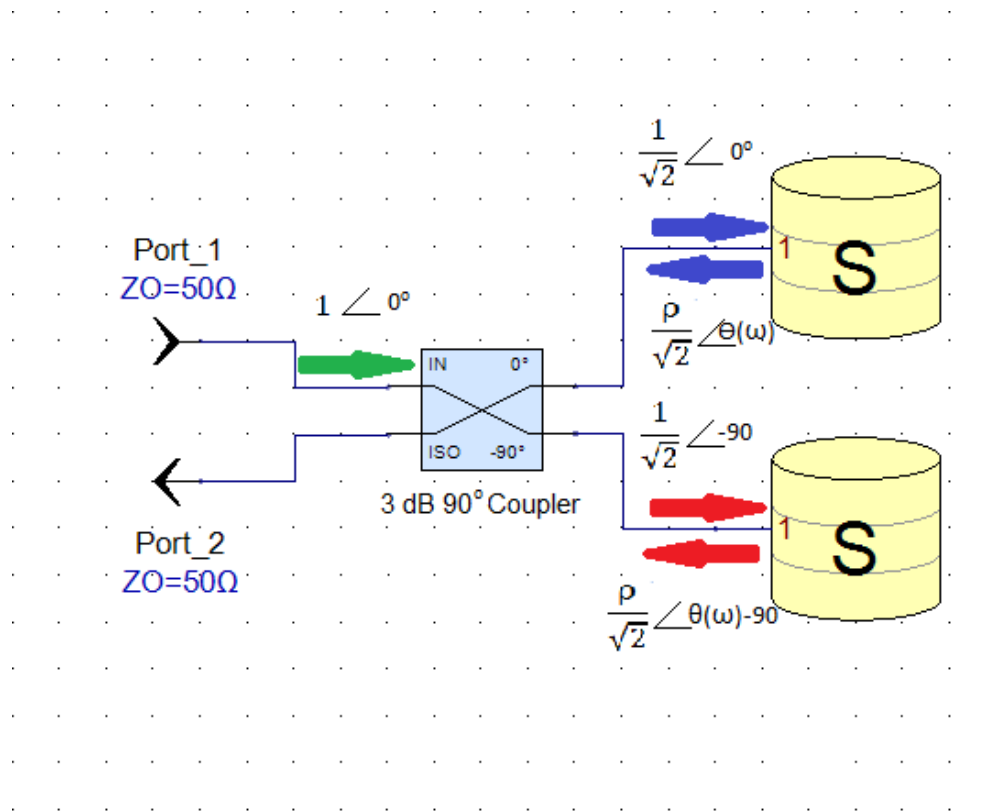
**Figure 3.3:** Simulation Results For Low-pass and High-pass Absorptive Filters



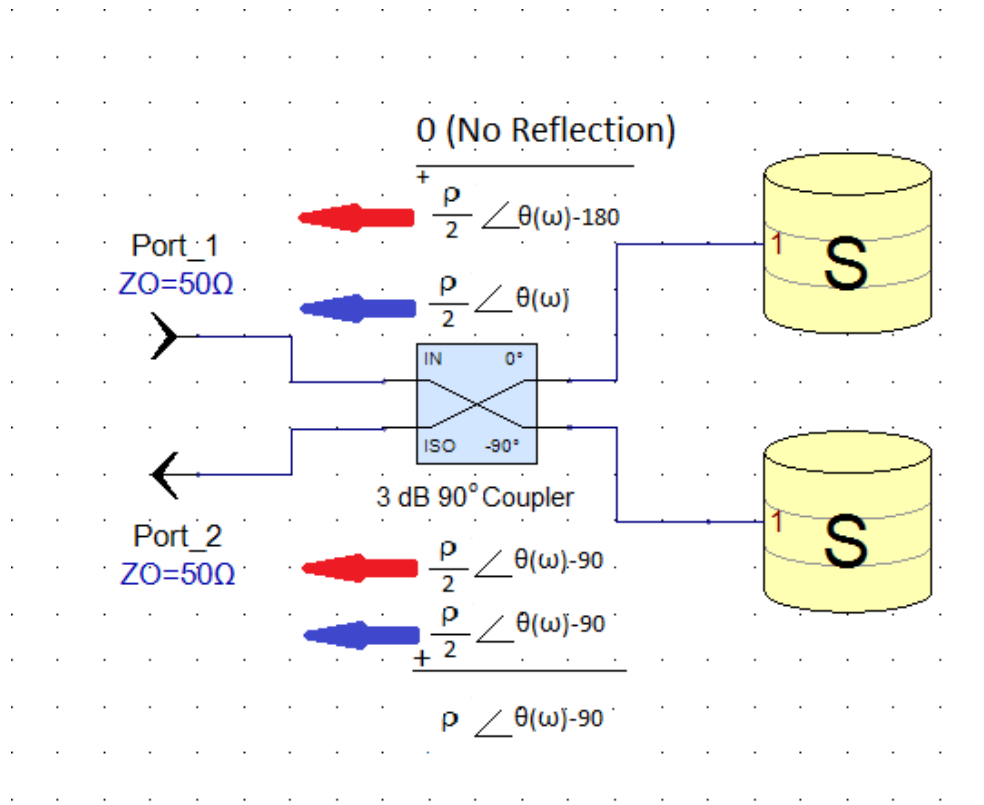


### 3.4 Absorptiveness by Using 3dB 90°Coupler

There is also another way to obtain absorptive filter characteristics by using 3 dB 90 degree couplers. In the case of using ideal coupler; if through and coupled ports are connected to two identical networks, there is no reflection in input port and reflected signals are exactly observed in isolation port with 90° phase shift. This can be explained as given in Figure 3.6 and Figure 3.7.



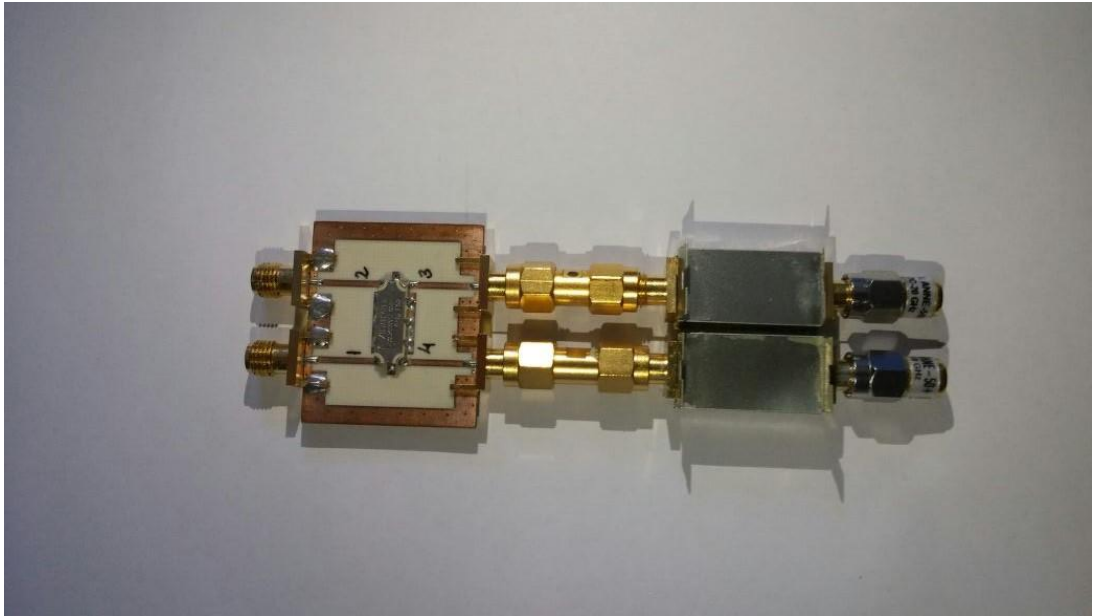
**Figure 3.6:** Explanation of Structure – 1



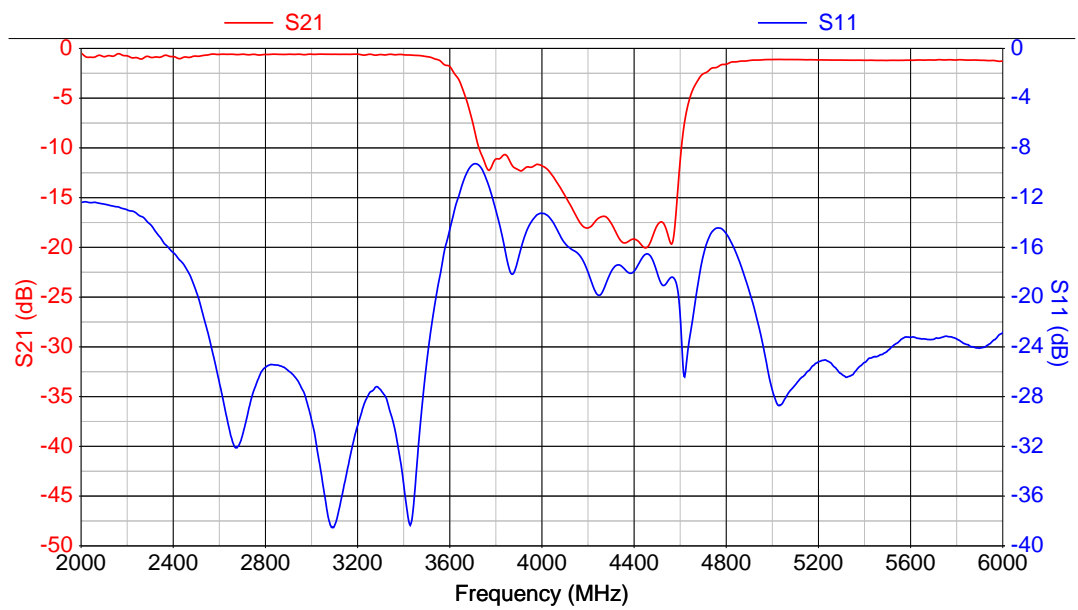
**Figure 3.7:** Explanation of Structure – 2

In the light of these figures, return loss of a single one port network becomes insertion loss of whole network. Therefore, to obtain good pass band characteristics, full reflection is required in one port network. On the other hand, for good suppression in stop band, good matching in that band of one port network is needed. As a result of these, to obtain low-pass absorptive filter with this method, terminated high-pass filters should be used and vice versa. Similarly, using terminated bandpass filters in these structures leads absorptive bandstop filters and vice versa.

An absorptive bandstop filter is constructed by using this method. For this purpose, a 3 dB 90° coupler of Anaren® Company, XMC2560E-03, and two bandpass interdigital filters are used (Appendix B). In addition to these components, ANNE-50+ 50Ω loads, Mini-Circuits® Company product, are used to terminate filters (Appendix C). Constructed absorptive filter is given in Figure 3.8 and its measurement result is given Figure 3.9.



**Figure 3.8:** Implemented Absorptive Filter



**Figure 3.9:** Measurement Result of Implemented Filter

To obtain good results in this topology terminated filters at through and coupled ports must be as identical as possible. Since operation band of this type is limited with the 3 dB 90° coupler performance, coupler should be chosen as wide band as possible. To improve absorptiveness property of this type of filters, phase errors and amplitude balance properties should also be taken into account.

## CHAPTER 4

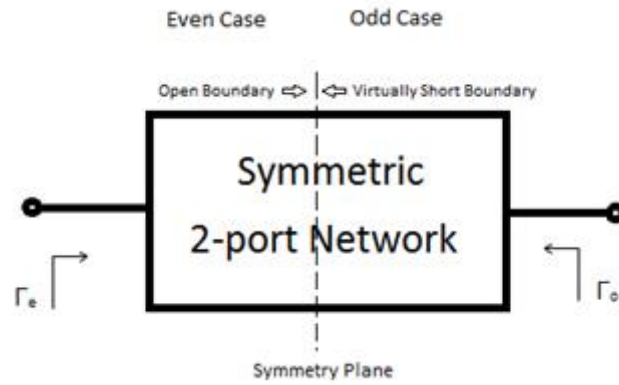
### REFLECTIONLESS FILTERS

#### 4.1 Introduction

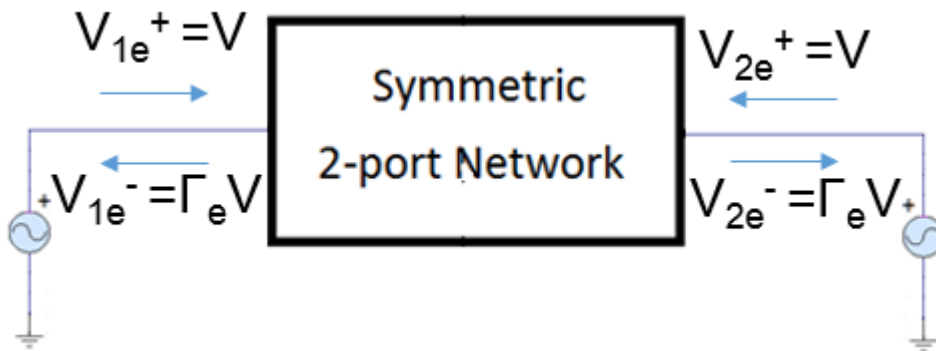
In this chapter, a different approach to absorptive filters, Matthew Morgan's Reflectionless Filter Topology, is examined [7]. Theory, design procedure, realization and measurement results of manufactured filters are given in this chapter

#### 4.2 Theory

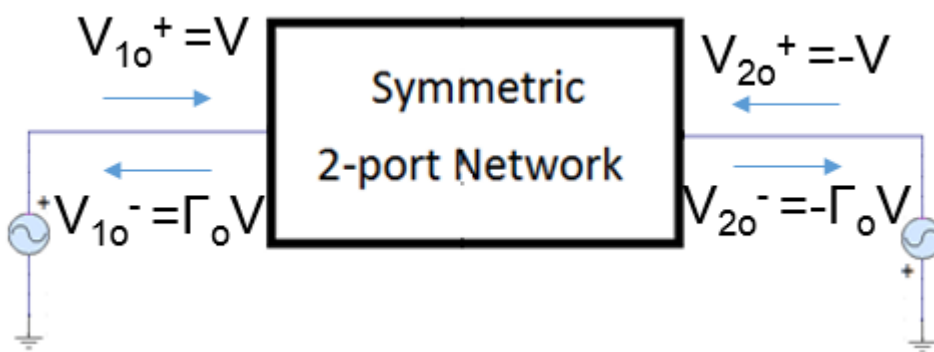
Main idea behind the Matthew Morgan's reflectionless filter can be derived using Even-/Odd-Mode Analysis (Bartlett's Bisection Theorem). In order to use this analysis, a symmetrical network is needed. For even-mode case, ports are driven with exactly same sources. In this case, there is no current crossing through the symmetry plane in which the symmetry plane can be assumed as open boundary. On the other hand, if the sources are equal in magnitude but they are  $180^\circ$  out-of-phase, nodes on symmetry plane become having zero potential with respect to ground. This is called odd-mode. For odd-mode case, symmetry plane becomes virtually short boundary. General characteristics of full network can be obtained by using superposition which helps to obtain the S-parameters.



**Figure 4.1:** Symmetric Two Port Network



**Figure 4.2:** Even Mode Case for Symmetric Two Port Network



**Figure 4.3:** Odd Mode Case for Symmetric Two Port Network

After superposition, incident and reflected voltages can be derived as,

$$V_1^+ = V_{1e}^+ + V_{1o}^+ = 2V \quad (4.1)$$

$$V_2^+ = V_{2e}^+ + V_{2o}^+ = 0 \quad (4.2)$$

$$V_1^- = V_{1e}^- + V_{1o}^- = (\Gamma_e + \Gamma_o)V \quad (4.3)$$

$$V_2^- = V_{2e}^- + V_{2o}^- = (\Gamma_e - \Gamma_o)V \quad (4.4)$$

S-parameters of whole two port network can be obtained by using the relations of superposed incident and reflected voltages given in equation 4.1, 4.2, 4.3 and 4.4.

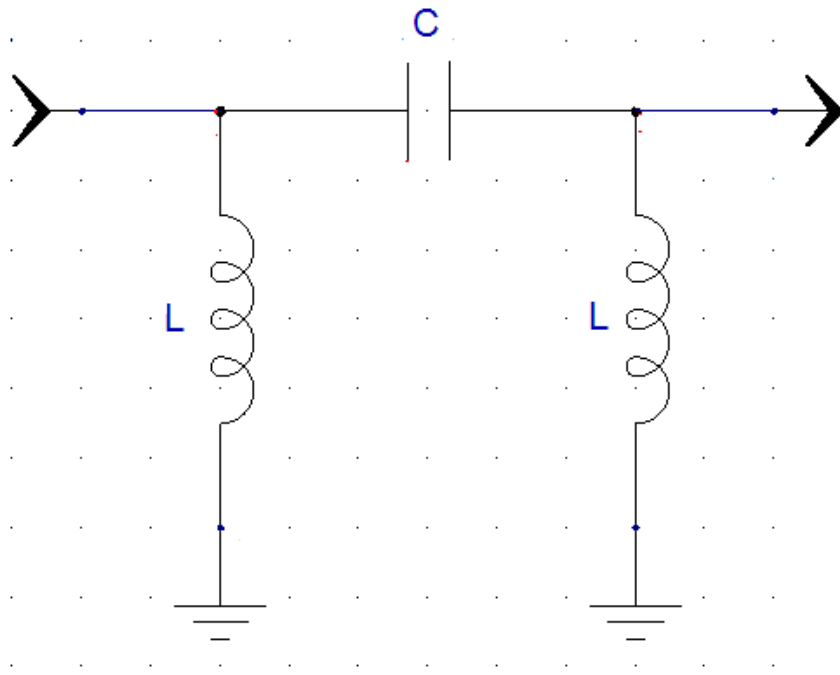
$$S_{11} = \frac{\Gamma_e + \Gamma_o}{2} \quad (4.5)$$

$$S_{21} = \frac{\Gamma_e - \Gamma_o}{2} \quad (4.6)$$

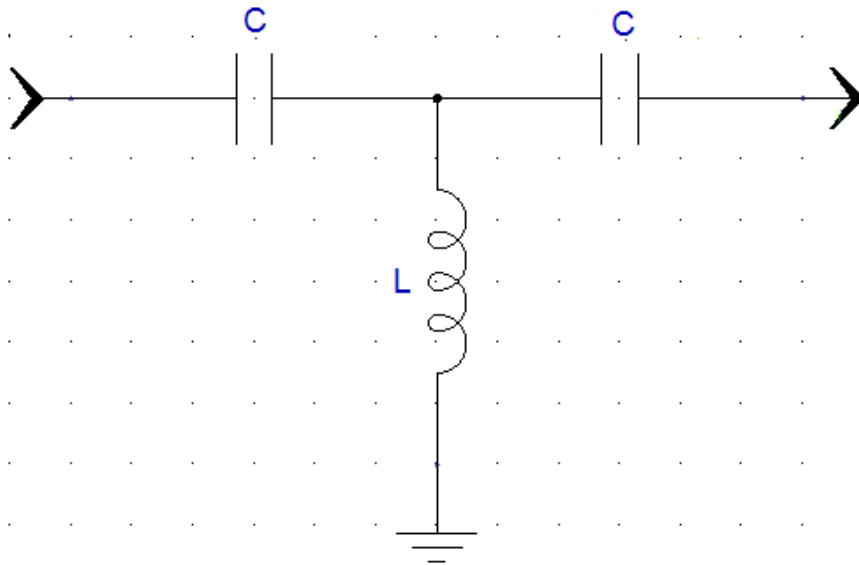
$\Gamma_o$  and  $\Gamma_e$  parameters used in equation 4.3, 4.4, 4.5 and 4.6 are the reflection coefficients of even and odd mode equivalent circuits. In the light of this result, if the even-mode and odd-mode reflection coefficients have same magnitude and  $180^\circ$  phase difference between them, the network is reflectionless ( $S_{11}=0$ ). In this case, resultant  $S_{21}$  is equal to  $\Gamma_e$ .

To better understand how a reflectionless filter is synthesized, low-pass reflectionless filter topology is considered at first. Since the transmission coefficient of reflectionless network equals to the reflection coefficient of odd-mode, high-pass filter topology should be used as even and odd-mode equivalent circuits.

Two dual third order high-pass filters having same normalized element values are given in Figure 4.4 and Figure 4.5.



**Figure 4.4:** High-Pass Filter Type-1



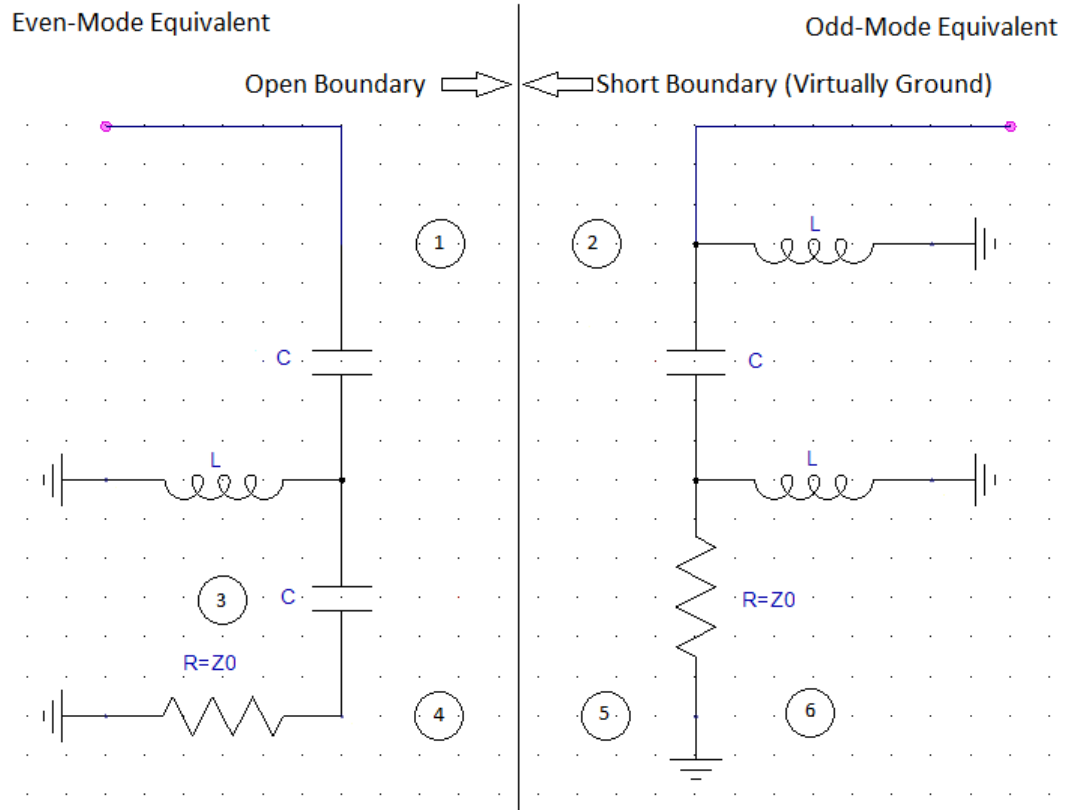
**Figure 4.5:** High-Pass Filter Type-2

If two filters are terminated with a resistor having impedance  $Z_0$ , it can be observed that responses of both one-port networks are equal in magnitude and they are  $180^\circ$  out of phase. Therefore, if odd mode equivalent of a two port network



is one of the given types and even mode equivalent is the other one, a reflectionless network which has low-pass response can be obtained.

Synthesis of low-pass reflectionless filter from these two one port networks is explained in Figure 4.6 step by step.



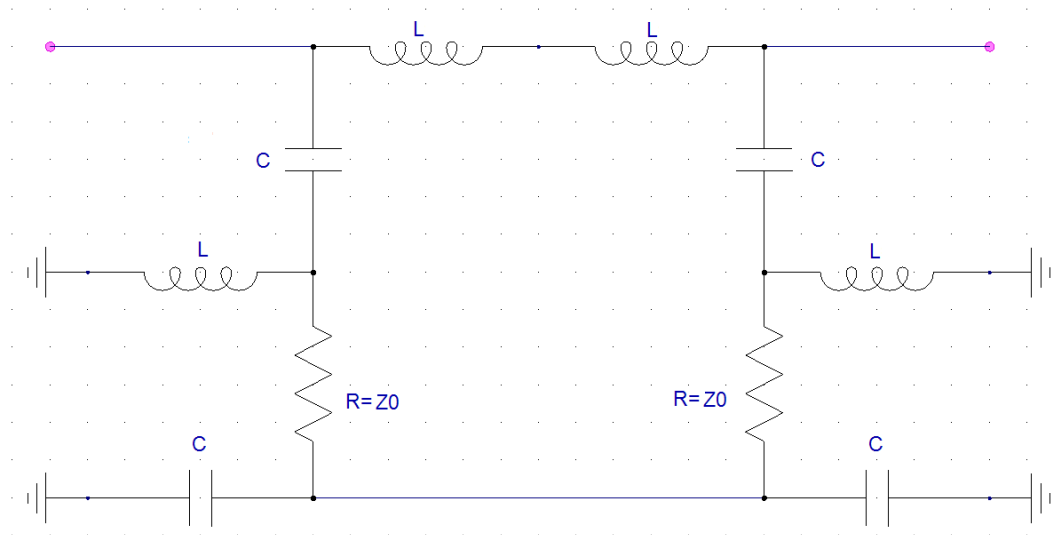
**Figure 4.6:** Derivation of Reflectionless Filter from Dual High-Pass Filters

### Steps

1. Since the symmetry plane of a symmetric two-port network is an open boundary for even mode, an inductor can be connected between input of the even-mode equivalent circuit and symmetry plane.
2. First shunt inductor at the input of the odd-mode equivalent can be connected through symmetry plane since it is virtually ground in this case.
3. Capacitor and resistor given in point 3 can be interchanged since they are connected in series.

4. Similarly, since the symmetry plane is an open boundary for even-mode equivalent case, there can be a connection between symmetry plane and circuit at point 4.
5. Since symmetry plane is virtually ground for odd-mode equivalent case, ground can be connected to symmetry plane at point 5 and ground can be omitted.
6. Since a capacitor between two grounded nodes has no effect, a shunt capacitor can be added at point 6.

Finalized two-port symmetrical network after all of these steps is given in the Figure 4.7.



**Figure 4.7:** Reflectionless Low-Pass Filters

To ensure duality property of even and odd-mode equivalent circuits, inductance value should be selected as  $L = Z_0^2 C$ . Under this condition, transmission characteristics of this two port network can be derived by using basic lumped element circuit analysis. Input impedance of even-mode equivalent circuit can be found as follows:

$$Z_{in,e} = \frac{1}{j\omega C} + (j\omega Z_0^2 C) // (\frac{1}{j\omega C} + Z_0) \quad (4.7)$$

$$Z_{in,e} = \frac{2Z_0^2 - \frac{1}{\omega^2 C^2} + j\omega Z_0^3 C - j\frac{Z_0}{\omega C}}{Z_0 + j\omega Z_0^2 C - j\frac{1}{\omega C}} \quad (4.8)$$

Since odd-mode equivalent circuit is dual of the even-mode equivalent circuit;

$$Z_{in,o} = Z_{in,e}^* \quad (4.9)$$

$$Z_{in,o} = \frac{2Z_0^2 - \frac{1}{\omega^2 C^2} - j\omega Z_0^3 C + j\frac{Z_0}{\omega C}}{Z_0 - j\omega Z_0^2 C + j\frac{1}{\omega C}} \quad (4.10)$$

As it is mentioned before, two port network's  $S_{21}$  parameter is equal to  $\Gamma_e$ . Return loss of odd-mode equivalent circuit is:

$$\Gamma_e = \frac{Z_{in,e} - Z_0}{Z_{in,e} + Z_0} \quad (4.11)$$

$$S_{21} = \Gamma_e = \frac{Z_0^2 - \frac{1}{\omega^2 C^2}}{3Z_0^2 - \frac{1}{\omega^2 C^2} + j2\omega Z_0^3 C - j\frac{2Z_0}{\omega C}} \quad (4.12)$$

It is seen that a transmission zero occurs in  $S_{21}$  characteristics at  $\omega_{tz}$  and it can be found by using Equation 4.12 as;

$$\omega_{tz} = \frac{1}{Z_0 C} \quad (4.13)$$

Angular transmission zero frequency,  $\omega_{tz}$ , is very critical parameter for transmission characteristics of reflectionless low-pass filter. When  $S_{21} = \Gamma_e$  relation is normalized with  $\omega_{tz}$  by inserting  $\omega = \omega_{tz} \omega'$ , the following relation is obtained.

$$S_{21} = \Gamma_e = \frac{1 - \frac{1}{\omega'^2}}{3 - \frac{1}{\omega'^2} + j2\omega' - j\frac{2}{\omega'}} \quad (4.14)$$

It is seen that  $S_{21}$  only depends on  $\omega_{tz}$ . Therefore,  $\omega_{tz}$  is chosen as the design parameter in this thesis. If any cut-off frequencies such as -1 dB cut-off frequency or -3 dB cut-off frequency is critical for an application, the relation between this cut-off frequency and transmission zero frequency can be found by using equation 4.14. For example, the relation between transmission zero frequency and -1 dB cut-off frequency can be found by equating the magnitude of equation 4.14 with -1 in logarithmic scale.

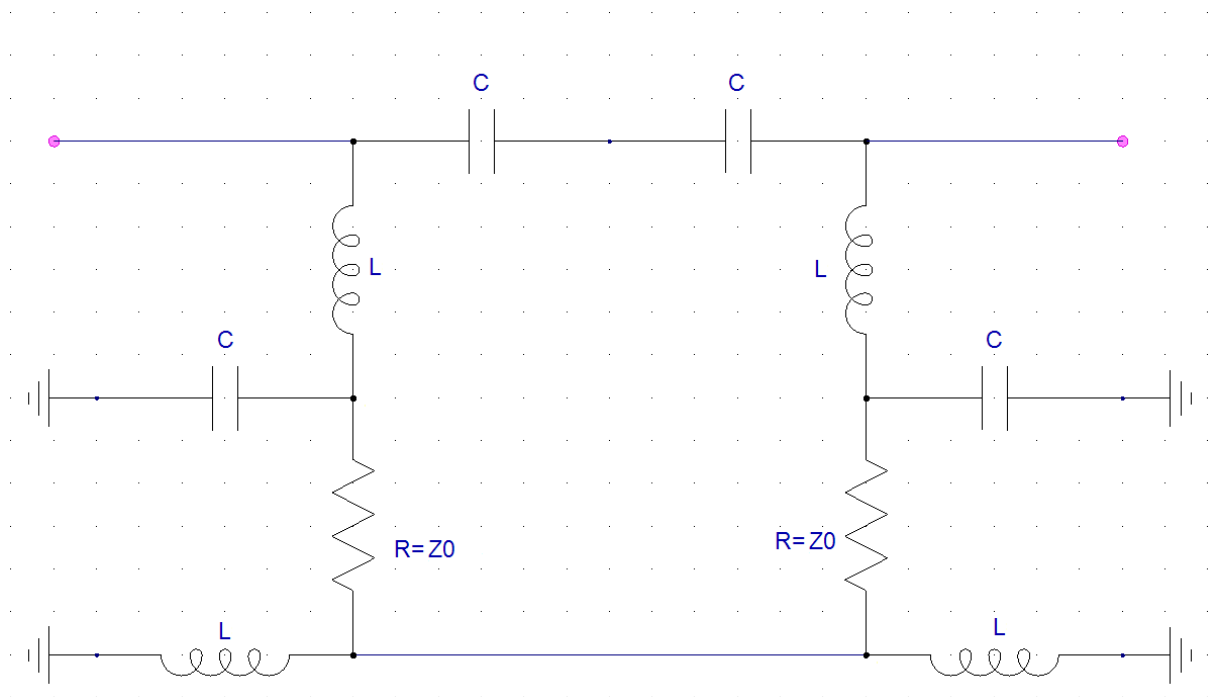
$$20 \log \left| \frac{1 - \frac{1}{\omega'^2}}{3 - \frac{1}{\omega'^2} + j2\omega' - j\frac{2}{\omega'}} \right| = -1 \quad (4.15)$$

Equation 4.15 has 2 real roots at  $\omega' = \pm 0.5592$ . This result shows the relation between transmission zero frequency. Similar relations can be found easily for -0.01 dB, -0.1 dB -0.5 dB and -3 dB. All results are given in Table 4.1.

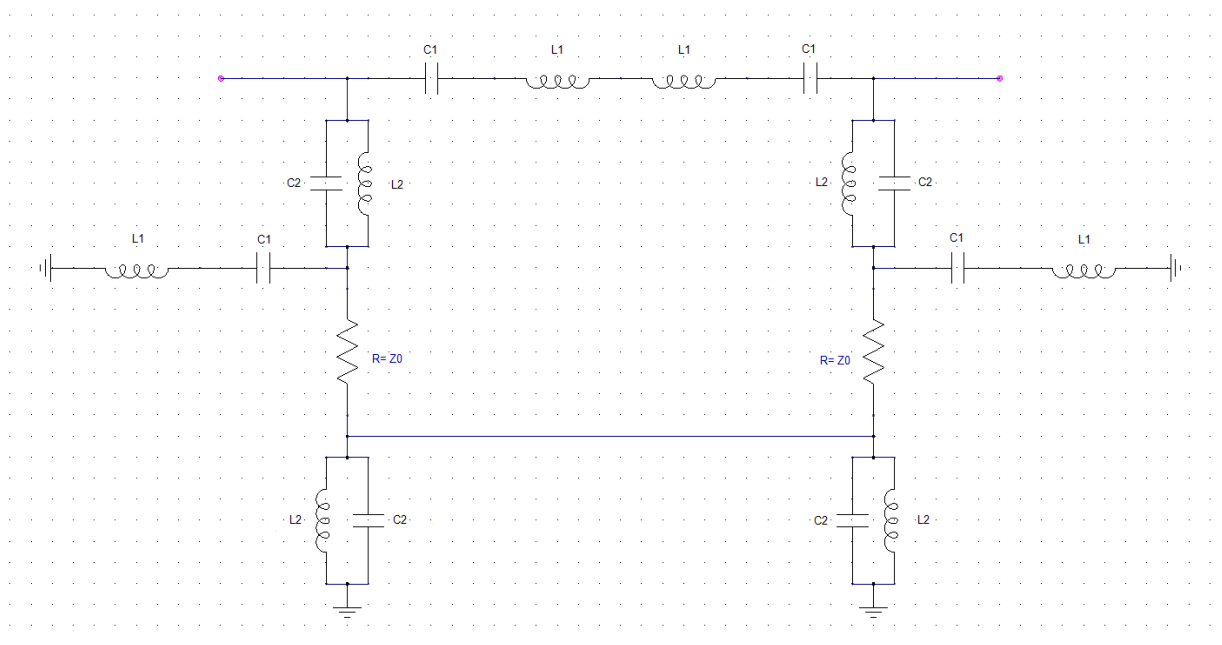
**Table 4.1** Relation Between  $f_c$  and  $f_{tz}$

$S_{21}$ at $f_c$	$f_c/f_{tz}$
-0.01	0.280691
-0.1	0.400186
-0.5	0.506405
-1	0.5592
-3	0.656953

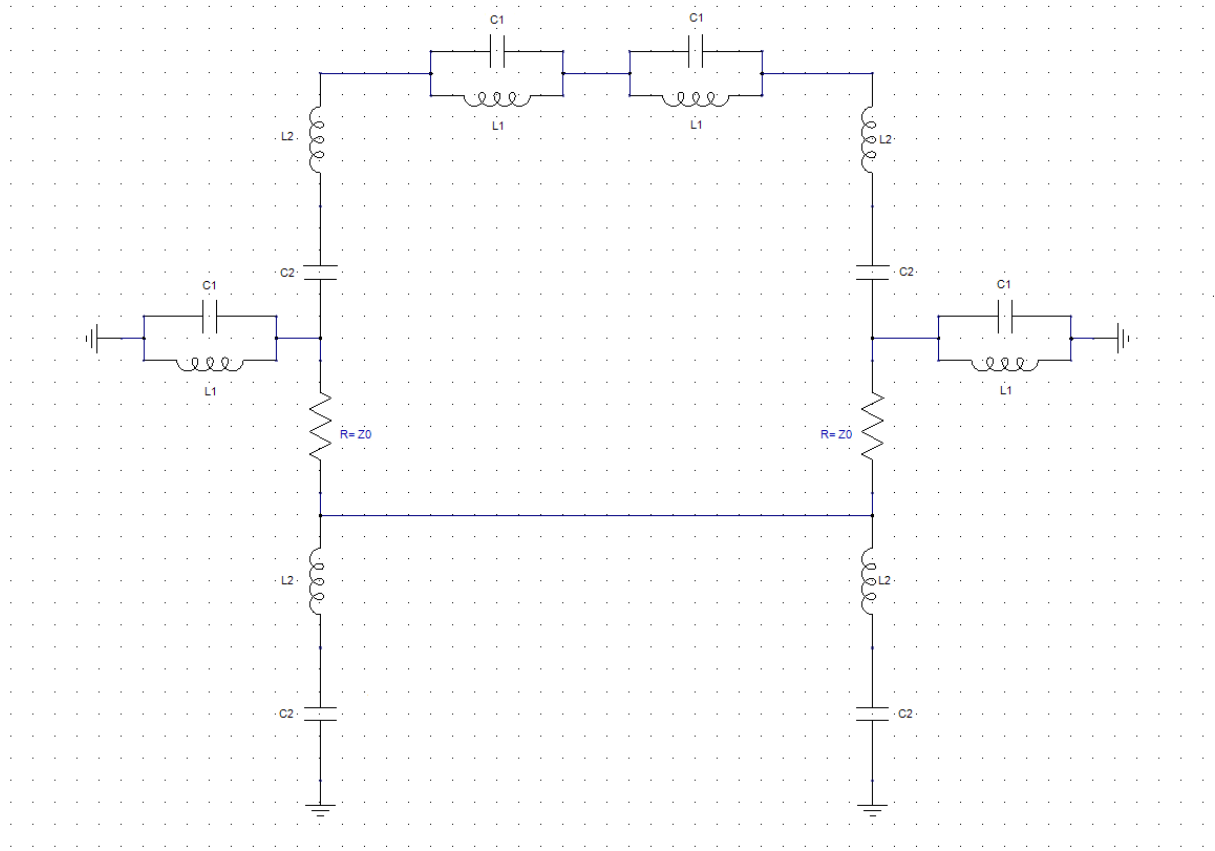
High-pass, bandpass and bandstop reflectionless filter structures can be developed and transmission zero relations can be found by following same procedure of low-pass reflectionless filter derivation. Generalized form of high-pass, bandpass and bandstop reflectionless filters are given in Figure 4.8, Figure 4.9 and Figure 4.10.



**Figure 4.8:** Reflectionless High-Pass Filters



**Figure 4.9:** Reflectionless Bandpass Filters



**Figure 4.10:** Reflectionless Bandstop Filters

When same approach is used to obtain transfer characteristics of high-pass reflectionless filter, it is seen that a transmission zero occurs in stop band and it can be found by using Equation 4.13 which is same as low-pass reflectionless filter. On the other hand, two transmission-zeroes occur for bandpass and bandstop filters. To understand the relation between those transmission zeroes and inductance-capacitance values for bandpass and bandstop filters, filter transformations can be used.

To use filter transformations, similar method given in reference books which is scaling a given low-pass prototype element value in terms of source resistance and cut-off frequency is followed. However, transmission-zero frequencies are used in scaling for these transformations instead of cut-off frequencies for the sake of simplicity.

Low-pass prototype normalized values are obtained from high-pass reflectionless filter inductance and capacitance values since its even/odd-mode

equivalent circuit has low-pass structure. When impedance scaling is applied to inductance value  $L$  and capacitance value  $C$ ; normalized inductance and capacitance values  $L'$  and  $C'$  are obtained as:

$$L' = \frac{L}{Z_0} \quad (4.16)$$

$$C' = Z_0 C \quad (4.17)$$

For frequency scaling, reactance value of series  $L$  and susceptance value of shunt  $C$  is considered:

$$\omega \longrightarrow \omega' = \frac{\omega}{\omega_{tz}} \quad (4.18)$$

$$j\omega L' = j\left(\frac{\omega}{\omega_{tz}}\right)\omega_{tz}L' \longrightarrow j\omega' L'' \quad (4.19)$$

$$L'' = \omega_{tz} L' \quad (4.20)$$

$$j\omega C' = j\left(\frac{\omega}{\omega_{tz}}\right)\omega_{tz}C' \longrightarrow j\omega' C'' \quad (4.21)$$

$$C'' = \omega_{tz} C' \quad (4.22)$$

By using Equation 4.13 capacitance and inductance values can be found as:

$$C = \frac{1}{Z_0 \omega_{tz}} \quad (4.23)$$

$$L = \frac{Z_0}{\omega_{tz}} \quad (4.24)$$

After all of these equations, it is seen that normalized values  $L''$  and  $C''$  are unity when normalization is made by using transmission-zero frequency.

For low-pass to high-pass transformation, following process applied:

$$\omega \longrightarrow \omega' = -\frac{\omega_{tz}}{\omega} \quad (4.25)$$

Reactance for series connection becomes,

$$j\omega L' \longrightarrow j\omega' L' = -j \frac{\omega_{tz}}{\omega} L' = \frac{1}{j\omega(\frac{1}{\omega_{tz} L'})} = \frac{1}{j\omega C'_{HP}} \quad (4.26)$$

Susceptance for shunt connection becomes,

$$j\omega C' \longrightarrow j\omega' C' = -j \frac{\omega_{tz}}{\omega} C' = \frac{1}{j\omega(\frac{1}{\omega_{tz} C'})} = \frac{1}{j\omega L'_{HP}} \quad (4.27)$$

When impedance de-normalization applied:

$$C_{HP} = \frac{1}{Z_0 \omega_{tz}} \quad (4.28)$$

$$L_{HP} = \frac{Z_0}{\omega_{tz}} \quad (4.29)$$

Results obtained in equations 4.28 and 4.29 show that the relation between transmission-zero frequency and inductance and capacitance values are same for low-pass and high-pass which is also mentioned before.

Similar transformation can also be used for bandpass and bandstop filters. Since bandpass and bandstop filters have 2 transmission-zeroes, following transformation process should be applied for bandpass filter:

$$\omega \longrightarrow \omega' = \frac{\omega_0}{\omega_{tz,2} - \omega_{tz,1}} \left( \frac{\omega}{\omega_0} - \frac{\omega_0}{\omega} \right) \quad (4.30)$$

Where  $\omega_{tz,1}$  is lower transmission-zero frequency,  $\omega_{tz,2}$  is upper transmission-zero frequency and  $\omega_0$ :

$$\omega_0 = \sqrt{\omega_{tz,2} \omega_{tz,1}} \quad (4.31)$$

For series arm:



$$j\omega L' \longrightarrow j\omega' L' = jL' \frac{\omega_0}{\omega_{t_z,2} - \omega_{t_z,1}} \left( \frac{\omega}{\omega_0} - \frac{\omega_0}{\omega} \right) = j\omega \frac{L'}{\omega_{t_z,2} - \omega_{t_z,1}} + \frac{L' \omega_0^2}{j\omega(\omega_{t_z,2} - \omega_{t_z,1})} = j\omega L'_{BP,1} + \frac{1}{j\omega C'_{BP,1}} \quad (4.32)$$

For shunt arm:

$$j\omega C' \longrightarrow j\omega' C' = jC' \frac{\omega_0}{\omega_{t_z,2} - \omega_{t_z,1}} \left( \frac{\omega}{\omega_0} - \frac{\omega_0}{\omega} \right) = j\omega \frac{C'}{\omega_{t_z,2} - \omega_{t_z,1}} + \frac{C' \omega_0^2}{j\omega(\omega_{t_z,2} - \omega_{t_z,1})} = j\omega L'_{BP,2} + \frac{1}{j\omega C'_{BP,2}} \quad (4.33)$$

When impedance de-normalization is applied:

$$C_{BP,1} = \frac{\omega_{t_z,2} - \omega_{t_z,1}}{Z_0 \omega_{t_z,1} \omega_{t_z,2}} \quad (4.34)$$

$$L_{BP,1} = \frac{Z_0}{\omega_{t_z,2} - \omega_{t_z,1}} \quad (4.35)$$

$$C_{BP,2} = \frac{1}{Z_0 (\omega_{t_z,2} - \omega_{t_z,1})} \quad (4.36)$$

$$L_{BP,2} = \frac{Z_0 (\omega_{t_z,2} - \omega_{t_z,1})}{\omega_{t_z,1} \omega_{t_z,2}} \quad (4.37)$$

Similarly, for bandstop filters:

$$\omega \longrightarrow \omega' = \frac{\omega_{t_z,2} - \omega_{t_z,1}}{\omega_0} \left( \frac{\omega}{\omega_0} - \frac{\omega_0}{\omega} \right)^{-1} \quad (4.38)$$

$$j\omega L' \longrightarrow j\omega' L' = jL' \frac{\omega_{t_z,2} - \omega_{t_z,1}}{\omega_0} \left( \frac{\omega}{\omega_0} - \frac{\omega_0}{\omega} \right)^{-1} = (j\omega C'_{BS,1} + \frac{1}{j\omega L'_{BS,1}})^{-1} \quad (4.39)$$

$$j\omega C' \longrightarrow j\omega' C' = jC' \frac{\omega_{t_z,2} - \omega_{t_z,1}}{\omega_0} \left( \frac{\omega}{\omega_0} - \frac{\omega_0}{\omega} \right)^{-1} = (j\omega L'_{BS,2} + \frac{1}{j\omega C'_{BS,2}})^{-1} \quad (4.40)$$

Thus;

$$C_{BS,1} = \frac{1}{Z_0(\omega_{tz,2} - \omega_{tz,1})} \quad (4.41)$$

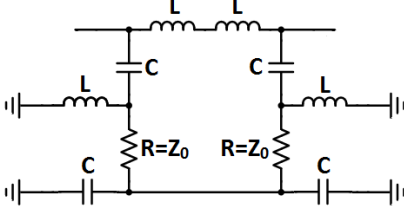

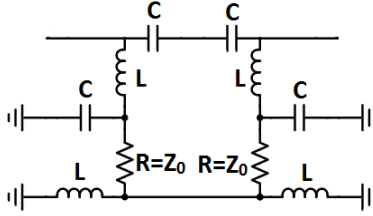

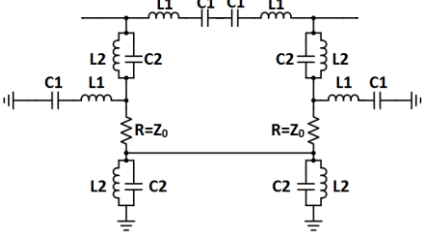

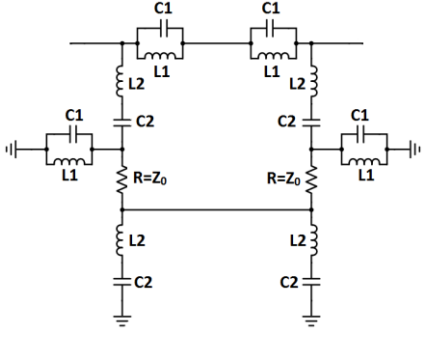
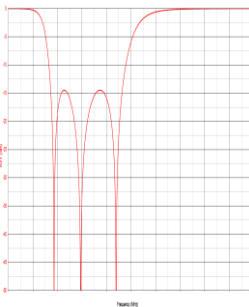
$$L_{BS,1} = \frac{Z_0(\omega_{tz,2} - \omega_{tz,1})}{\omega_{tz,1}\omega_{tz,2}} \quad (4.42)$$

$$C_{BS,2} = \frac{(\omega_{tz,2} - \omega_{tz,1})}{Z_0\omega_{tz,2}\omega_{tz,1}} \quad (4.43)$$

$$L_{BS,2} = \frac{Z_0}{\omega_{tz,2} - \omega_{tz,1}} \quad (4.44)$$

The reason why all of these derivations are made is to understand the relation between transmission zeroes and inductance and capacitance values. All results are given in the following Table.

**Table 4.2** Summary of Basic Reflectionless Filter Structures

Reflectionless Filter Type	Filter Schematic	Filter $S_{21}$ Response	Element Values
Low-Pass			$C = \frac{1}{Z_0 \omega_{tz}}$ $L = \frac{Z_0}{\omega_{tz}}$
High-Pass			$C = \frac{1}{Z_0 \omega_{tz}}$ $L = \frac{Z_0}{\omega_{tz}}$
Bandpass			$L_1 = \frac{Z_0}{\omega_{tz,2} - \omega_{tz,1}}$ $C_1 = \frac{(\omega_{tz,2} - \omega_{tz,1})}{Z_0 \omega_{tz,2} \omega_{tz,1}}$ $C_2 = \frac{1}{Z_0 (\omega_{tz,2} - \omega_{tz,1})}$ $L_2 = \frac{Z_0 (\omega_{tz,2} - \omega_{tz,1})}{\omega_{tz,1} \omega_{tz,2}}$
Bandstop			$L_1 = \frac{Z_0 (\omega_{tz,2} - \omega_{tz,1})}{\omega_{tz,1} \omega_{tz,2}}$ $C_1 = \frac{1}{Z_0 (\omega_{tz,2} - \omega_{tz,1})}$ $L_2 = \frac{Z_0}{\omega_{tz,2} - \omega_{tz,1}}$ $C_2 = \frac{\omega_{tz,2} - \omega_{tz,1}}{Z_0 \omega_{tz,1} \omega_{tz,2}}$

### 4.3 Design

In previous part, theoretical explanation of Matthew Morgan's reflectionless structures and its characteristics are given. In design procedure, the results obtained in previous part are used during creating schematics and determining transmission zero frequencies.

Several filters are designed with different transfer characteristics and cut-off frequencies. All designs are simulated by using GENESYS™ by using ideal lumped elements and more realistic elements by importing S-parameter data files of inductors and capacitors. Each type of reflectionless filters is treated in separate sections.

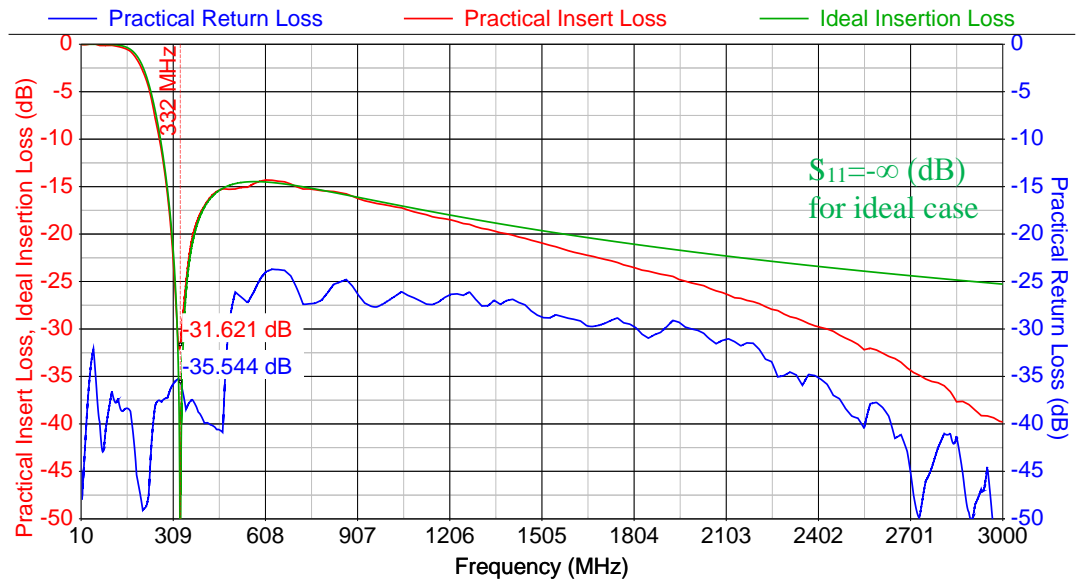
#### 4.3.1 Reflectionless Low-Pass Filter Design

Three different reflectionless low-pass filters are designed with different cut-off frequencies. Simulation results are in good agreement with theoretical explanation given previously.

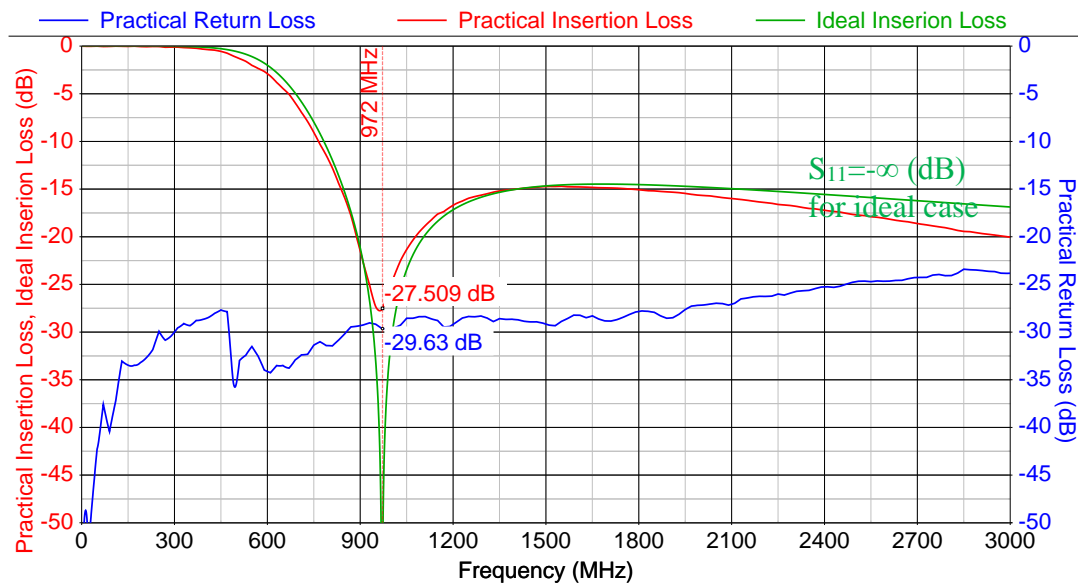
Simulation results of all designs are given below for both ideal and non-ideal inductor and capacitor models. Explanations about them are given Table 4.2.

**Table 4.3** Reflectionless Low-Pass Filter Specifications

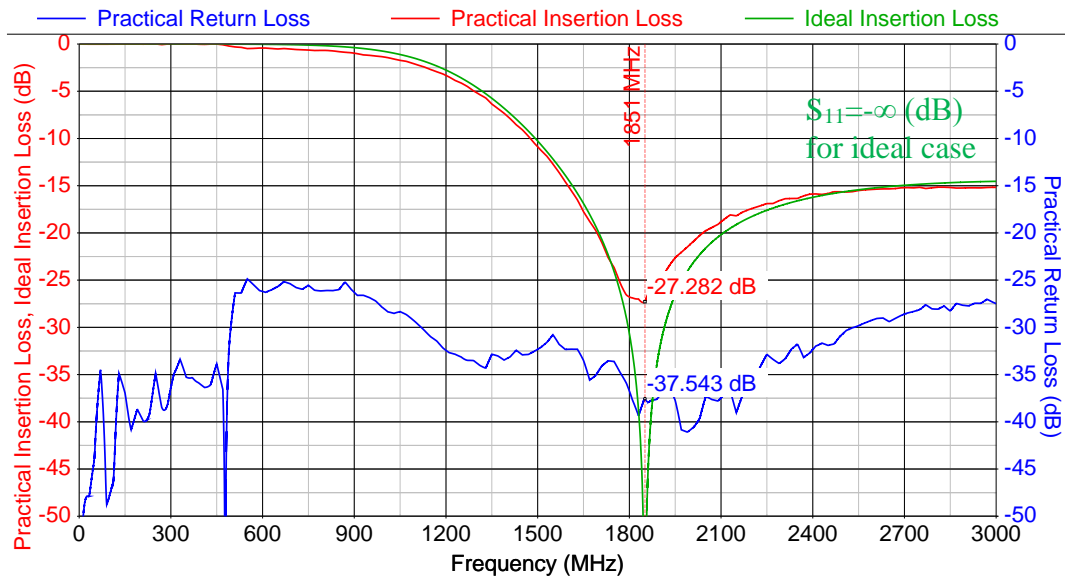
Filter Number	Cut-off Frequency ( $f_c$ )	Transmission Zero Frequency ( $f_{tz}$ )	Inductance	Capacitance
LPF-1	185 MHz	332 MHz	24 nH	9.6 pF
LPF-2	543 MHz	972 MHz	8.2 nH	3.3 pF
LPF-3	1035 MHz	1851 MHz	4.3 nH	1.7 pF



**Figure 4.11:** Simulation Results for Reflectionless Low-Pass Filter-1



**Figure 4.12:** Simulation Results for Reflectionless Low-Pass Filter-2



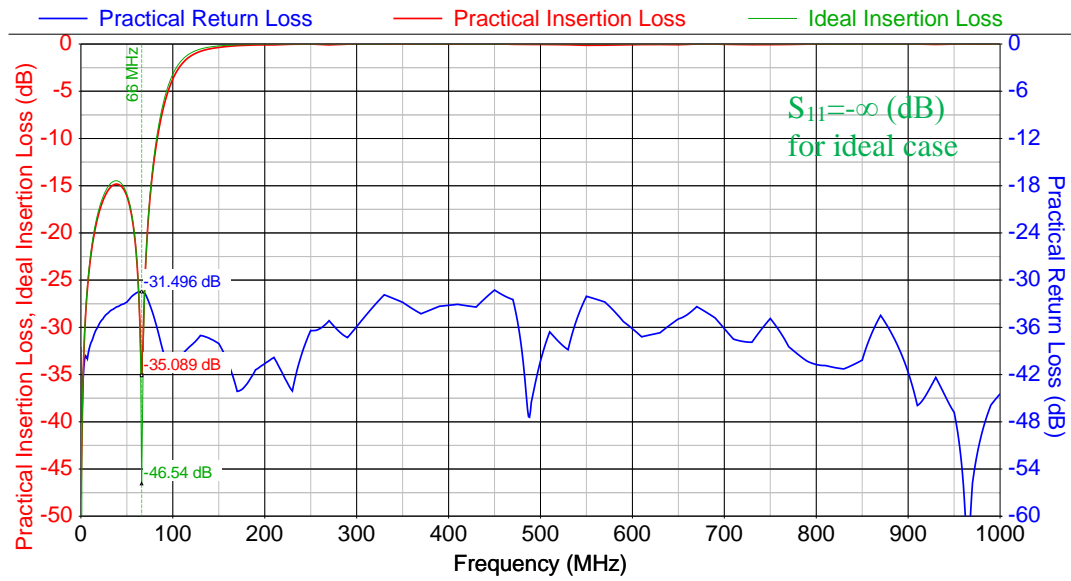
**Figure 4.13:** Simulation Results for Reflectionless Low-Pass Filter-3

#### 4.3.2 Reflectionless High-Pass Filter Design

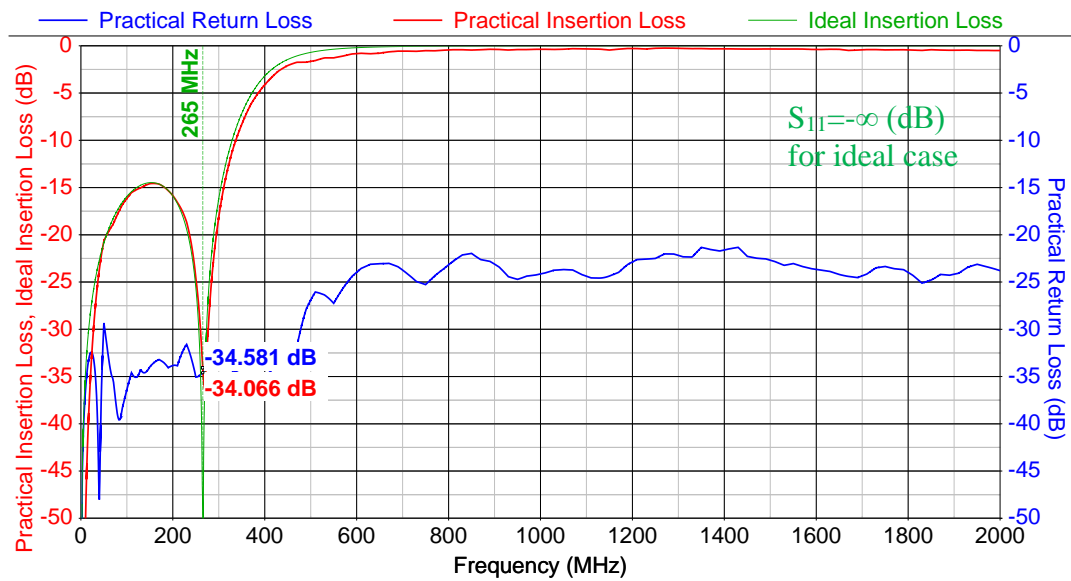
There are four different reflectionless high-pass filter designs with different cut-off frequencies. Simulation results of all designs are given below for both ideal and non-ideal inductor and capacitor models. Explanations about them are given Table 4.3.

**Table 4.4** Reflectionless High-Pass Filter Specifications

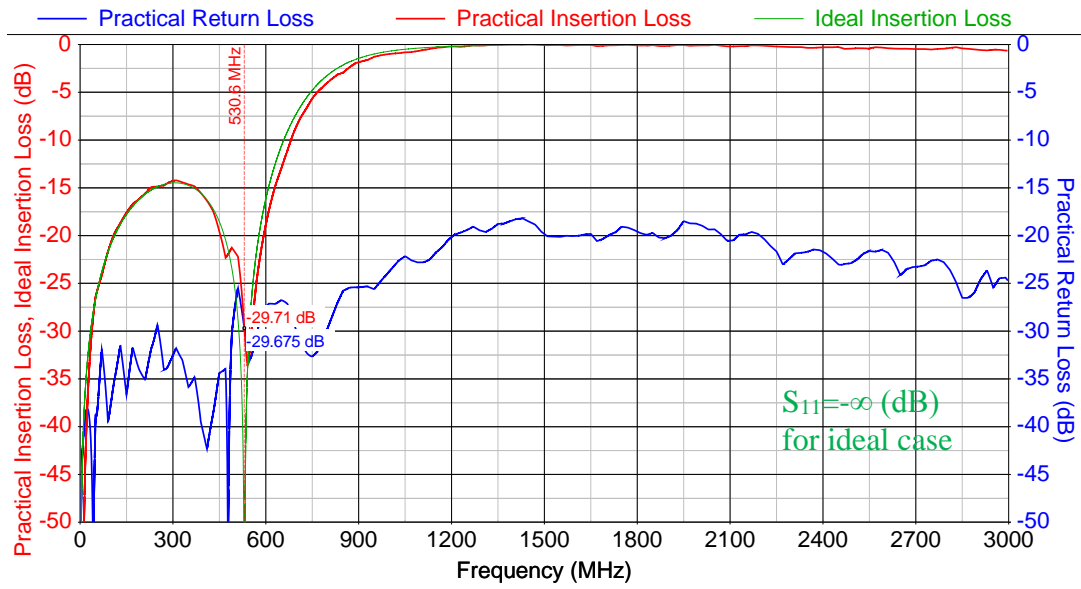
Filter Number	Cut-off Frequency ( $f_c$ )	Transmission Zero Frequency ( $f_{tz}$ )	Inductance	Capacitance
HPF-1	119 MHz	66.3 MHz	120 nH	48 pF
HPF-2	475 MHz	265.25 MHz	30 nH	12 pF
HPF-3	950 MHz	530.5 MHz	15 nH	6 pF
HPF-4	1897 MHz	1061 MHz	7.5 nH	3 pF



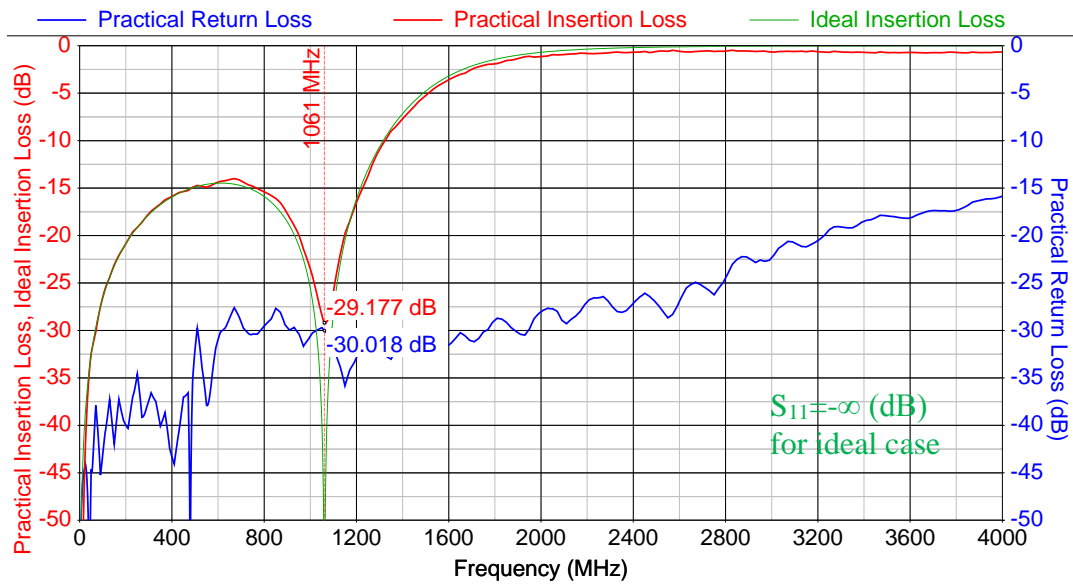
**Figure 4.14:** Simulation Results for Reflectionless High-Pass Filter-1



**Figure 4.15:** Simulation Results for Reflectionless High-Pass Filter-2



**Figure 4.16:** Simulation Results for Reflectionless High-Pass Filter-3



**Figure 4.17:** Simulation Results for Reflectionless High-Pass Filter-4



### 4.3.3 Reflectionless Bandpass Filter Design

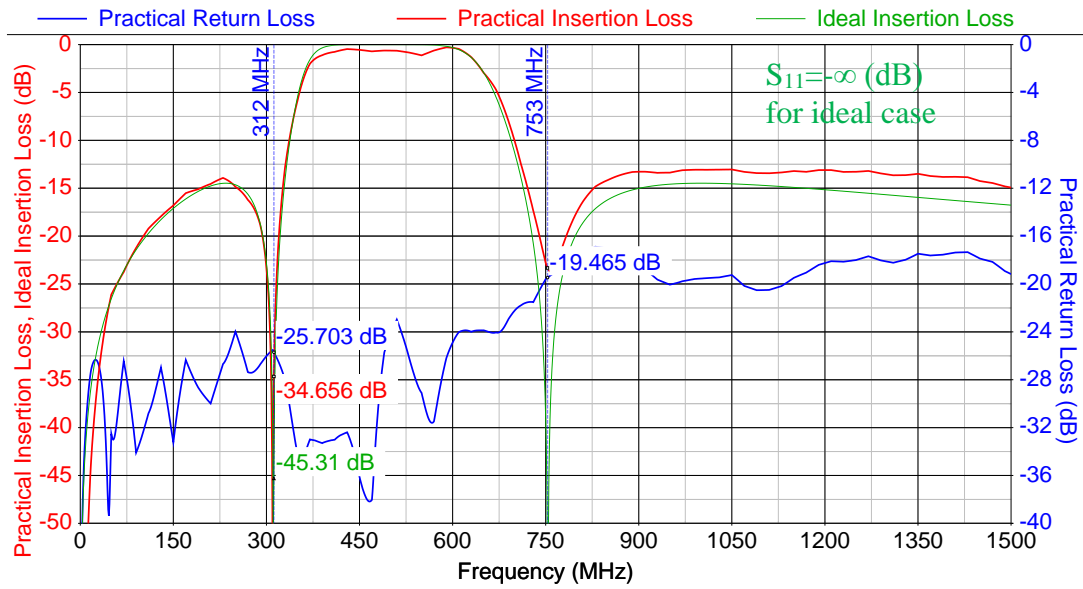
There are four different reflectionless bandpass filter designs with different cut-off frequencies. Simulation results of all designs are given below for both ideal and non-ideal inductor and capacitor models. Explanations about them are given Table 4.4.

**Table 4.5** Reflectionless Bandpass Filter Specifications

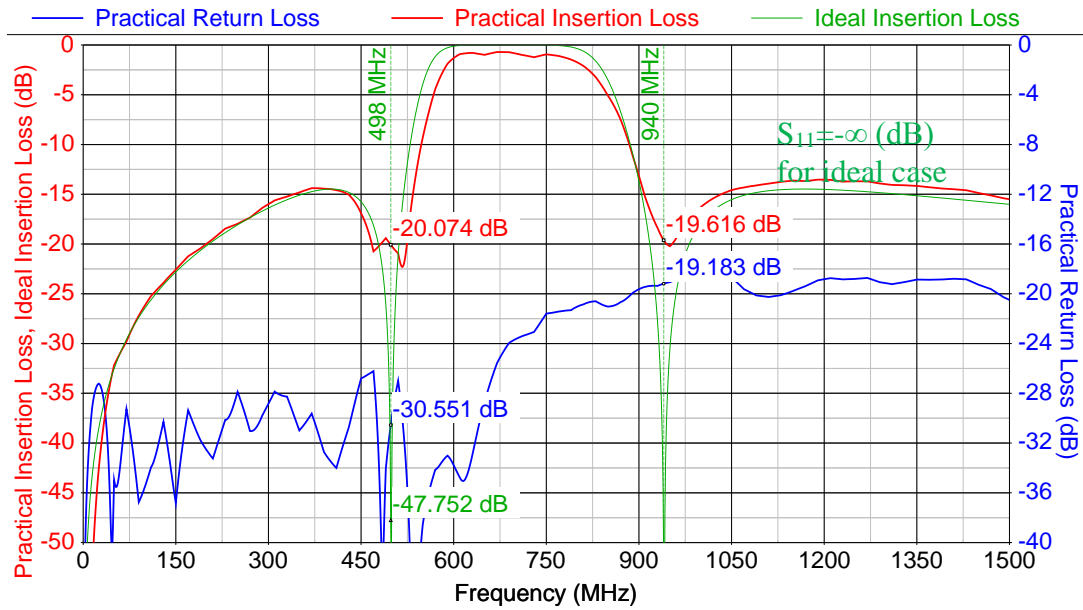
Filter Number	Cut-off Frequencies ( $f_{c1} - f_{c2}$ )	Transmission Zero Frequencies ( $f_{tz1} - f_{tz2}$ )	L1	L2	C1	C2
BPF-1	122-176 MHz	108-202 MHz	82 nH	36 nH	14.4 pF	32.8 pF
BPF-2	376-624 MHz	312-753 MHz	18 nH	15 nH	6 pF	7.2 pF
BPF-3	572-820 MHz	498-940 MHz	18 nH	7.5 nH	3 pF	7.2 pF
BPF-4	8051398 MHz	657-1714 MHz	7.5 nH	7.5 nH	3 pF	3 pF



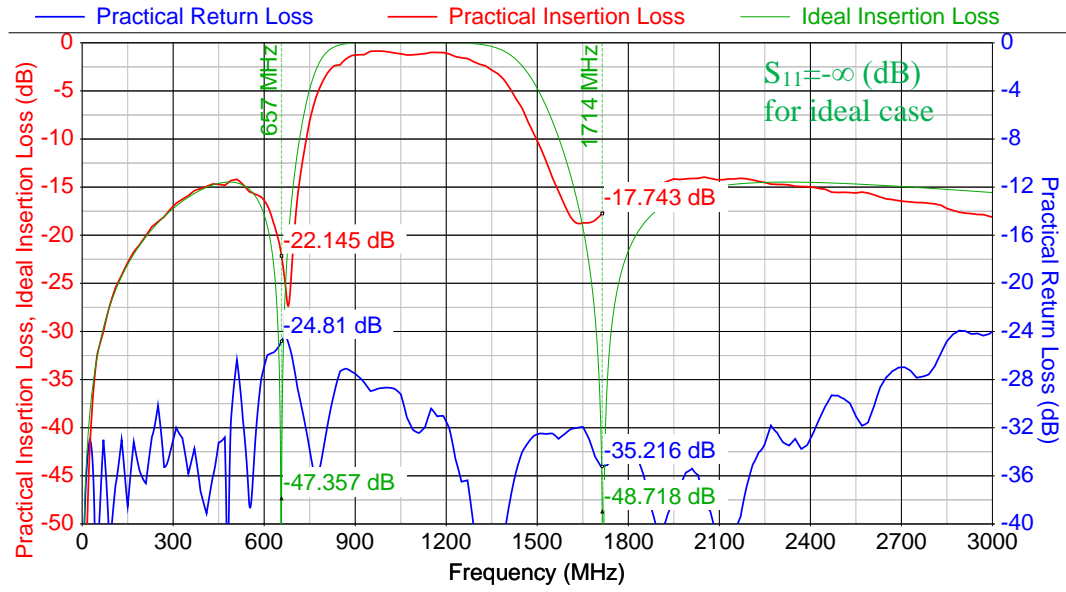
**Figure 4.18:** Simulation Results for Reflectionless Bandpass Filter-1



**Figure 4.19:** Simulation Results for Reflectionless Bandpass Filter-2



**Figure 4.20:** Simulation Results for Reflectionless Bandpass Filter-3



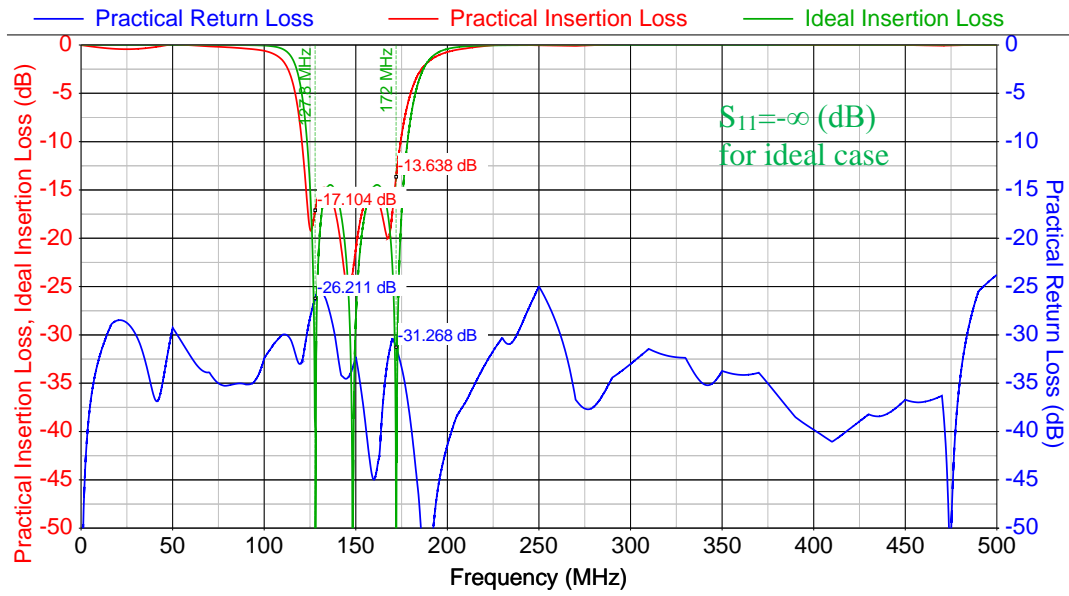
**Figure 4.21:** Simulation Results for Reflectionless Bandpass Filter-4

#### 4.3.4 Reflectionless Bandstop Filter Design

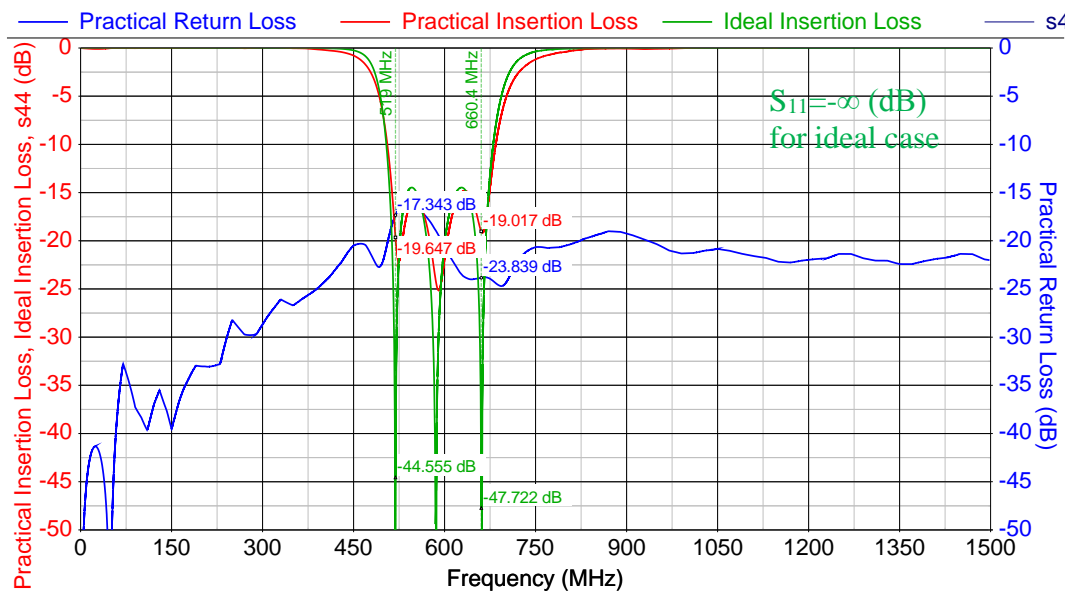
Similarly, there are three different reflectionless bandstop filter designs with different cut-off frequencies. Simulation results of all designs are given below for both ideal and non-ideal inductor and capacitor models. Explanations about them are given Table 4.5.

**Table 4.6** Reflectionless Bandstop Filter Specifications

Filter Number	Cut-off Frequencies ( $f_{c1} - f_{c2}$ )	Transmission Zero Frequencies ( $f_{tz1} - f_{tz2}$ )	L1	L2	C1	C2
BSF-1	114-193.2 MHz	108-202 MHz	16 nH	180 nH	72 pF	6.4 pF
BSF-2	471.8-725.9 MHz	312-753 MHz	3.3 nH	56 nH	22.4 pF	1.32 pF
BSF-3	1127.6-2550.6 MHz	1344.4-2140.5 MHz	2.2 nH	10 nH	4 pF	0.88 pF



**Figure 4.22:** Simulation Results for Reflectionless Bandstop Filter-1



**Figure 4.23:** Simulation Results for Reflectionless Bandstop Filter-2

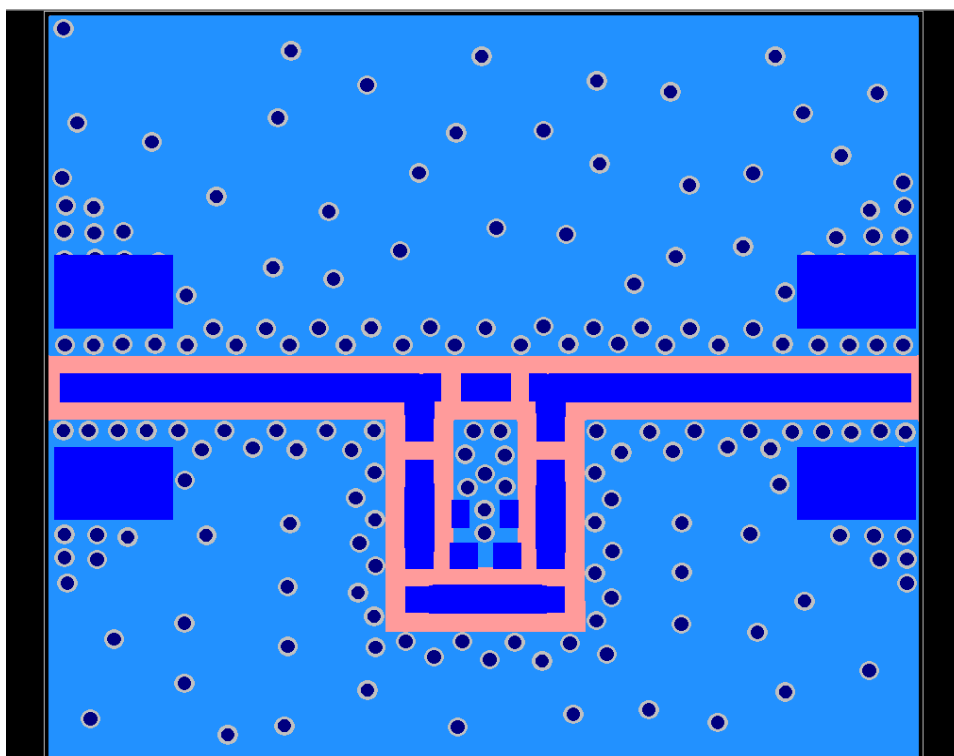


**Figure 4.24:** Simulation Results for Reflectionless Bandstop Filter-3

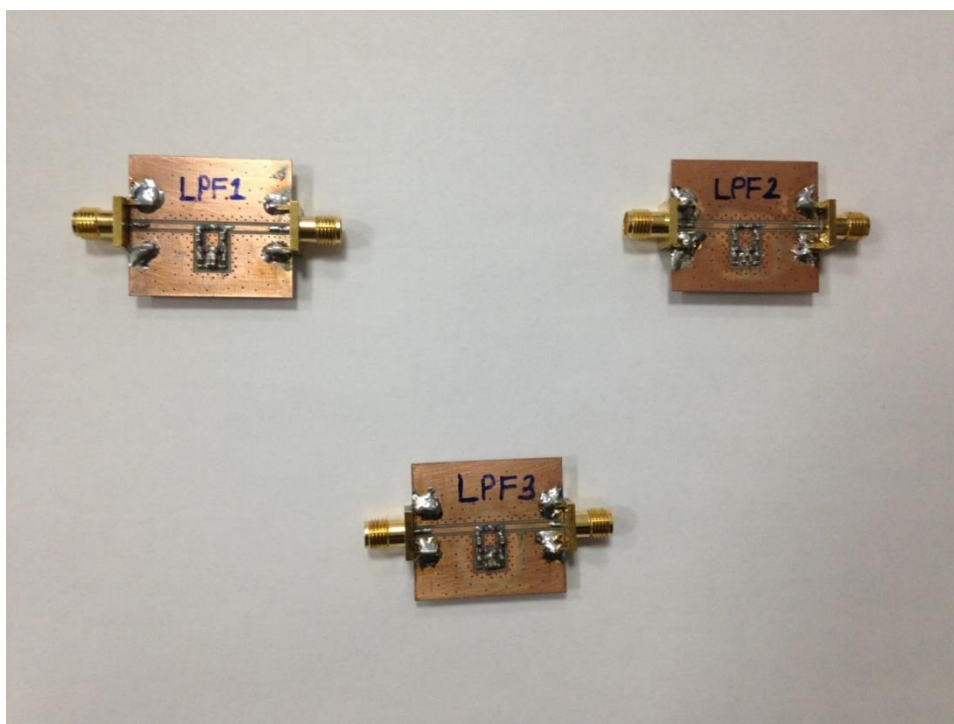
#### 4.4 Realization and Measurement

As it is seen from design part, there is a good agreement between ideal and non-ideal simulations. These filters are realized by using the capacitors and inductors that are used in non-ideal simulations. For this purpose, lay-outs for each type of reflectionless filters are designed. All lay-outs are designed for Rogers 4003C 20 mil substrate(Appendix D). Four reflectionless filter typers are handled in separate sections. Designed layouts, fabricated filters and measurement result of each filter are given in these sections.

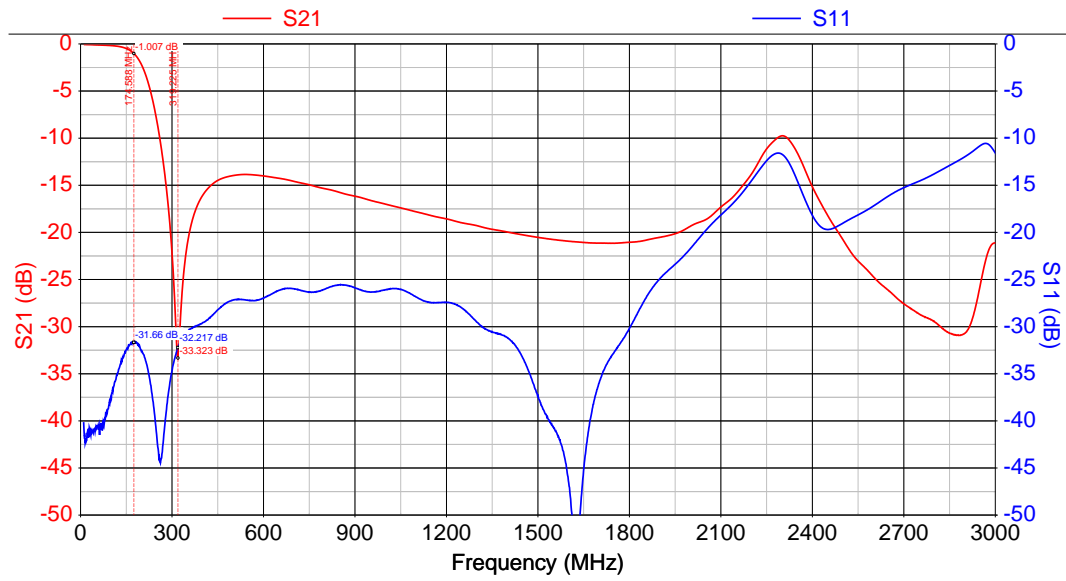
#### 4.4.1 Implemented Reflectionless Low-Pass Filters



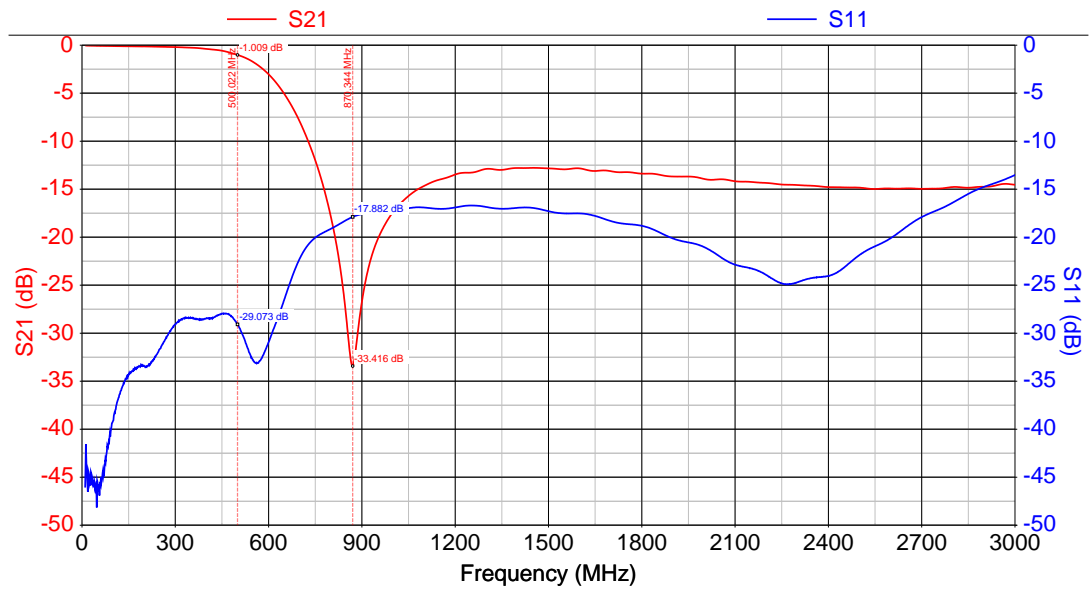
**Figure 4.25:** Lay-out of Reflectionless Low-Pass Filter



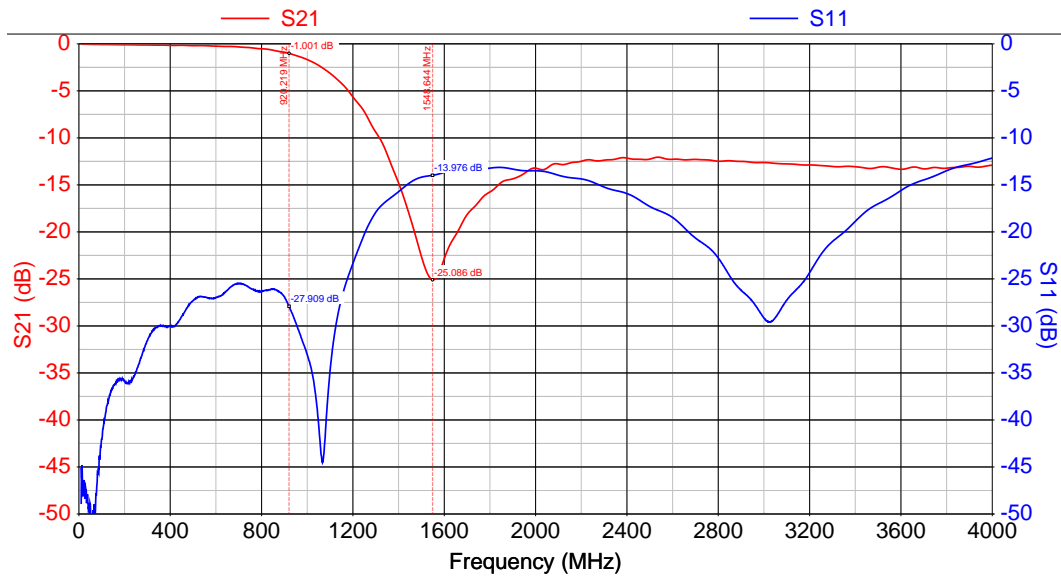
**Figure 4.26:** Fabricated Reflectionless Low-Pass Filters



**Figure 4.27:** Measurement Result of Reflectionless LPF-1

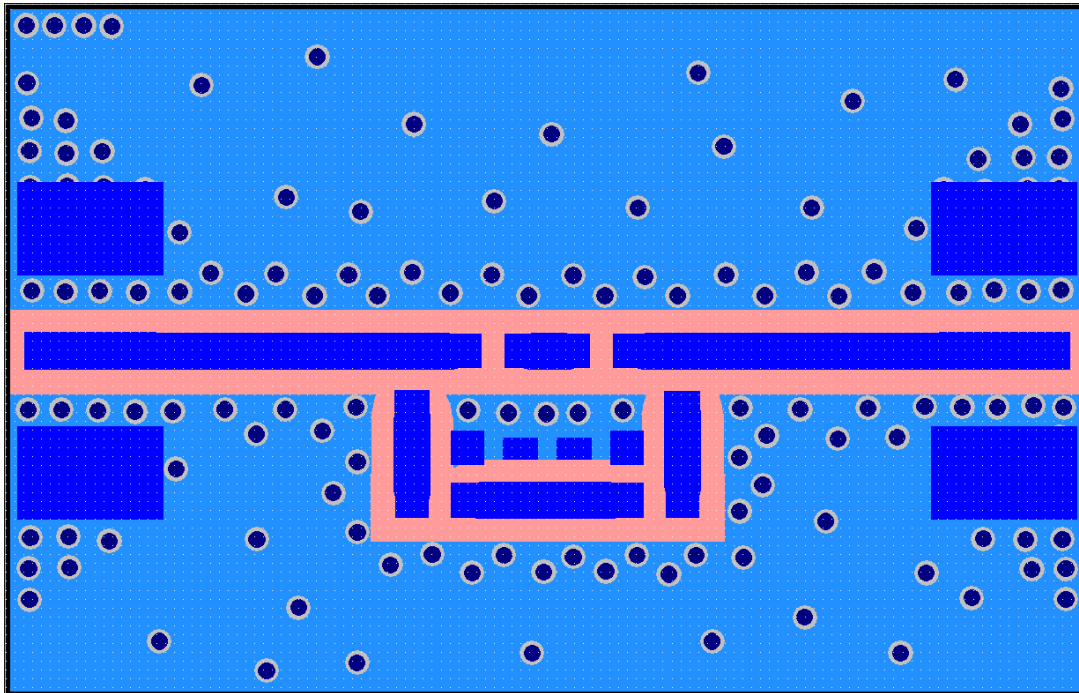


**Figure 4.28:** Measurement Result of Reflectionless LPF-2



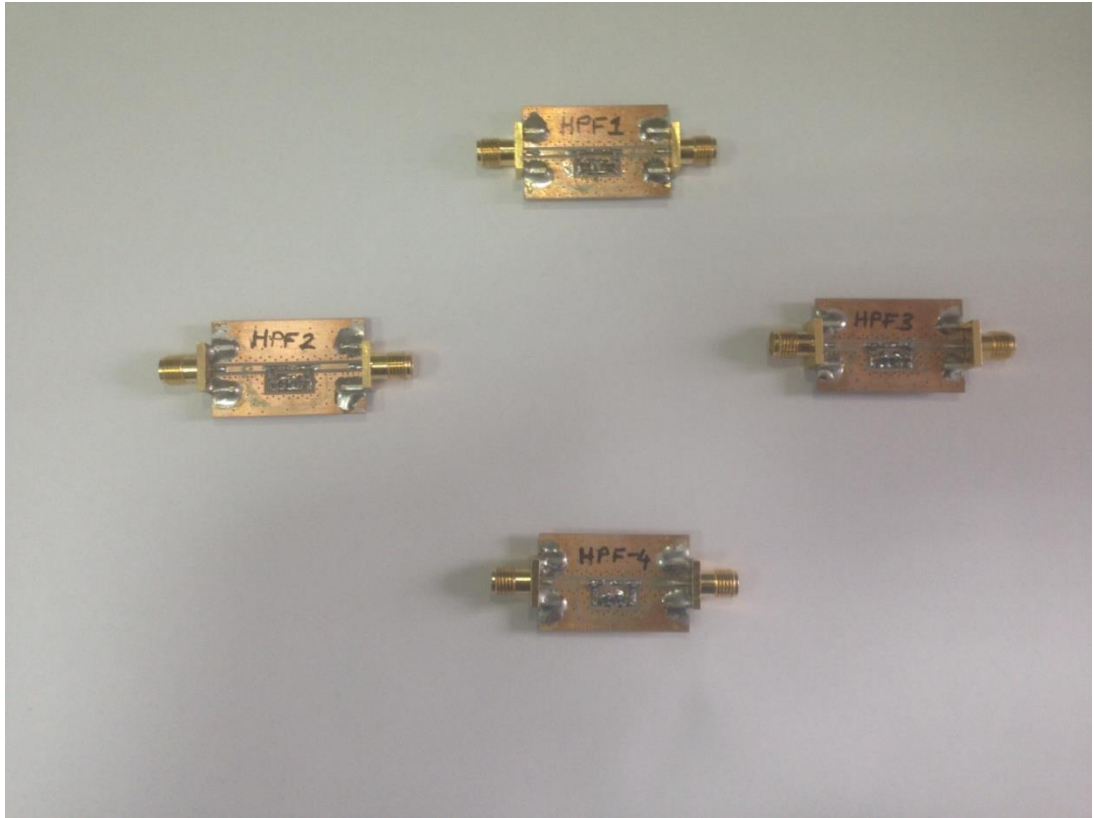
**Figure 4.29:** Measurement Result of Reflectionless LPF-3

#### 4.4.2 Implemented Reflectionless High-Pass Filters

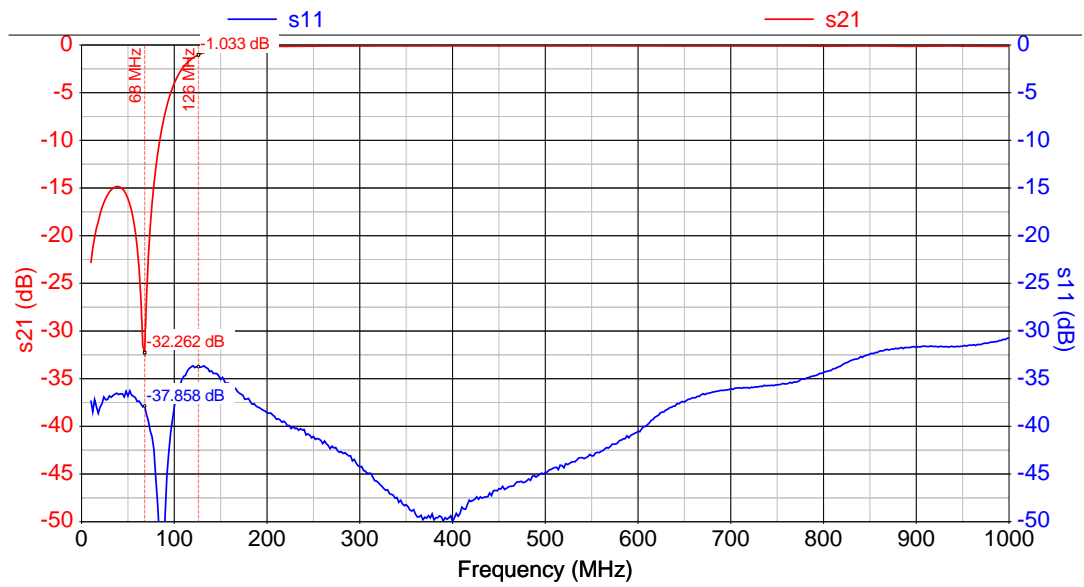


**Figure 4.30:** Lay-out of Reflectionless High-Pass Filter

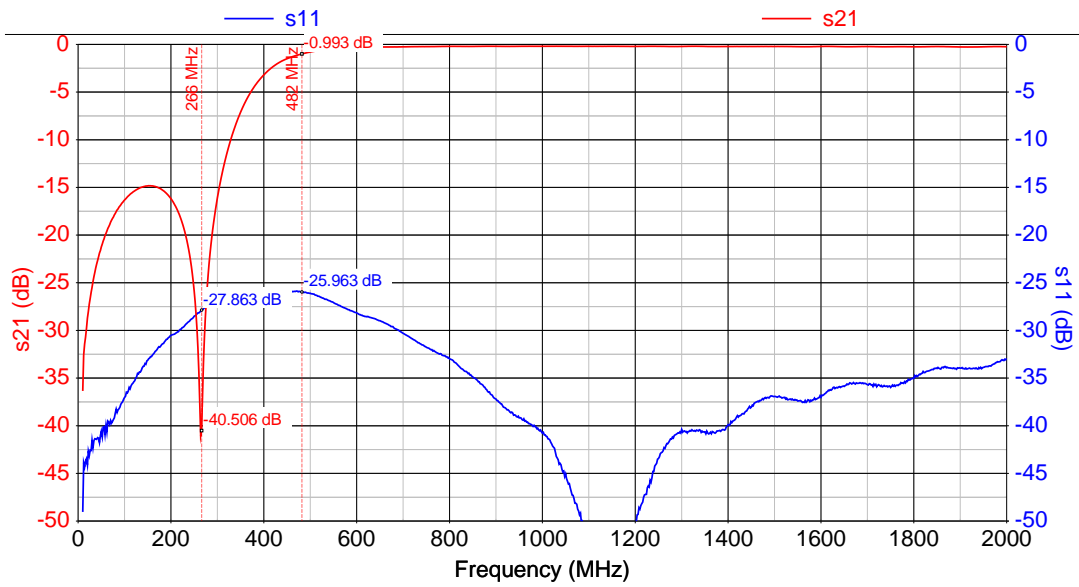




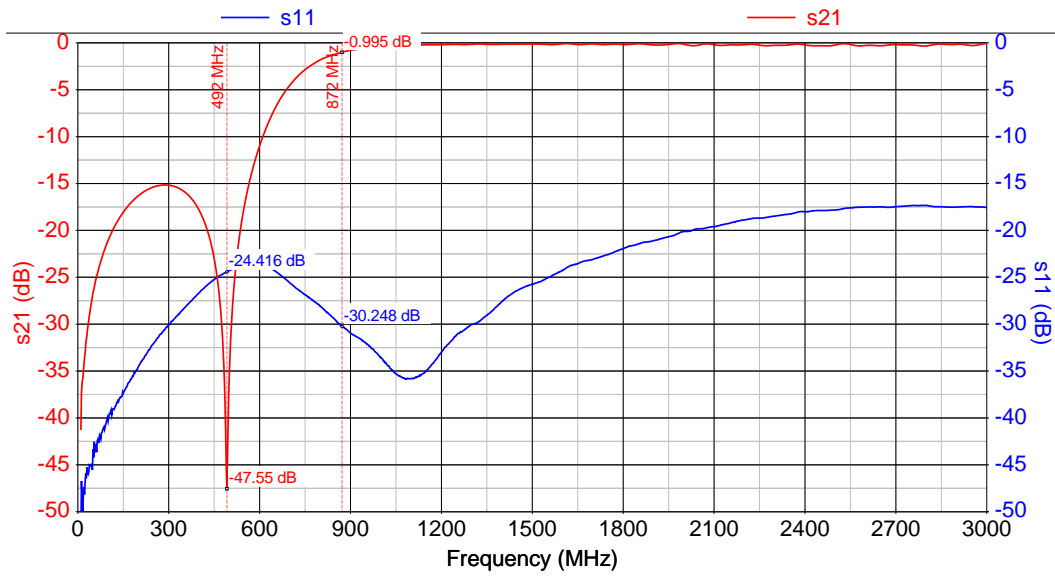
**Figure 4.31:** Fabricated Reflectionless High-Pass Filters



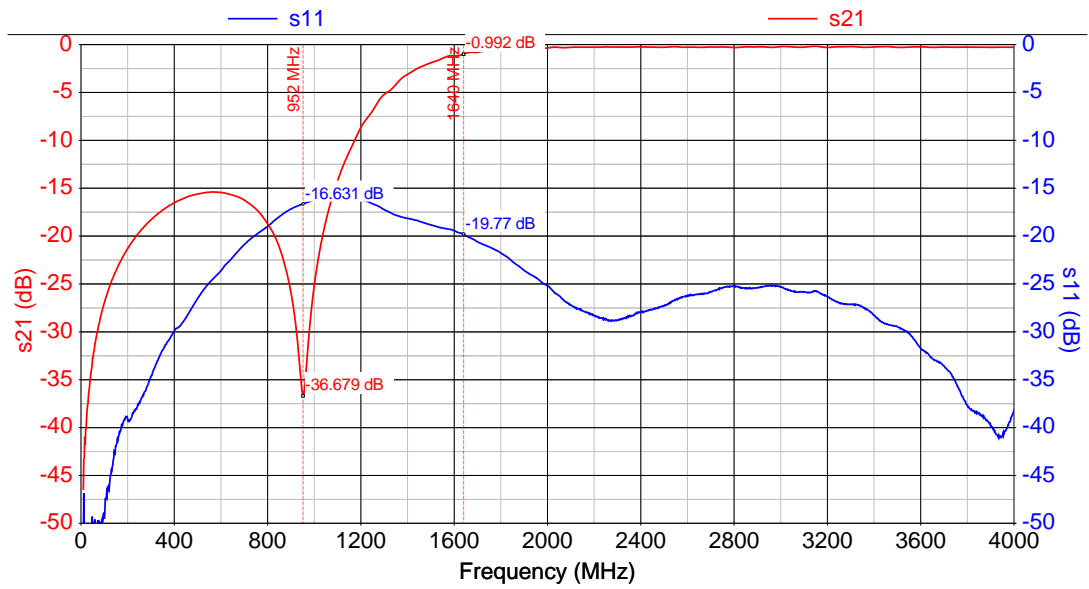
**Figure 4.32:** Measurement Result of Reflectionless HPF-1



**Figure 4.33:** Measurement Result of Reflectionless HPF-2

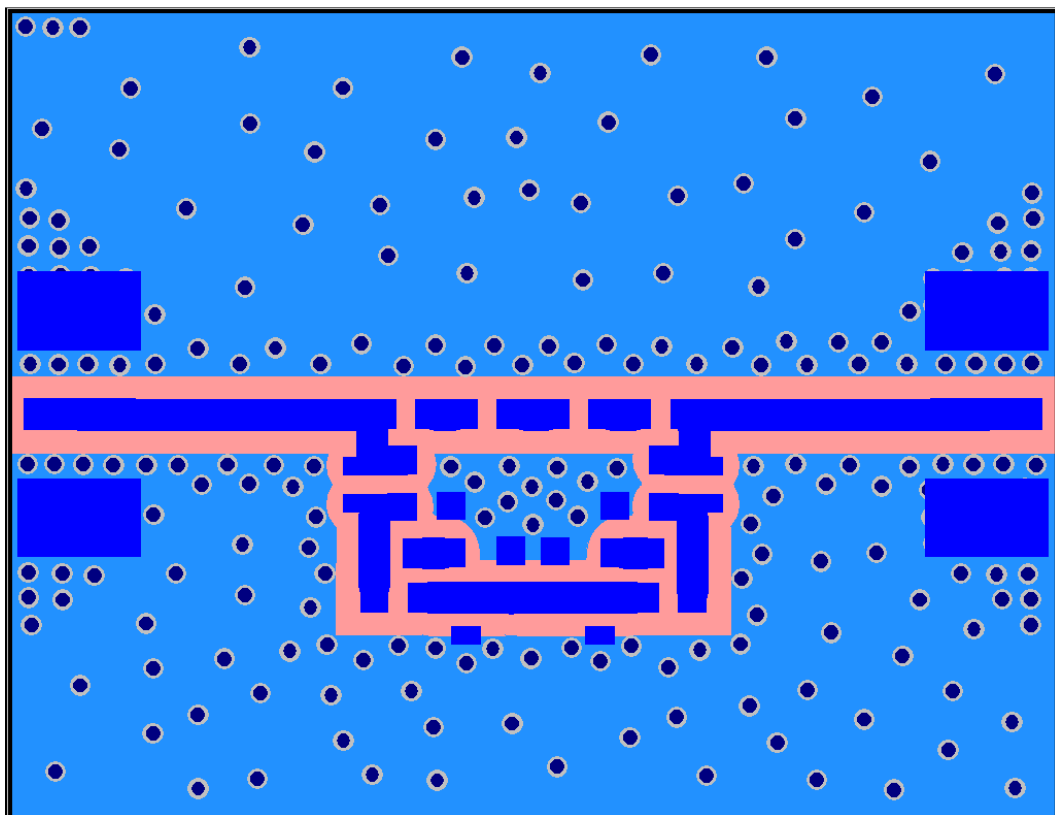


**Figure 4.34:** Measurement Result of Reflectionless HPF-3

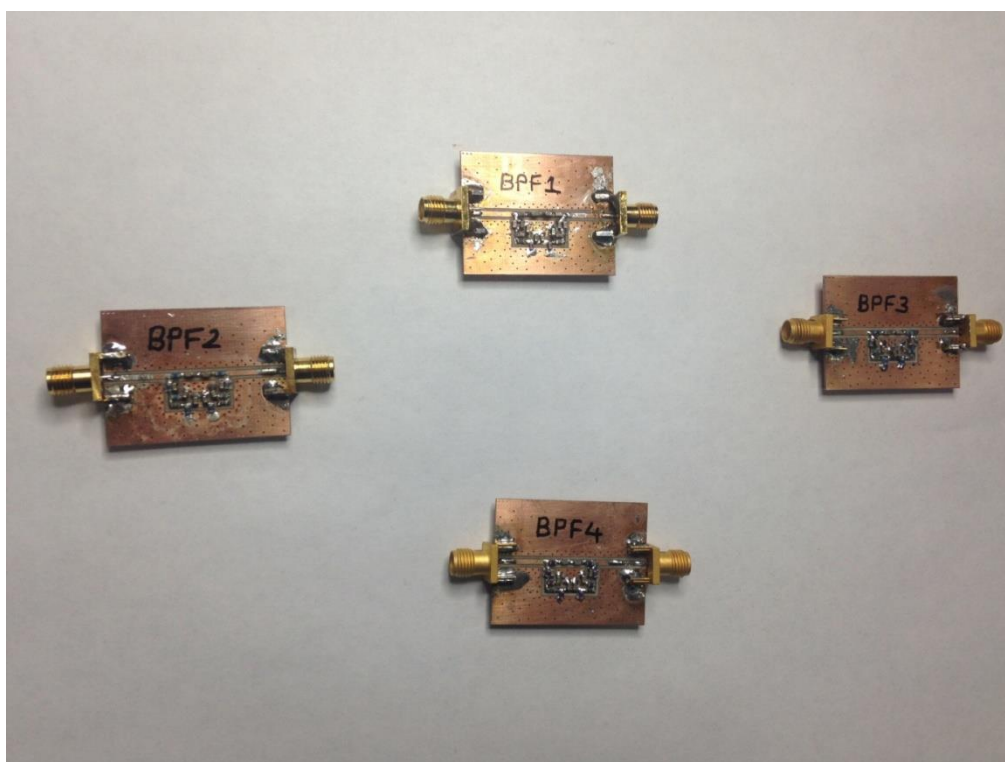


**Figure 4.35:** Measurement Result of Reflectionless HPF-4

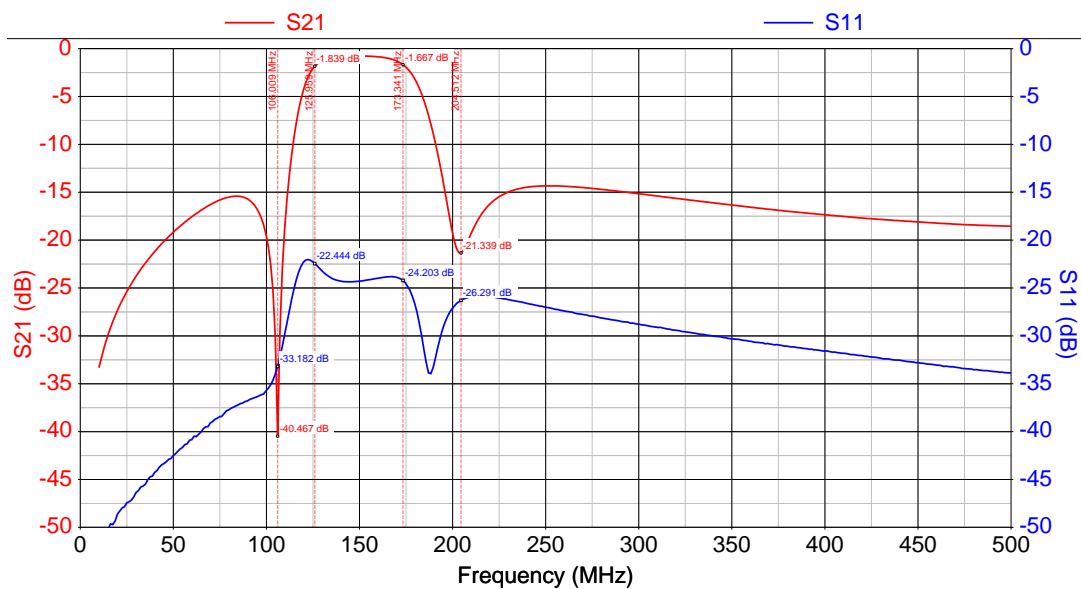
#### 4.4.3 Implemented Reflectionless Bandpass Filters



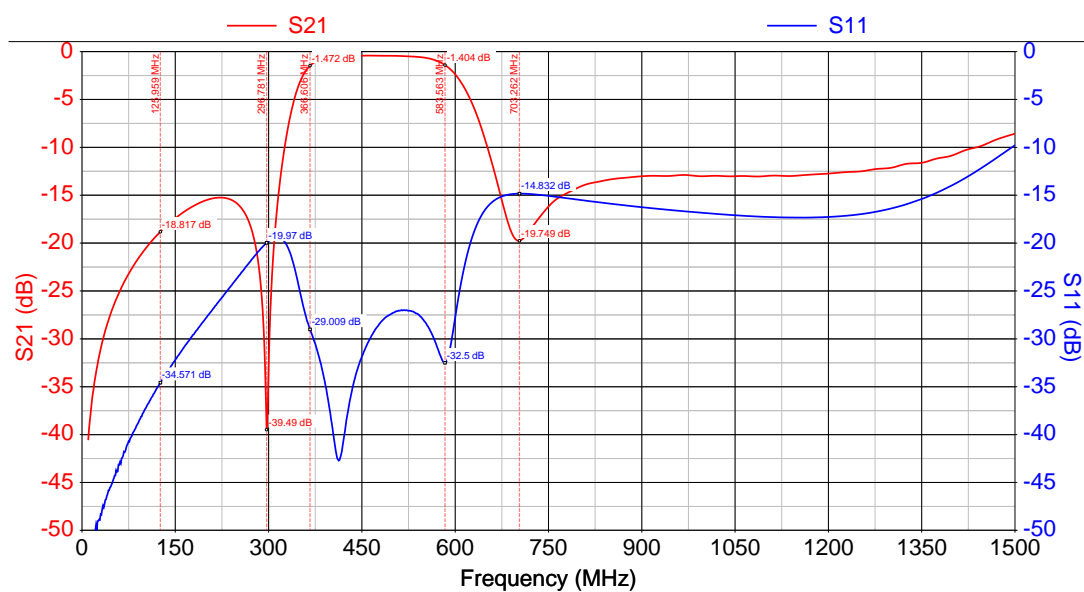
**Figure 4.36:** Lay-out of Reflectionless Bandpass Filter



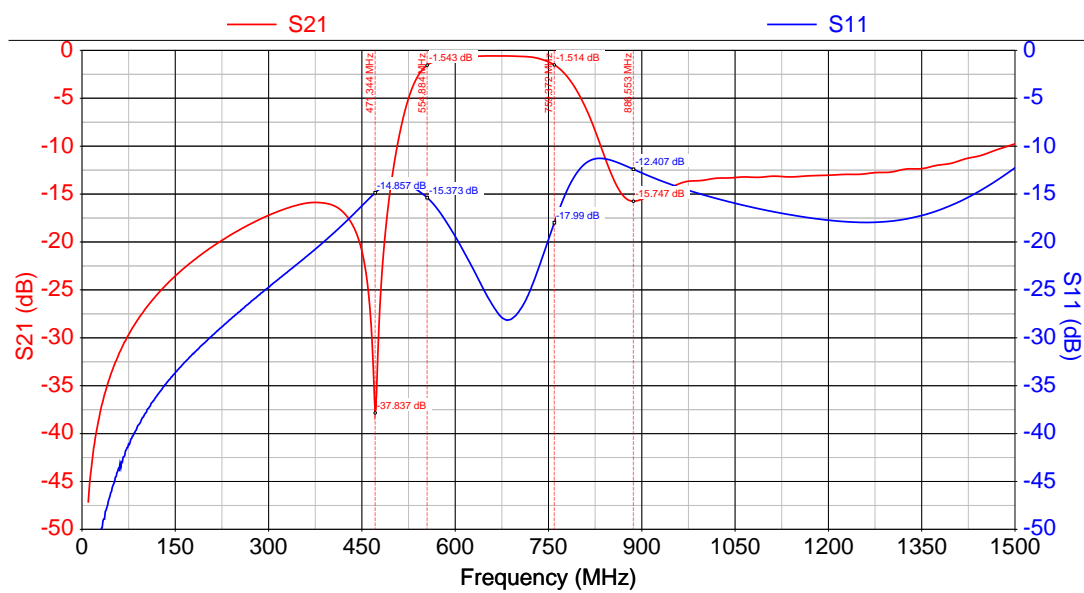
**Figure 4.37:** Fabricated Reflectionless Band-Pass Filters



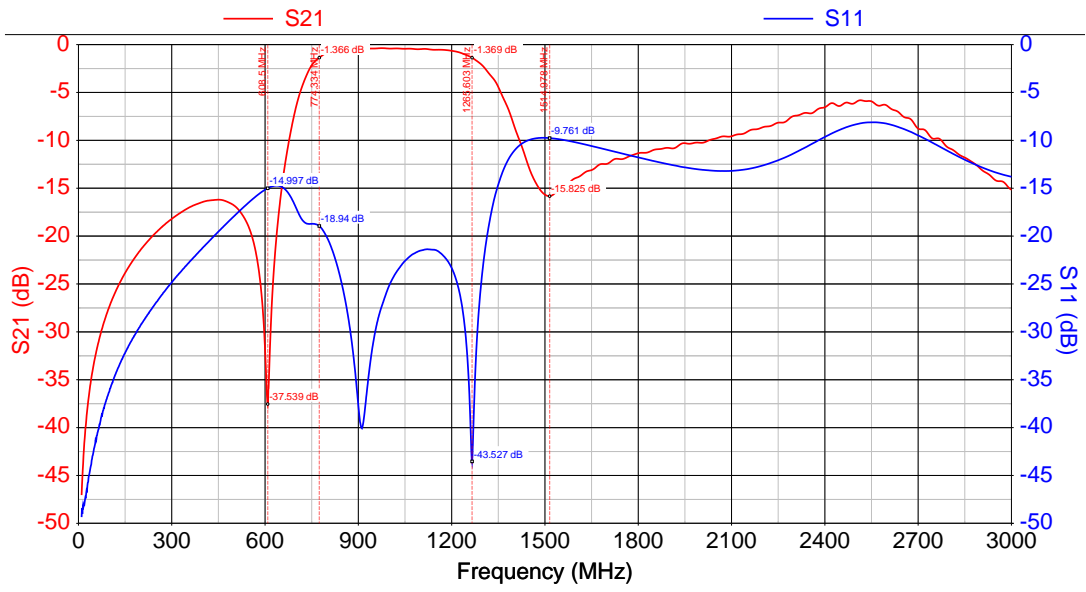
**Figure 4.38:** Measurement Result of Reflectionless BPF-1



**Figure 4.39:** Measurement Result of Reflectionless BPF-2

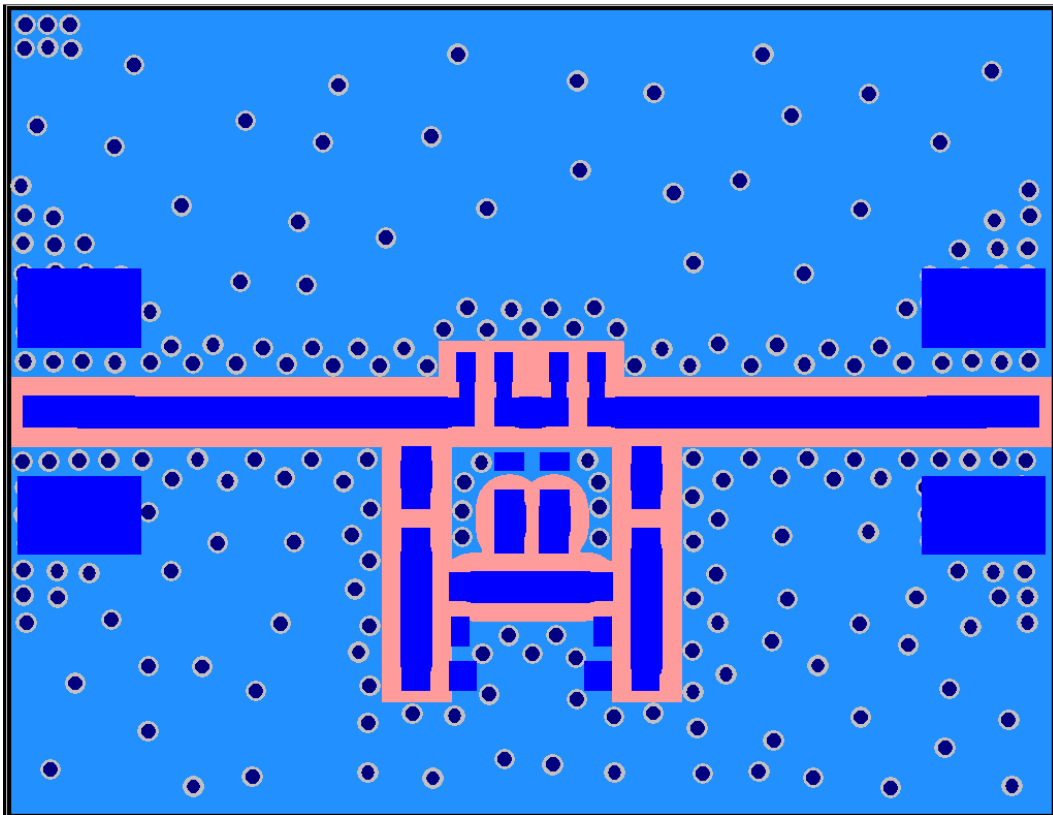


**Figure 4.40:** Measurement Result of Reflectionless BPF-3

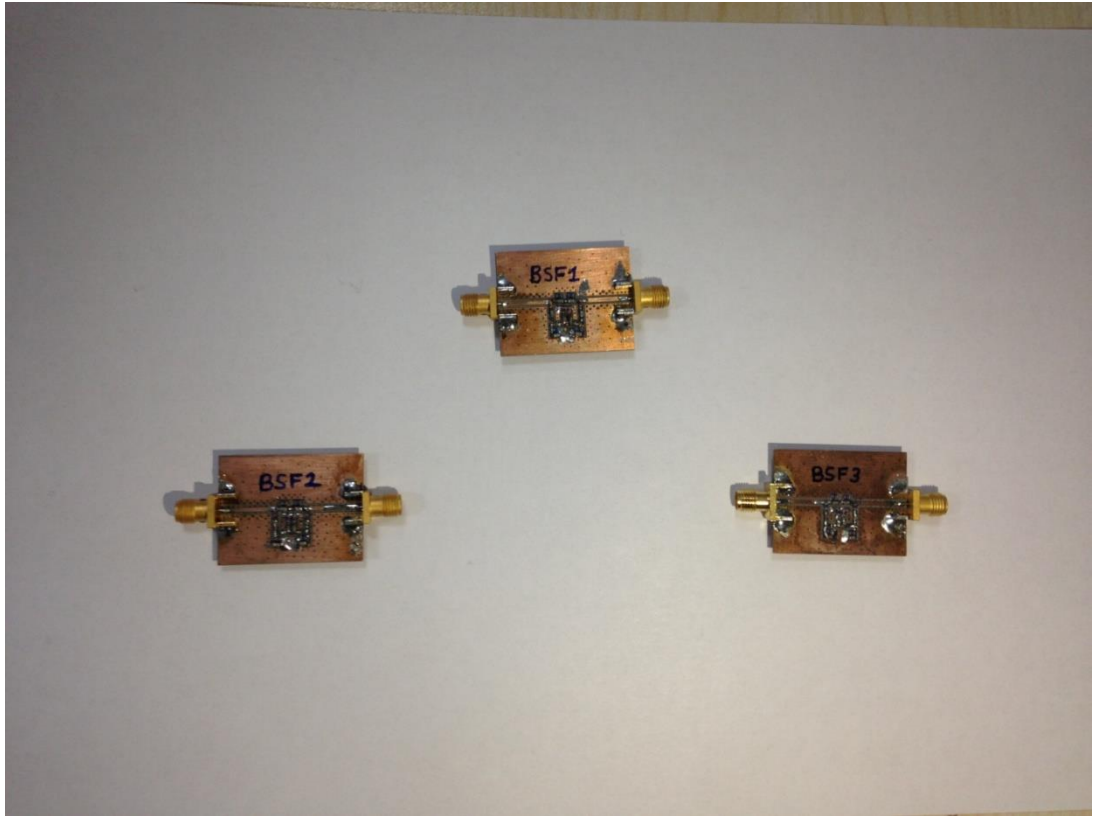


**Figure 4.41:** Measurement Result of Reflectionless BPF-4

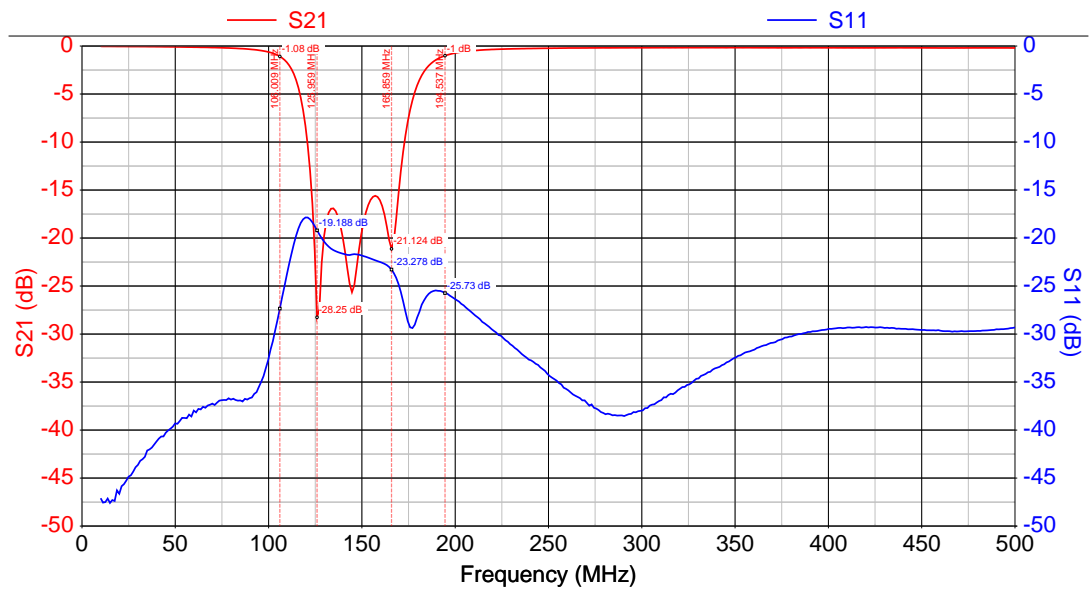
#### 4.4.4 Implemented Reflectionless Bandstop Filters



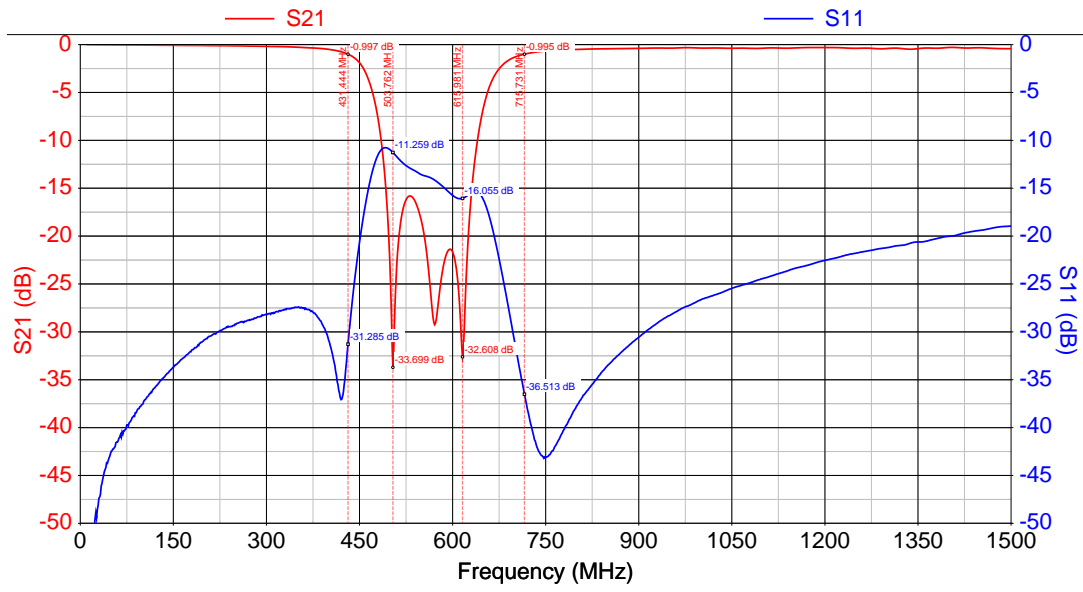
**Figure 4.42:** Lay-out of Reflectionless Bandstop Filter



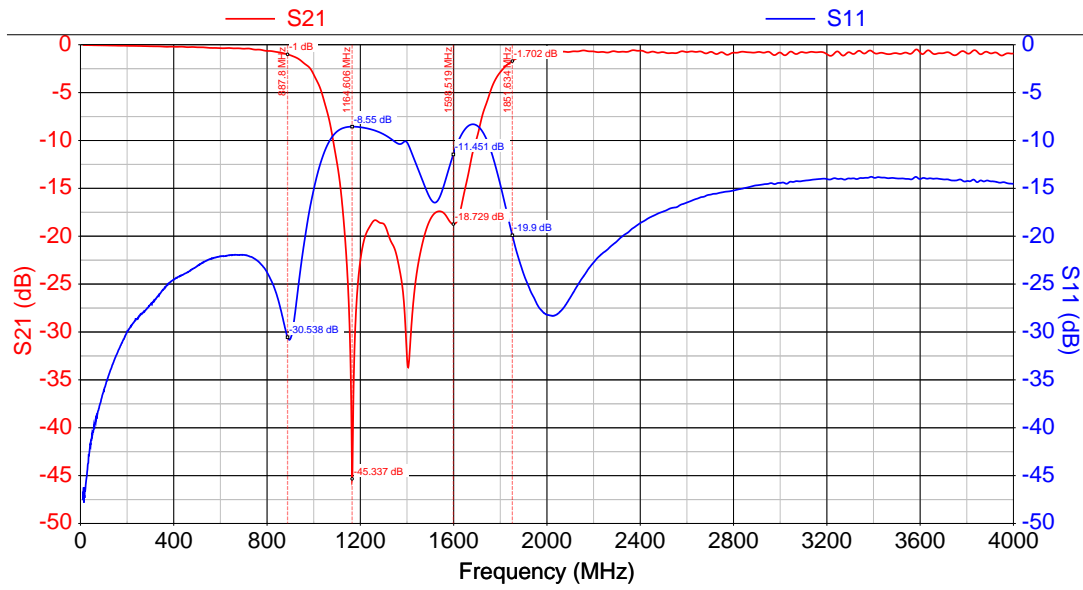
**Figure 4.43:** Fabricated Reflectionless Bandstop Filters



**Figure 4.44:** Measurement Result of Reflectionless BSF-1



**Figure 4.45:** Measurement Result of Reflectionless BSF-2



**Figure 4.46:** Measurement Result of Reflectionless BSF-3



As it is seen from measurement result graphs given above, there is a good agreement between simulation and measurement results. A difference is observed for stopband characteristics of some low-pass reflectionless filters and upper stop band of some bandpass filters. The reason behind this difference is about lumped components' self resonance frequencies and metalization capacitances of layouts. Metal connection lengths between pads of capacitors, inductors and resistors become comparable with wavelength as frequency increases and this affect filter characteristics.



## CHAPTER 5

### IMPROVED REFLECTIONLESS FILTERS

#### 5.1 Introduction

Various types of reflectionless filters are examined and experimented in Chapter 4. A strong consistency between simulation and measurement results is observed. These easy to design and easy to implement filters can be very useful in microwave systems. However, as it can be observed from the results found in Chapter 4, the suppression of reflectionless filter can be inadequate for some applications which is about 14.47 dB characteristically.

In order to improve the suppression performance of this type of filters, two approaches are explained. First of them is using different resistor termination at the end of the even and odd mode equivalent circuits. Other approach examines the reflectionless filter as a diplexer and constructs different structures.

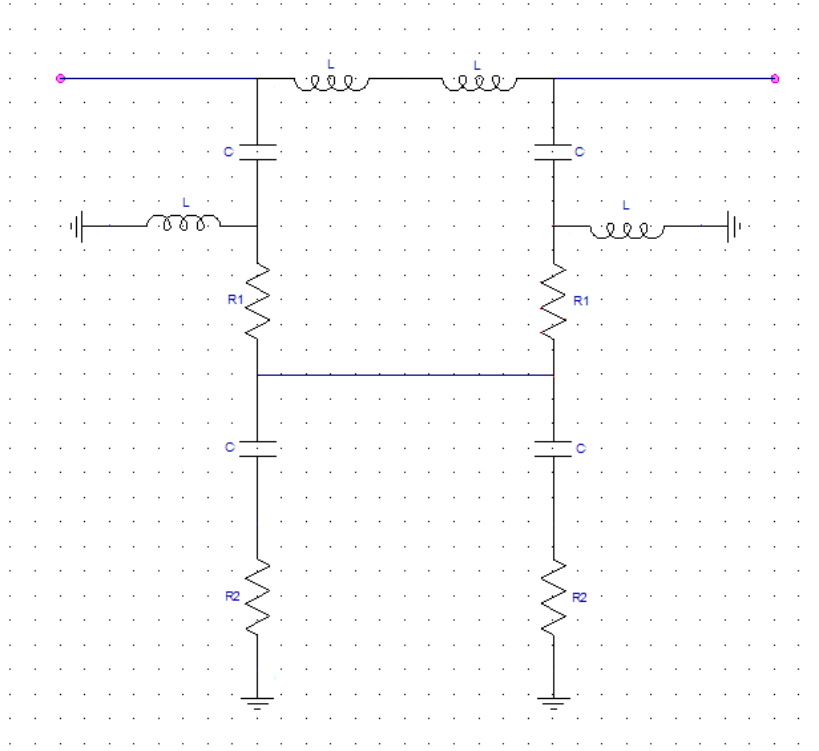
#### 5.2 Termination Resistor Approach

The reflectionless filters explained in Chapter 4 are designed by using resistors having the values of characteristic impedance,  $Z_0$ . In this section, effect of using different resistor values is analyzed. However, using same resistors different from  $Z_0$  in even and odd mode violates duality property of even and odd mode circuits. Therefore, resistor used in even mode,  $R_e$  and odd mode  $R_o$  should satisfy the following conditions to preserve reflectionlessness.

$$\frac{R_o - Z_0}{R_o + Z_0} = -\frac{R_e - Z_0}{R_e + Z_0} \quad (5.1)$$

$$R_o R_e = Z_0^2 \quad (5.2)$$

In order to show how this approach is applied to reflectionless filter structures, a low-pass reflectionless filter is used and two extra resistors are added after capacitors at the bottom side. Related schematic is given in Figure 5.1



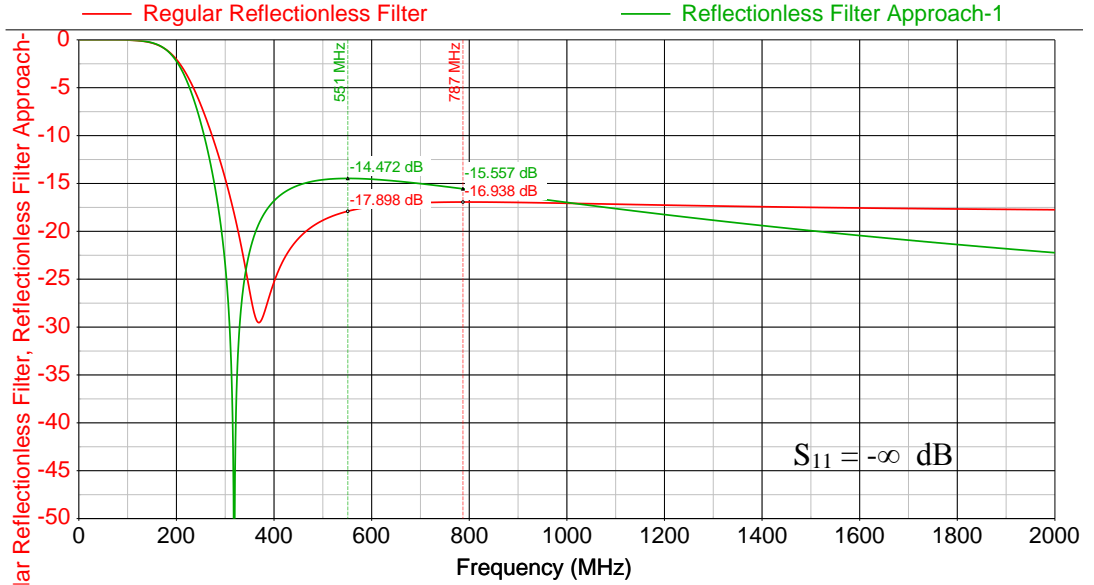
**Figure 5.1:** Reflectionless Low Pass Filters Constructed by First Approach

Since symmetry plane is virtually short for odd mode,  $R_2$  has no effect on odd mode equivalent circuit. On the other hand, it becomes effective for even mode case. The relation between  $R_1$ ,  $R_2$  and  $R_e$ ,  $R_o$  is given in equation 5.3 and 5.4.

$$R_o = R_1 \quad (5.3)$$

$$R_e = R_1 + R_2 \quad (5.4)$$

Reflectionless property of two port network is preserved; therefore, no reflection is observed in this network too. To compare the suppression performance of this network and regular reflectionless low-pass filter, two networks are simulated by using same capacitors and inductors. Simulation results are shared in Figure 5.2.

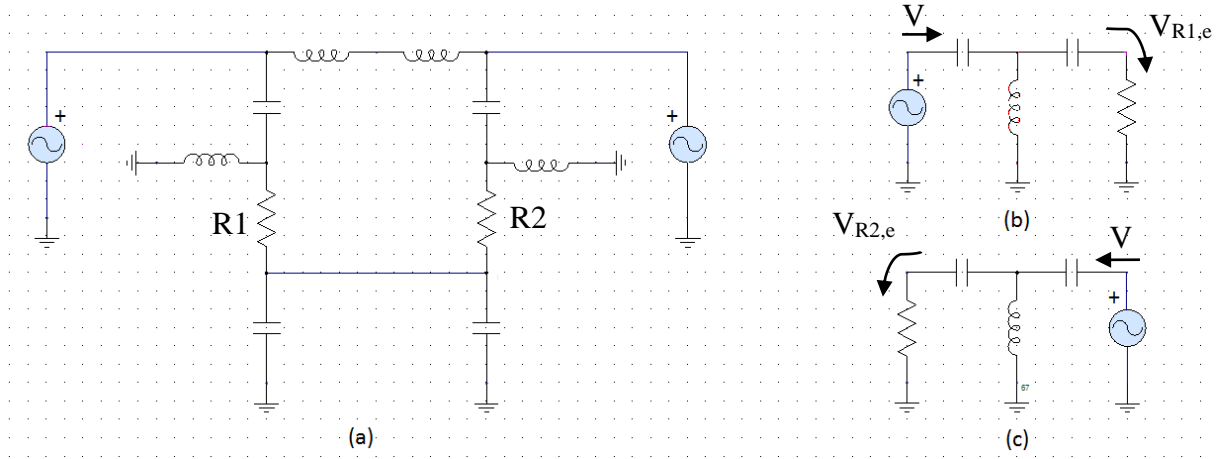


**Figure 5.2:** Simulation Result for First Approach

As it can be seen from Figure 5.2, local maxima after transmission zero is suppressed almost 2.5 dB more by following this approach. It is noted that, resistors  $R_1$  and  $R_2$  are  $39 \Omega$  and  $25.103 \Omega$ , respectively and 10 pF capacitors and 25 nH inductors are used in these simulations. Consequently, stop band maxima decreases by using this approach; however, suppression degrades as frequency increases.

### 5.3 Reflectionless Filter as a Diplexer Approach

When a simple reflectionless filter is driven from one port, the dissipation behavior on resistors can be understood by using even – odd mode analysis as explained in Chapter 4. For even mode, ports of symmetric network are driven with same sources. Figure 5.3 explains even mode case.

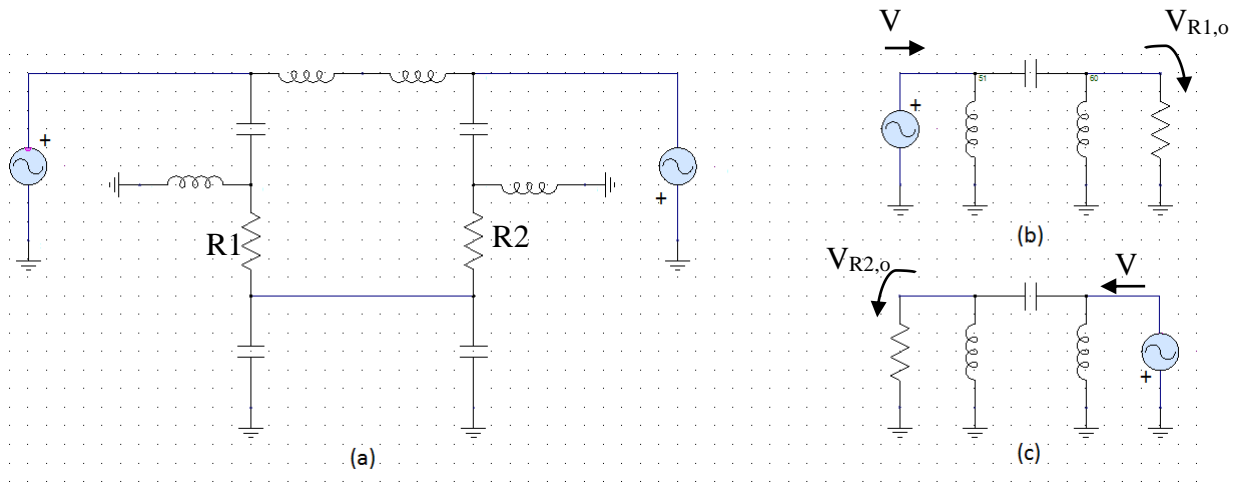


**Figure 5.3:** (a) Even Mode Case (b) Even Mode Equivalent for Left Side Circuitry (c) Even Mode Equivalent for Right Side Circuitry

Transfer function of high pass network between source and resistor for even mode equivalent circuits is  $T_e$  and relation between  $V_{R1,e}$ ,  $V_{R2,e}$ , and  $V$  is:

$$V_{R1,e} = V_{R2,e} = T_e V \quad (5.5)$$

Similarly for odd mode:



**Figure 5.4:** (a) Odd Mode Case (b) Odd Mode Equivalent for Left Side Circuitry (c) Odd Mode Equivalent for Right Side Circuitry

Transfer function of high-pass network between source and resistor for odd mode equivalent circuits is  $T_o$  and relation between  $V_{R1,o}$ ,  $V_{R2,o}$ , and  $V$  is:

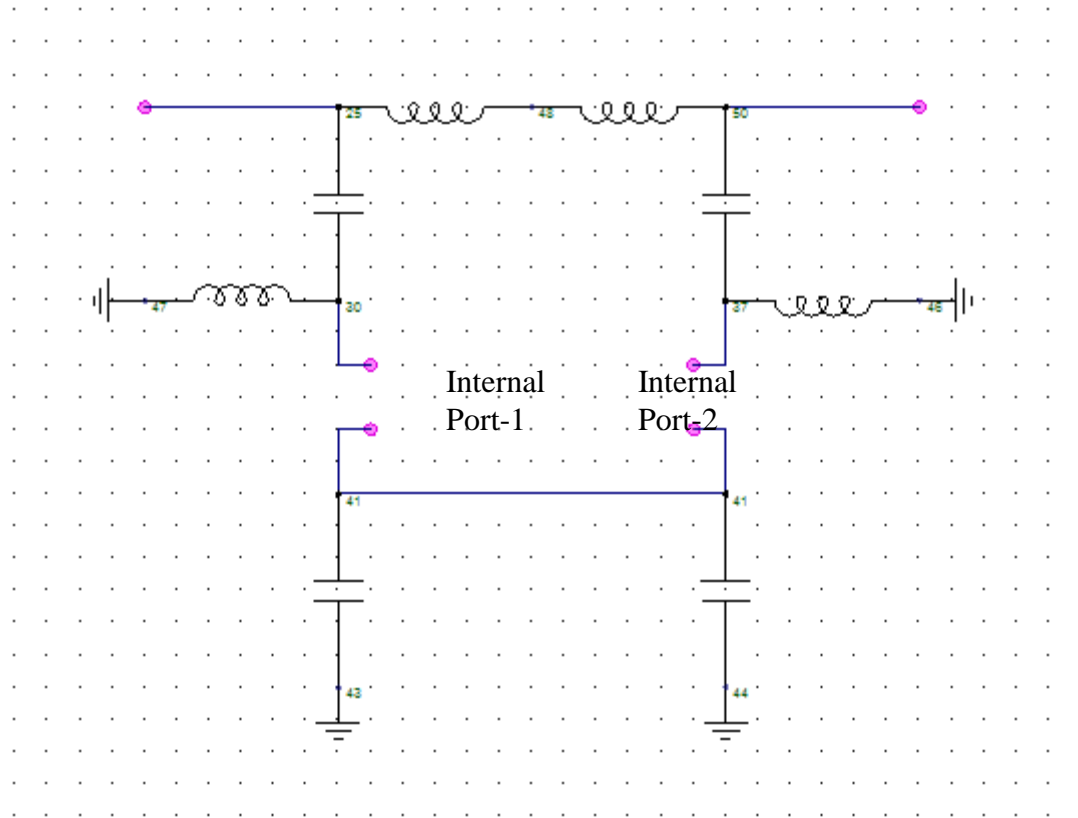
$$V_{R1,o} = -V_{R2,o} = T_o V \quad (5.6)$$

Since networks for even and odd mode cases are dual, transfer functions are equal.

$$T_e = T_o \quad (5.7)$$

By using results obtained from equations 5.5, 5.6, 5.7 and superposition property, it is seen that there is no voltage incident to resistor R2. Therefore, no dissipation occurs at R2 when reflectionless network is driven from left port. Similarly, if network is driven from right port, no dissipation occurs at R1. This results shows that, left input port and right resistor are isolated and vice-versa.

By taking this result into account, this filter is considered as dual-directional diplexer wherein the out of band energy is routed to internal ports for this approach. [reflectionless filter structures] Resultant schematics for this dual-directional diplexer given in Figure 5.5 [3].

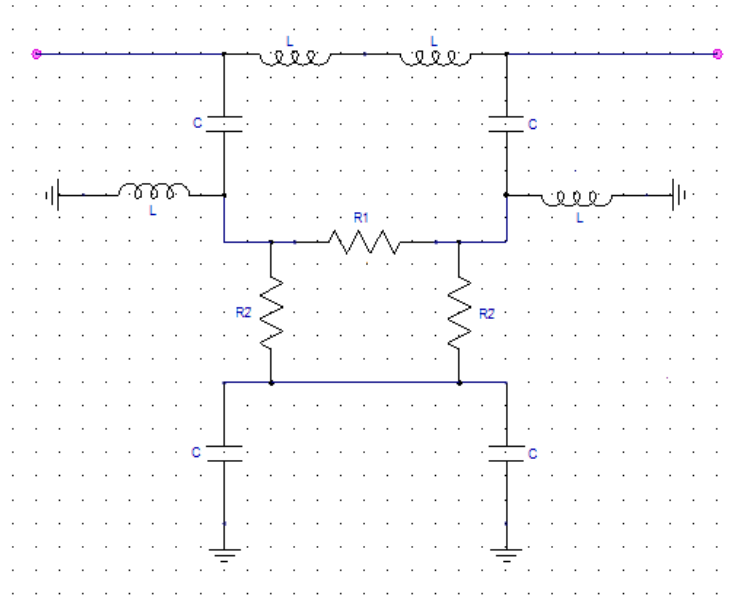


**Figure 5.5:** Dual-Directional Diplexer

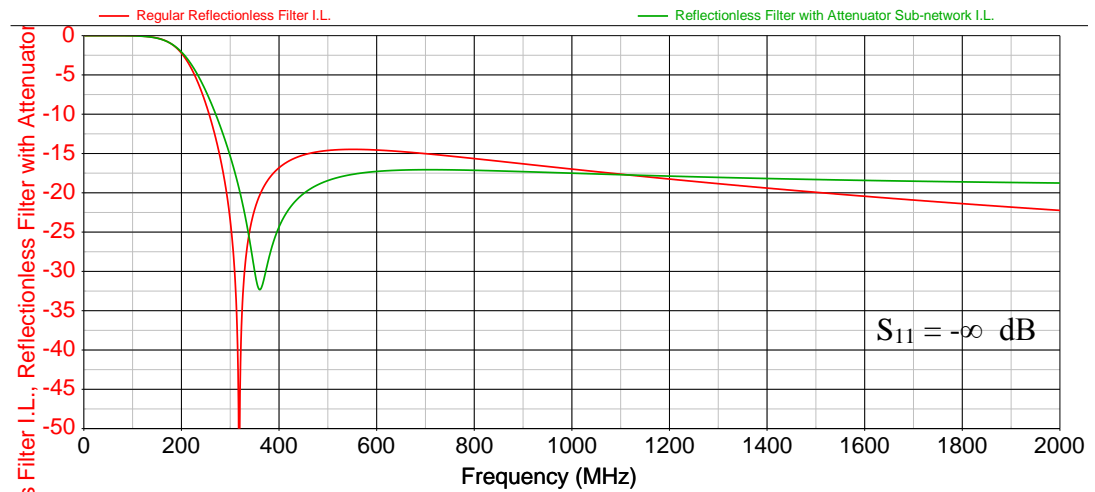
The basic idea behind this approach is that any matched network connected between these internal ports does not violate reflectionless property of overall network. For example, resistive attenuators or other reflectionless filters can be connected to the internal ports as sub-networks.

By using this approach, some reflectionless filter structures are designed and simulated. Related filters and simulation results are given in following figures.





**Figure 5.6:** Reflectionless Filter with Attenuator Sub-network

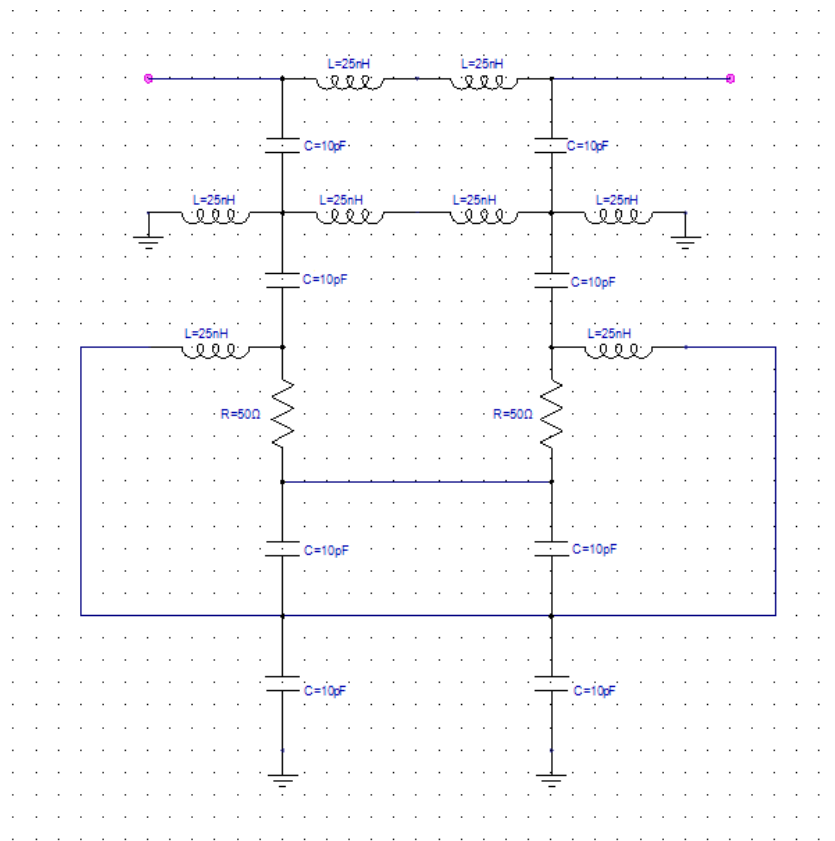


**Figure 5.7:** Simulation Result for Reflectionless Filter with Attenuator Sub-network

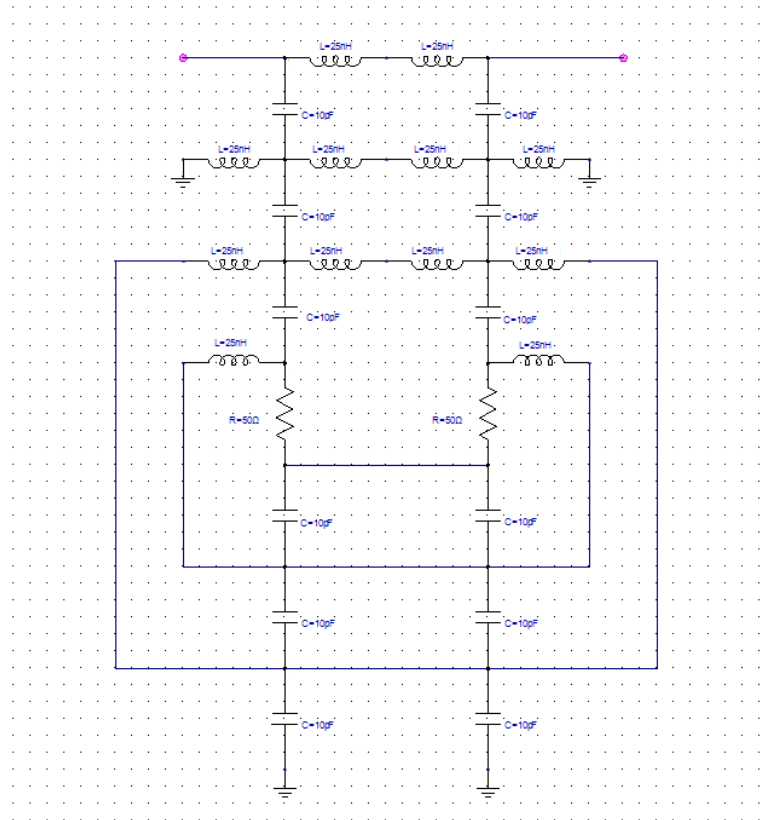
Attenuation value of attenuator used as sub-network affects overall response. In order to decrease the maxima in suppression band as much as possible, 20 dB pi-attenuator is used as sub-network. Although the maxima decreases in out of band, regular reflectionless filter have better suppression as frequency increases which is very similar to first approach result. In fact, schematic obtained in first

approach can also be thought as reflectionless filter with tee attenuator sub-network. Therefore, obtaining similar responses is an expected result.

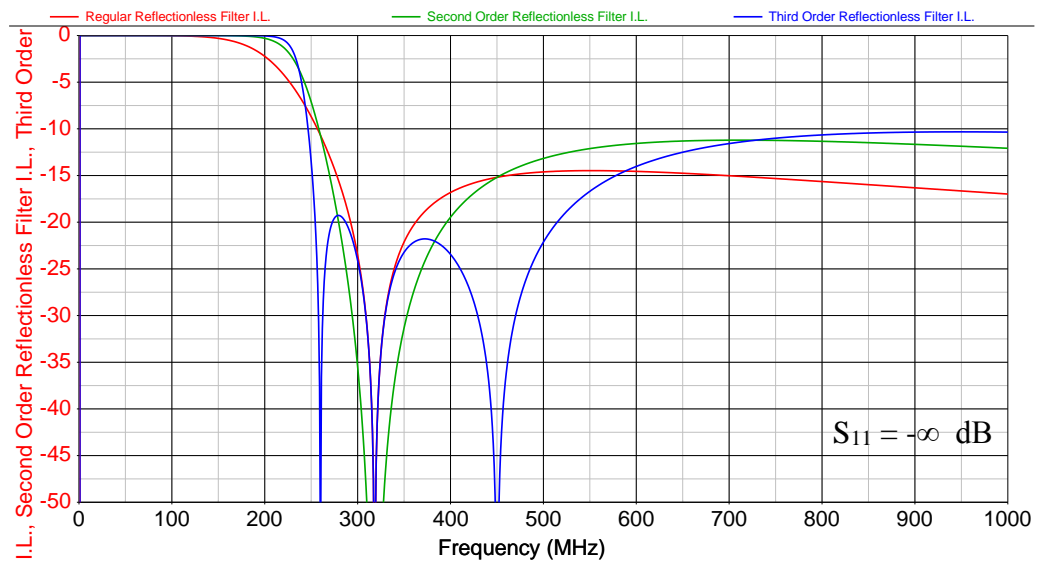
Other reflectionless filter topologies can also be used as sub-networks. Various reflectionless filters with different sub-networks are presented in following figures.



**Figure 5.8:** Second Order Reflectionless Filter



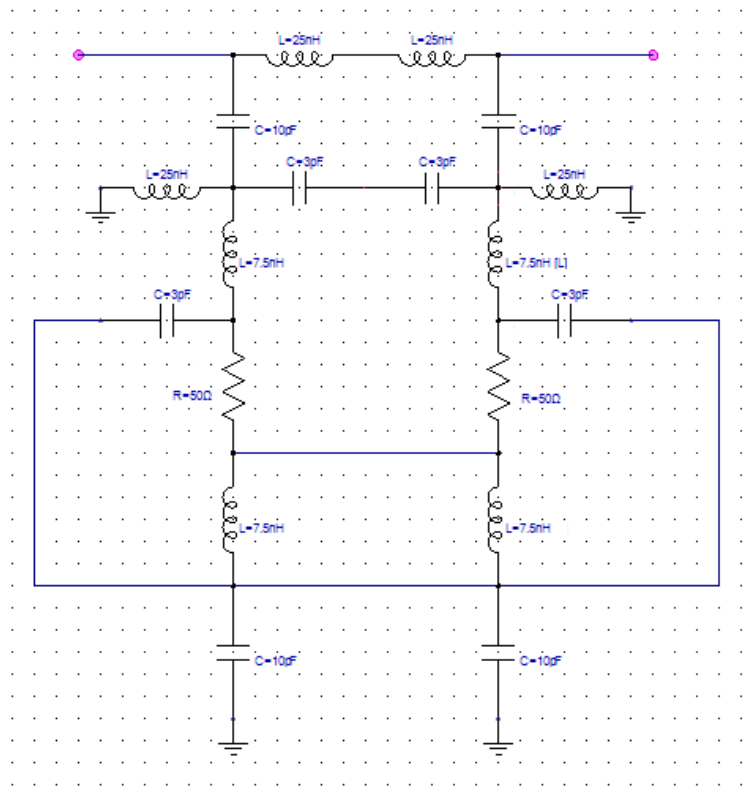
**Figure 5.9:** Third Order Reflectionless Filter



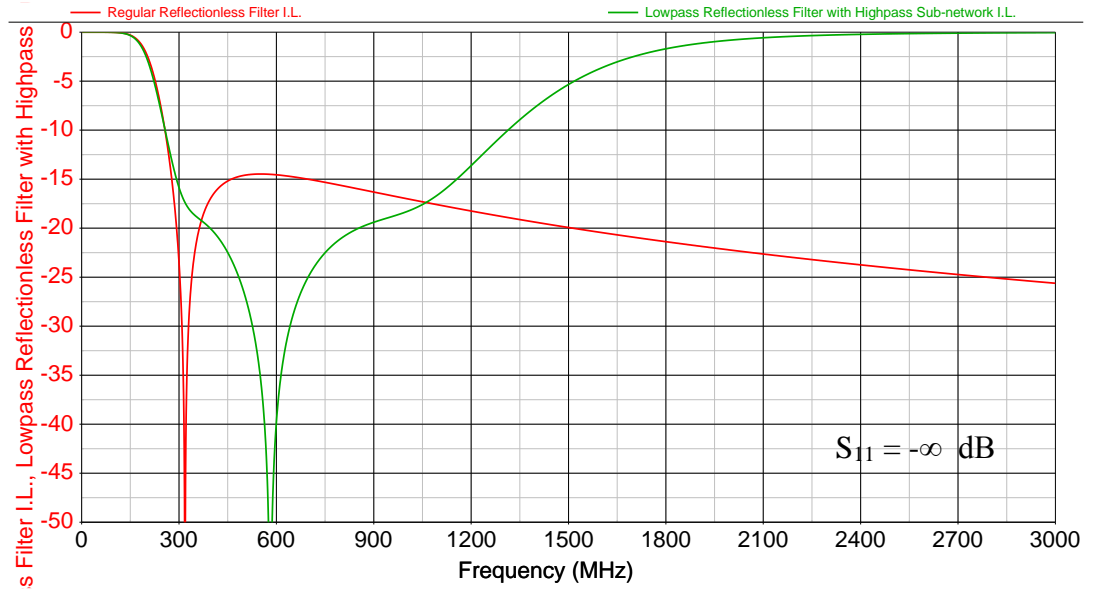
**Figure 5.10:** Comparison of First, Second and Third Order Reflectionless Filters

Adding a reflectionless filter to internal ports improves steepness of the pass band response. In addition, the maxima that occurred in first order regular reflectionless filter is suppressed in third order reflectionless filter. However, this causes greater peak at higher frequencies.

Different type of reflectionless filter can also be used as sub-networks. For example, a high-pass reflectionless filter is connected to internal ports of a low-pass reflectionless filter and different response is obtained.



**Figure 5.11:** Reflectionless Low-Pass Filter with High-Pass Sub-network



**Figure 5.12:** Comparison of Regular Reflectionless Low-Pass Filter and Reflectionless Filter in Figure 5.9

When a reflectionless low-pass filter is internally terminated with a high-pass reflectionless filter, a bandstop response is obtained as given in Figure 5.10. It is understood from this result that sub-networks are not only used for better suppression, but also to shape the overall response.



## **CHAPTER 6**

### **CONCLUSION AND FUTURE WORK SUGESTIONS**

In this thesis, the importance of out of band matching is handled and several absorptive filtering techniques are treated. According to examples given in Chapter 2, out of band performance of some RF and microwave components also affects in-band performance such as degradation in its return loss and ripples in passband. The problems given in these examples are well known by RF and microwave system engineers. However, they choose different solutions instead of using absorptive filters to overcome these problems. For example, engineers commonly use matching attenuators in front of the ports of mixers in up-conversion and down-conversion applications. Although this is a solution for matching problem, this degrades overall gain of system. Therefore, there is a need of absorptive filters and because of this; Chapter 3, Chapter 4 and Chapter 5 are devoted to absorptive filter design and implementation methods.

Four different absorptive filter design methods are given in Chapter 3 and Chapter 4 which are absorptive filters by using isolators, multiplexers, 3 dB 90° couplers and Matthew Morgan's reflectionless filters. Using isolators in absorptive filtering may be seen as the simplest method; however, this is not an easy to integrate method for most of the microwave systems. In addition, finding wide band isolator can be problematic. On the other hand, using 3 dB 90° couplers in absorptive filters is also an easy method to use. Absorptiveness band of this kind of filters depends on the operation band of couplers and this is not critical because there are a lot of wide band couplers in market. However, this type of absorptive filters need more space when it is compared with Matthew Morgan's reflectionless filters. In addition to space advantage of reflectionless filters, this topology also has

a wide band absorptiveness in applications, which depends on properties of lumped capacitors, inductors and resistors. On the other hand, the disadvantage of reflectionless filters is its suppression performance which may be inadequate for some applications. In order to obtain a satisfied suppression in stopband, reflectionless filters can be cascaded as long as required because of its absorptiveness property. However, space requirements may not let this much filters in cascaded form for this case.

According to this information, reflectionless filter topology has only one disadvantage, having poor suppression performance. In order to improve it, two different approaches are mentioned in Chapter 5. Related approaches are explained and approaches are verified by using simulations. All simulation results are compared with classical reflectionless filters and better suppression and steeper pass band is observed.

RF and microwave filters are used not only to suppress the unwanted signal but also to reject out of band noise for some applications. For example, filters are used in front of mixers to reject image frequency noise and this improves overall noise figure. However, reflectionless filters does not reflect out of band noise back because of their resistive characteristics. However, reflective filters affect return loss characteristics of frequency conversion systems. The detailed analysis for this problem and alternative solutions are thought as future work.

In addition to this, detailed analysis of improved reflectionless filters and alternative sub-networks are thought as future works. Furthermore, some other absorptive filters by using hybrid filtering techniques as given in [8], [9] and [10] are thought as future works of this thesis.



## REFERENCES

- [1] D. M. Pozar, *Microwave Engineering*, John Wiley & Sons, 2005.
- [2] Levy, R., Cohn, S. B., "A History of Microwave Filter Research, Design, and Development," *IEEE Transactions on Microwave Theory and Techniques*, vol. 32, no. 9, pp. 1055 - 1067, 1984.
- [3] Morgan, M. A., Boyd, T. A., "Reflectionless Filter Structures," *IEEE Transactions on Microwave Theory and Techniques*, vol. 63, no. 4, pp. 1263 - 1271, 2015.
- [4] "FILPRO Manual," METU.
- [5] "GENESYS User's Manual," Eagleware Software Inc..
- [6] "SONNET User's Manual," Sonnet Software Inc..
- [7] Morgan, M. A., Boyd, T. A., "Theoretical and Experimental Study of New Class of Reflectionless Filter," *IEEE Transactions on Microwave Theory and Techniques*, vol. 59, no. 5, pp. 1214 - 1221, 2011.
- [8] Huang, G. J., Yi-Hsin, P., Huang, H. C., "A 90 Degree Hybrid with Wideband Filtering Characteristic," *Asia-Pacific Microwave Conference (APMC)*, vol. 1, pp. 1 - 3, 2015.
- [9] Wu, L. S., Xia, B., Yin, W. Y., Mao, J., "Collaborative Design of a New Dual-Bandpass 180 Degree Hybrid Coupler," *IEEE Transactions on Microwave Theory and Techniques*, vol. 61, no. 3, pp. 1053 - 1066, 2013.

- [10] Liu, W. R., Huang, T. Y., Chen, C. F., Shen, T. M., "Design of a 180-Degree Hybrid with Chebyshev Filtering Response Using Coupled Resonators," *Microwave Symposium Digest (IMS)*, pp. 1 -3, 2013.

## APPENDIX A

### ZX05-5+ DATA SHEET

## Coaxial Frequency Mixer

Level 7 (LO Power +7 dBm) 5 to 1500 MHz

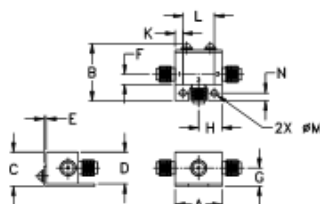
#### Maximum Ratings

Operating Temperature	-40°C to 85°C
Storage Temperature	-55°C to 100°C
RF Power	50mW
IF Current	40mA

#### Coaxial Connections

LO	1
RF	2
IF	3

#### Outline Drawing



#### Outline Dimensions (Inch mm)

A	B	C	D	E	F	G
.74	.90	.54	.50	.04	.16	.23
18.80	22.86	13.72	12.70	1.02	4.06	7.37

H	J	K	L	M	N	#M
.37	—	.122	.426	.106	.122	grams
9.40	—	3.10	10.80	2.69	3.10	20.0

#### Features

- rugged construction
- small size
- low conversion loss
- high L-R isolation
- protected by US Patents 6,133,525 & 6,790,049

#### Applications

- cellular
- PCS
- instrumentation
- satellite communication

## ZX05-5+ ZX05-5



CASE STYLE: FL905

Connectors	Model	Price	Qty.
BMA	ZX05-5-B(+)	\$37.95 ea.	(1-24)

**+ RoHS compliant in accordance with EU Directive (2002/95/EC)**

The +Suffix identifies RoHS Compliance. See our web site for RoHS Compliance methodologies and qualifications.

#### Electrical Specifications (T<sub>AMB</sub>=25°C)

FREQUENCY (MHz)		CONVERSION LOSS (dB)		LO-RF ISOLATION (dB)						LO-IF ISOLATION (dB)						IP3 at center band (dBm)								
LO/RF	IF	Mid-Band		Total Range	L			M			U			L			M			U				
$f_{LO}/f_{IF}$		$f_{LO}$	$f_{IF}$			Type	Min.	Typ.	Max.	Type	Min.	Typ.	Max.	Type	Min.	Typ.	Max.	Type	Min.	Typ.	Max.	Type	Min.	Typ.
5-1500	DC-1000	6.6	0.1	7.5	9.3	50	40	40	25	33	23	50	40	30	20	20	10	15						

1 dB COMP: +1 dBm typ.

Positive direction: positive output with in-phase RF & LO signals

L = low range (5 to 101)

m = mid band (20 to 100)

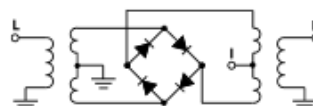
M = mid range (101 to 1000)

U = upper range (1000 to 1500)

#### Typical Performance Data

Typical Performance Data						
Frequency (MHz)		Conversion Loss (dB)	Isolation L-R (dB)	Isolation L-I (dB)	VSWR RF Port (-1)	VSWR LO Port (-1)
RF	LO	LO +7dBm	LO +7dBm	LO +7dBm	LO +7dBm	LO +7dBm
5.10	35.10	6.93	32.10	36.28	1.48	1.83
35.10	65.10	6.51	35.10	36.21	1.38	1.80
50.10	80.10	6.48	61.74	59.65	1.37	1.80
100.10	70.10	6.60	55.18	36.54	1.36	1.77
171.43	141.43	6.54	50.58	45.84	1.35	1.80
354.10	324.10	6.51	47.52	39.83	1.33	1.78
336.77	336.77	6.56	45.52	36.24	1.32	1.78
419.43	389.43	6.63	43.47	34.05	1.31	1.78
502.10	472.10	6.58	42.13	31.37	1.30	1.81
584.77	554.77	6.56	40.30	30.33	1.28	1.82
667.43	637.43	6.64	37.49	29.33	1.25	1.84
750.10	720.10	6.78	35.27	28.03	1.24	1.87
831.53	801.53	6.81	34.84	25.74	1.19	1.90
934.39	904.39	6.70	33.83	23.50	1.09	1.91
1057.24	1027.24	6.59	33.85	22.24	1.05	1.97
1140.10	1110.10	6.66	33.54	21.45	1.20	2.09
1242.96	1212.96	7.02	32.75	20.75	1.41	2.22
1345.81	1315.81	7.59	31.63	19.50	1.52	2.15
1448.67	1418.67	7.75	29.54	17.12	1.84	2.01
1500.10	1470.10	7.94	28.84	17.08	1.93	2.06

#### Electrical Schematic



**Mini-Circuits®**  
ISO 9001 ISO 14001 CERTIFIED

P.O. Box 350166, Brooklyn, New York 11235-0003 (718) 934-4500 Fax (718) 332-4661 For detailed performance specs & shopping online see Mini-Circuits web site



The Design Engineers Search Engine Provides ACTUAL Data Instantly From MINI CIRCUITS/SAL [www.minicircuits.com](http://www.minicircuits.com)

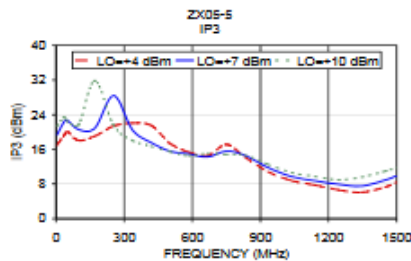
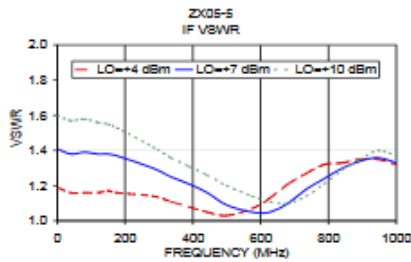
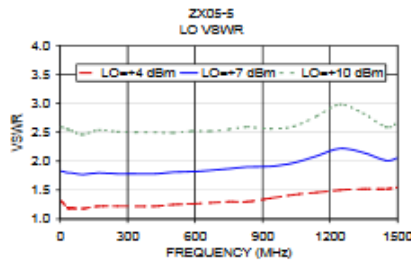
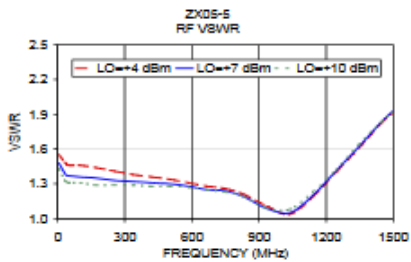
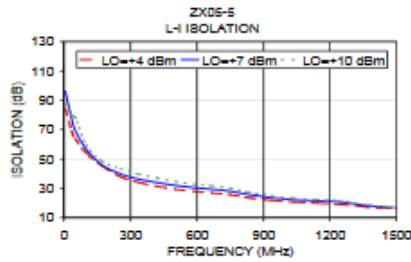
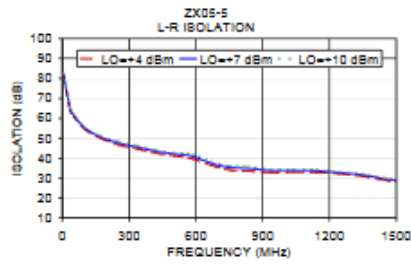
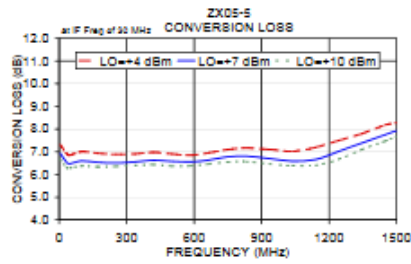
RF/RF MICROWAVE COMPONENTS

**mini-circuits.com**

REV. C  
M111705  
2/05-5  
B/A/DC/CP  
07/02/25  
Page 1 of 2

## Performance Charts

**ZX05-5+  
ZX05-5**



**Mini-Circuits®**  
ISO 9001 ISO 14001 CERTIFIED

P.O. Box 350166, Brooklyn, New York 11235-0003 (718) 934-4500 Fax (718) 332-4661 For detailed performance specs & shopping online see Mini-Circuits web site  
The Design Engineers Search Engine Provides ACTUAL Data Instantly From MINI-CIRCUITS At: [www.minicircuits.com](http://www.minicircuits.com)



RF/MICROWAVE COMPONENTS

**ALL NEW**  
[minicircuits.com](http://minicircuits.com)

Page 2 of 2

## APPENDIX B

### XMC2560E-03 DATA SHEET

**Anaren®**

**Model XMC2560E-03**

Rev B

**Xinger**



#### Wideband Hybrid Coupler, 3 dB, 90° Military Grade

##### Description

The XMC2560E-03 is a low profile, high performance 3dB hybrid coupler in an easy to use, manufacturing friendly surface mount package. It is designed primarily for defense applications. The XMC2560E-03 is designed particularly for balanced power and low noise amplifiers, plus signal distribution and other applications where low insertion loss and tight amplitude and phase balance is required. It can be used in high power applications up to 100 watts.

Parts have been subjected to rigorous qualification testing and they are manufactured using materials with coefficients of thermal expansion (CTE) compatible with common substrates such as FR4, G-10, RF-35, RO4350 and polyimide.

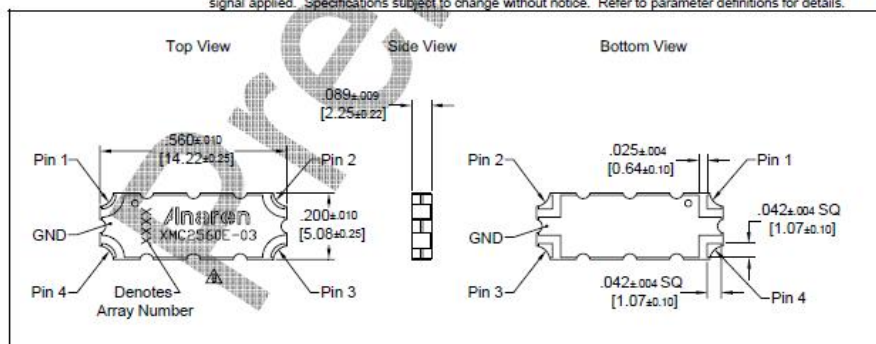
##### Features:

- 2500 – 6000 MHz
- Defense Applications
- High Power
- Very Low Loss
- Tight Amplitude Balance
- High Isolation
- Production Friendly
- Tape and Reel
- Available in Lead-Free (as illustrated) or Tin-Lead
- Reliable, FIT=0.53

##### Electrical Specifications\*\*

Frequency	Isolation	Insertion Loss	VSWR	Amplitude Balance
MHz	dB Min	dB Max	Max : 1	dB Max
2500-6000	21	0.22	1.25	± 0.75
Phase Error	Power	θJC	Operating Temp.	
Degrees	Avg. CW Watts	°C/Watt	°C	
± 4.0	TBD	39	-55 to +95	

\*\*Specification based on performance of unit properly installed on Anaren Test Board 54608-0003 with small signal applied. Specifications subject to change without notice. Refer to parameter definitions for details.



**Anaren**  
What'll we think of next?™



Available on Tape  
and Reel for Pick and  
Place Manufacturing.

USA/Canada: (315) 432-8909  
Toll Free: (800) 411-6596  
Europe: +44 2392-232392

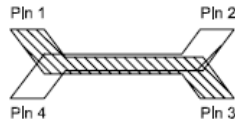
## Model XMC2560E-03

Rev B

**Anaren®**

### Hybrid Coupler Pin Configuration

The XMC2560E-03 has an orientation marker to denote Pin 1. Once port one has been identified the other ports are known automatically. Please see the chart below for clarification:



Configuration	Pin 1	Pin 2	Pin 3	Pin 4
Splitter	Input	Isolated	$-3\text{dB } \angle \theta - 90$	$-3\text{dB } \angle \theta$
Splitter	Isolated	Input	$-3\text{dB } \angle \theta$	$-3\text{dB } \angle \theta - 90$
Splitter	$-3\text{dB } \angle \theta - 90$	$-3\text{dB } \angle \theta$	Input	Isolated
Splitter	$-3\text{dB } \angle \theta$	$-3\text{dB } \angle \theta - 90$	Isolated	Input
*Combiner	$A \angle \theta - 90$	$A \angle \theta$	Isolated	Output
*Combiner	$A \angle \theta$	$A \angle \theta - 90$	Output	Isolated
*Combiner	Isolated	Output	$A \angle \theta - 90$	$A \angle \theta$
*Combiner	Output	Isolated	$A \angle \theta$	$A \angle \theta - 90$

\*Note: "A" is the amplitude of the applied signals. When two quadrature signals with equal amplitudes are applied to the coupler as described in the table, they will combine at the output port. If the amplitudes are not equal, some of the applied energy will be directed to the isolated port.

USA/Canada: (315) 432-8909  
Toll Free: (800) 411-6596  
Europe: +44 2392-232392

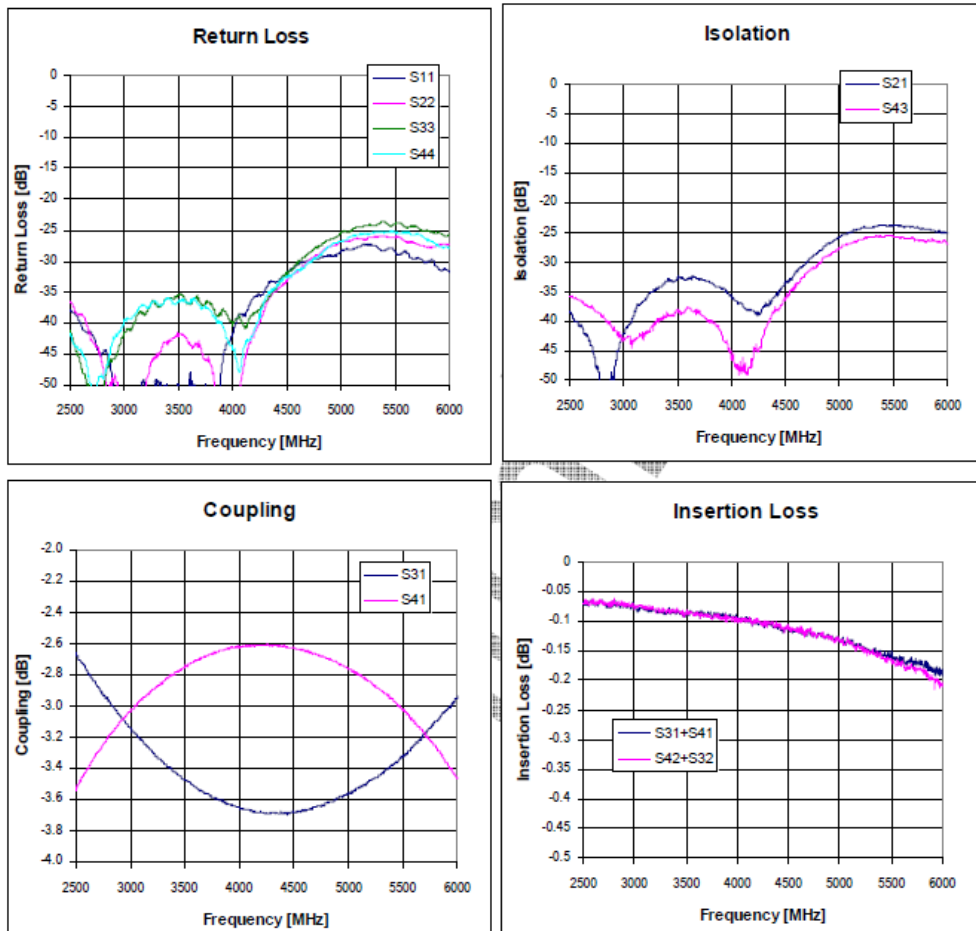
Available on Tape and  
Reel for Pick and Place  
Manufacturing.

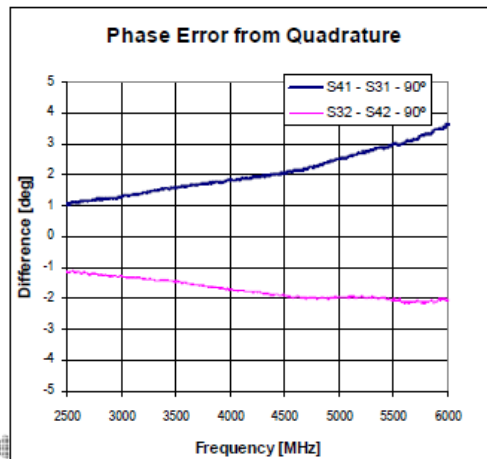
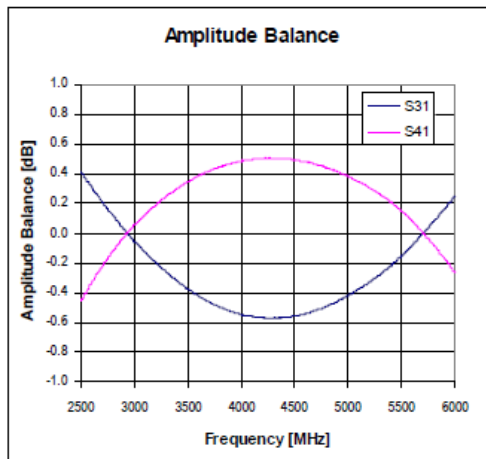


**Anaren**

What'll we think of next?™

### XMC2560E-03 Typical Performance





USA/Canada: (315) 432-8909  
Toll Free: (800) 411-6596  
Europe: +44 2392-232392

Available on Tape and  
Reel for Pick and Place  
Manufacturing.



**Anaren**  
What'll we think of next?™



## APPENDIX C

### ANNE-50+ DATA SHEET

## Termination SMA

50Ω

DC to 18000 MHz

## ANNE-50+



### Maximum Ratings

Operating Temperature -55°C to 100°C  
Storage Temperature -55°C to 100°C  
Permanent damage may occur if any of these limits are exceeded.

### Features

- wideband coverage, DC to 18000 MHz
- return loss, 35 dB typ. up to 4000 MHz and 27 dB typ. 10000 to 18000 MHz
- rugged construction

### Applications

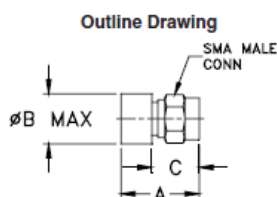
- cellular communications
- satellite communications
- test set-up
- defense & radar

CASE STYLE: LL561

Connectors	Model	Price	Qty.
SMA-Male	ANNE-50+	\$9.96 ea.	(1-9)

**+ RoHS compliant in accordance with EU Directive (2002/95/EC)**

The +Suffix has been added in order to identify RoHS Compliance. See our web site for RoHS Compliance methodologies and qualifications.



### Outline Dimensions (inch/mm)

A	B	C	wt
0.58	0.37	0.35	grams
14.73	9.40	8.89	4.0



To order ANNE-50+ with 3½ length chain and end coupling with .130" diameter mtg. hole, use part no. ANNE-50CN+. Price is \$11.95, Qty. (1-9)

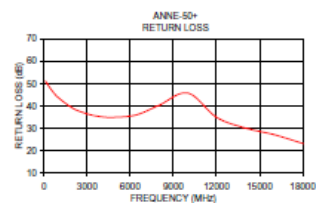
### Electrical Specifications T<sub>AMB</sub>=25°C

FREQUENCY (MHz)	IMPEDANCE (OHMS)	RETURN LOSS (dB) MIN.				POWER RATING* (W)
		DC-4 GHz	4-8 GHz	8-12 GHz	12-18 GHz	
DC-18000	50	30	27	23	21	1.0

\*At 50°C, derate linearly to 350mW at 100°C.

### Typical Performance Data

Frequency (MHz)	Return Loss (dB)
100	51.21
506	46.64
1072	43.38
2004	38.95
2800	36.93
3400	35.82
4000	35.20
4800	34.92
6400	35.97
8000	40.29
10000	45.79
12000	34.97
14000	30.16
16000	27.19
18000	23.24



**Mini-Circuits®**  
ISO 9001 ISO 14001 AS 9100 CERTIFIED

For detailed performance specs & shipping online see web site

P.O. Box 350100, Brooklyn, New York 11235-0003 (718) 934-4500 Fax (718) 332-4001 The Design Engineers Search Engine Provides ACTUAL Data Instantly at [minicircuits.com](http://minicircuits.com)

IEEE MICROWAVE COMPONENTS

Notice: 1. Performance and quality attributes and conditions not expressly stated in this specification sheet are intended to be excluded and do not form a part of this specification sheet. 2. Electrical specifications and performance data contained herein are based on Mini-Circuit's applicable established test performance criteria and measurement instructions. 3. The parts covered by this specification sheet are subject to Mini-Circuit's standard limited warranty and terms and conditions (collectively "Standard Terms"). Purchasers of this part are entitled to the rights and benefits contained therein. For a full statement of the Standard Terms and the exclusive rights and remedies thereunder, please visit Mini-Circuit's website at [www.minicircuits.com/MCUStore/terms.jsp](http://www.minicircuits.com/MCUStore/terms.jsp).

REV. F  
M120594  
ANNE-50+  
ED-11192A  
090526

## APPENDIX D

### ROGERS 4003C DATA SHEET



Advanced Circuit Materials

Advanced Circuit Materials Division  
100 S. Roosevelt Avenue  
Chandler, AZ 85226  
Tel: 480-961-1382, Fax: 480-961-4533  
www.rogerscorporation.com

Data Sheet

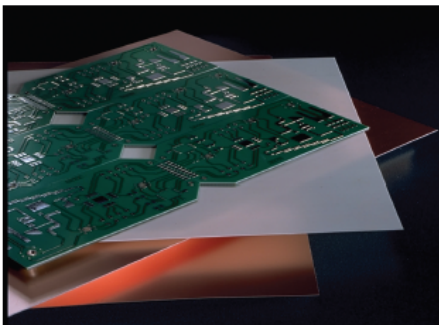
### RO4000® Series High Frequency Circuit Materials

#### Features:

- Not-PTFE
- Excellent high frequency performance due to low dielectric tolerance and loss
- Stable electrical properties versus frequency
- Low thermal coefficient of dielectric constant
- Low Z-Axis expansion
- Low in-plane expansion coefficient
- Excellent dimensional stability
- Volume manufacturing process

#### Some Typical Applications:

- LNB's for Direct Broadcast Satellites
- Microstrip and Cellular Base Station Antennas and Power Amplifiers
- Spread Spectrum Communications Systems
- RF Identifications Tags



RO4000® Series High Frequency Circuit Materials are glass reinforced hydrocarbon/ceramic laminates (Not PTFE) designed for performance sensitive, high volume commercial applications.

RO4000 laminates are designed to offer superior high frequency performance and low cost circuit fabrication. The result is a low loss material which can be fabricated using standard epoxy/glass (FR4) processes offered at competitive prices.

The selection of laminates typically available to designers is significantly reduced once operational frequencies increase to 500 MHz and above. RO4000 material possesses the properties needed by designers of RF microwave circuits and allows for repeatable design of filters, matching networks and controlled impedance transmission lines. Low dielectric loss allows RO4000 series material to be used in many applications where higher operating frequencies limit the use of conventional circuit board laminates. The temperature coefficient of dielectric constant is among the lowest of any circuit board material (Chart 1), and the dielectric constant is stable over a broad frequency range (Chart 2). This makes it an ideal substrate for broadband applications.

RO4000 material's thermal coefficient of expansion (CTE) provides several key benefits to the circuit designer. The expansion coefficient of RO4000 material is similar to that of copper which allows the material to exhibit excellent dimensional stability, a property needed for mixed dielectric multilayer boards constructions. The low Z-axis CTE of RO4000 laminates provides reliable plated through-hole quality, even in severe thermal shock applications. RO4000 series material has a Tg of >280°C (536°F) so its expansion characteristics remain stable over the entire range of circuit processing temperatures.

RO4000 series laminates can easily be fabricated into printed circuit boards using standard FR4 circuit board processing techniques. Unlike PTFE based high performance materials, RO4000 series laminates do not require specialized via preparation processes such as sodium etch. This material is a rigid, thermoset laminate that is capable of being processed by automated handling systems and scrubbing equipment used for copper surface preparation.

RO4003™ laminates are currently offered in various configurations utilizing both 1080 and 1674 glass fabric styles, with all configurations meeting the same laminate electrical performance specification. Specifically designed as a drop-in replacement for the RO4350 material, RO4350B laminates utilize RoHS compliant flame-retardant technology for applications requiring UL 94V-0 certification. These materials conform to the requirements of IPC-4103, slash sheet /10 for RO4003C and /11 for RO4350B.

The world runs better with Rogers.®

Chart 1: RO4000 Series Materials  
Dielectric Constant vs. Temperature

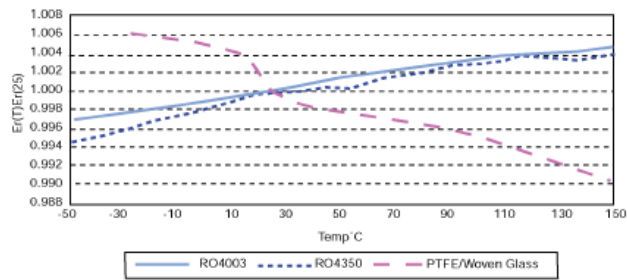


Chart 2: RO4000 Series Materials  
Dielectric Constant vs. Frequency

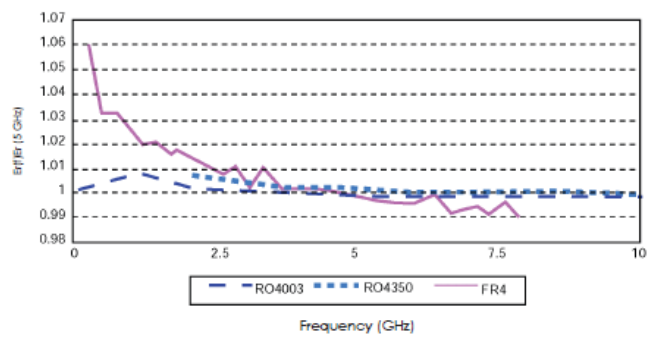
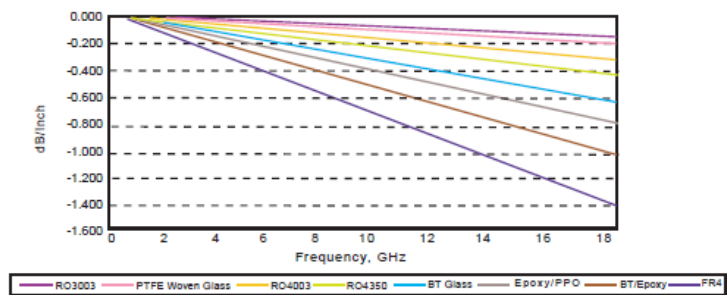


Chart 3: Microstrip Insertion Loss  
(0.030" Dielectric Thickness)



The information contained in this fabrication guide is intended to assist you in designing with Rogers' circuit materials and prepreg. It is not intended to and does not create any warranties, express or implied, including any warranty of merchantability or fitness for a particular purpose or that the results shown on this fabrication guide will be achieved by a user for a particular purpose. The user is responsible for determining the suitability of Rogers' circuit materials and prepreg for each application.

Property	Typical Value		Direction	Units	Condition	Test Method
	RO4003C™	RO4350B™				
Dielectric Constant, $\epsilon_r$ (Process specification)	3.38 ± 0.05	<sup>(1)</sup> 3.48 ± 0.05	Z	--	10 GHz/23°C	IPC-TM-650 2.5.5.5 <sup>(2)</sup> Clamped Stripline
<sup>(2)</sup> Dielectric Constant, $\epsilon_r$ (Recommended for use in circuit design)	3.55	3.66	Z	--	FSR/23°C	IPC-TM-650 2.5.5.6 Full Sheet Resonance
Dissipation Factor tan, $\delta$	0.0027 0.0021	0.0037 0.0031	Z	--	10 GHz/23°C 2.5 GHz/23°C	IPC-TM-650 2.5.5.5
Thermal Coefficient of $\epsilon_r$	+40	+50	Z	ppm/°C	-100°C to 250°C	IPC-TM-650 2.5.5.5
Volume Resistivity	1.7 X 10 <sup>10</sup>	1.2 X 10 <sup>10</sup>		MΩ•cm	COND A	IPC-TM-650 2.5.17.1
Surface Resistivity	4.2 X 10 <sup>9</sup>	5.7 X 10 <sup>9</sup>		MΩ	COND A	IPC-TM-650 2.5.17.1
Electrical Strength	31.2 (780)	31.2 (780)	Z	KV/mm (V/mil)	0.51mm (0.020")	IPC-TM-650 2.5.6.2
Tensile Modulus	26,889 (3900)	11,473 (1664)	Y	MPa (kpsi)	RT	ASTM D638
Tensile Strength	141 (20.4)	175 (25.4)	Y	MPa (kpsi)	RT	ASTM D638
Flexural Strength	276 (40)	255 (37)		MPa (kpsi)		IPC-TM-650 2.4.4
Dimensional Stability	<0.3	<0.5	X,Y	mm/m (mils/inch)	after etch +E2/150°C	IPC-TM-650 2.4.39A
Coefficient of Thermal Expansion	11 14 46	14 16 35	X Y Z	ppm/°C	-55 to 288°C	IPC-TM-650 2.1.41
Tg	>280	>280		°C DSC	A	IPC-TM-650 2.4.24
Td	425	390		°C TGA		ASTM D3850
Thermal Conductivity	0.64	0.62		W/m•K	100°C	ASTM F433
Moisture Absorption	0.06	0.06		%	48 hrs immersion 0.060" sample Temperature 50°C	ASTM D570
Density	1.79	1.86		gm/cm <sup>3</sup>	23°C	ASTM D792
Copper Peel Strength	1.05 (6.0)	0.88 (5.0)		N/mm (pli)	after solder float 1 oz. EDC Foil	IPC-TM-650 2.4.8
Flammability	N/A	94V-0				UL
Lead-Free Process Compatible	Yes	Yes				

(1) Dielectric constant typical value does not apply to 0.004" (0.101mm) laminates. Dielectric constant specification value for 0.004 RO4350B material is 3.36.

(2) Clamped stripline method can potentially lower the actual dielectric constant due to presence of airgap. Dielectric constant in practice may be higher than the values listed.

(3) Typical values are a representation of an average value for the population of the property. For specification values contact Rogers Corporation.

Prolonged exposure in an oxidative environment may cause changes to the dielectric properties of hydrocarbon based materials. The rate of change increases at higher temperatures and is highly dependent on the circuit design. Although Rogers' high frequency materials have been used successfully in innumerable applications and reports of oxidation resulting in performance problems are extremely rare, Rogers recommends that the customer evaluate each material and design combination to determine fitness for use over the entire life of the end product.

Standard Thickness	Standard Panel Size	Standard Copper Cladding
<b>RO4003C:</b> 0.008" (0.203mm), 0.012 (0.305mm), 0.016" (0.406mm), 0.020" (0.508mm) 0.032" (0.813mm), 0.060" (1.524mm) <b>RO4350B:</b> *0.004" (0.101mm), 0.0066" (0.168mm) 0.010" (0.254mm), 0.0133 (0.338mm), 0.0166 (0.422mm), 0.020" (0.508mm) 0.030" (0.762mm), 0.060" (1.524mm)	12" X 18" (305 X 457 mm) 24" X 18" (610 X 457 mm) 24" X 36" (610 X 915 mm) 48" X 36" (1.224 m X 915 mm) *0.004" material is not available in panel sizes larger than 24"x18" (610 X 457mm).	½ oz. (17µm), 1 oz. (35µm) and 2 oz. (70µm) electrodeposited copper foil.

The information contained in this fabrication guide is intended to assist you in designing with Rogers' circuit materials and prepreg. It is not intended to and does not create any warranties, express or implied, including any warranty of merchantability or fitness for a particular purpose or that the results shown on this fabrication guide will be achieved by a user for a particular purpose. The user is responsible for determining the suitability of Rogers' circuit materials and prepreg for each application.